REMARKS

Claims 12-14 and 23-33 are pending and rejected.

CLAIM REJECTIONS UNDER 35 U.S.C. § 112

Claims 12-14 and 23-33 are rejected under 35 USC 112 ¶¶ 1 and 2.

Applicants respectfully request reconsideration. Applicants incorporate their previous arguments of record as reasons why they have met their burden under 35 U.S.C. § 112 ¶¶ 1 and 2. Applicants further provide with this Amendment a Declaration under 37 C.F.R. §1.132 (Buolamwini Declaration) from another independent third party skilled in this art.

The Examiner maintains his rejection over the previously submitted Declaration under 37 C.F.R. §1.132 by Dr. Erlanger; one stated reason being that

> Although Prof. Erlanger has an undergraduate and a master's degree in chemistry, he would appear to have no special expertise in medicinal chemistry, small molecule ligands, or in organic chemistry generally (Office Action page 2).

Applicants refute this characterization. Because the Examiner has indicated his preference for a Declarant's credentials, applicants herein include the Buolamwini Declaration. Dr. Buolamwini is a full Professor of Medicinal Chemistry and holds a Ph.D. in Medicinal Chemistry. Dr. Buolamwini has "special expertise in medicinal chemistry, small molecule ligands, and in organic chemistry generally" as the Examiner requested. He, like Dr. Erlanger, provides examples and analysis of how 35 U.S.C. § 112 ¶¶ 1 and 2 requirements are met.

With this submission, applicants' position is supported by two Declarations, each made under oath and penalty of perjury, from each of two independent third parties. Applicants' position is further supported by two Declarations made under oath and penalty of perjury from an inventor. Thus, applicants have provided four Declarations of record that contain specific examples supporting applicants' position that the claimed methods are enabled and described. Applicants therefore respectfully request a Notice of Allowance. If the Examiner maintains his rejection in view of this extensive record, applicants respectfully request the Examiner to provide an affidavit under 37 C.F.R. 1.104(d)(2) which states: 1.104 Nature of examination...(d) Citation of references....

> (2) When a rejection in an application is based on facts within the personal knowledge of an employee of the Office, the data shall be as specific as possible, and the reference must be supported, when called for by the applicant, by the affidavit of such employee, and such affidavit shall be subject to contradiction or explanation by the affidavits of the applicant and other persons.

The attached Buolamwini Declaration contains substantive support for enablement and description, but does not number paragraphs. Applicants believe this format is necessary to preempt the Examiner's paragraph by paragraph rejections of previous Declarations without considering their import in totality. For example, the Erlanger Declaration contains 24 numbered paragraphs. The Examiner, however, does not consider the entire 24 paragraphs, but critiques individual paragraphs and uses this to negate the

Declarant's analysis. For example, Erlanger paragraph 7 summarizes opinions that are fully explained in subsequent paragraphs 10-15 (including explanations of structures, the chemistry involved, and methods to make the particular compounds claimed). Yet, the Examiner summarily dismisses the content of paragraph 7 as "expert opinion ... not entitled to any weight", without considering supporting paragraphs 10-15 and without considering the Declaration in its entirety.

With respect to the references that applicants previously submitted as evidence that structures of each of the receptor binding molecules were known to one skilled in the art, the Examiner stated these were deficient because none supplied the "known or disclosed correlation between function and structure", citing MPEP §2161II.A.2(a) (Office Action page 3). However, the MPEP requires such a structure/function relationship only "where an invention is described solely in terms of a method of its making coupled with its function and there is no described or art-recognized correlation or relationship between the structure of the invention and its function." MPEP § 2163I.A.

This is not the case here. The Buolamwini Declaration, like the Erlanger Declaration, supports applicants' assertion that one skilled in the art does recognize a correlation or relationship between applicants' claimed sulfenate and its claimed function, refuting this basis for rejection. Applicants have provided both the structure (both chemical formula and specific identities of each component), and the function (the chromophore or dye is the photosensitizer, which induces sulfenate radicals, that destroy tissues by

necrosis or apoptosis at the receptor to which the sulfenate is located by the receptor binding portion of the compound).

Using steroid receptor binding compounds as an example, a large number of ligands does not make a claim indefinite by reciting "steroid receptor binding molecules". One skilled in the art knows that steroid hormone receptors are proteins that have a binding site for a particular steroid molecule. One skilled in the art would determine specific compounds empirically, by a literature search, etc. such that their scope is not "unknown and unknowable". Applicants have cited in the Erlanger Declaration estradiol as one example. The Examiner has supplied his own examples of which steroids would and would not work, supporting applicants' position that such compounds are not "unknown and unknowable". For example, the Examiner states that diethylstilbesterol is not a steroid but strongly binds to the estrogen receptor; testosterone does not bind to the estrogen receptor, testosterone and esterone do not bind to the corticosteroid receptors, cortisone and aldosterone do not bind to the sex hormone receptors (Office Action page 4).

As further evidence, the attached Buolamwini Declaration provides listings for additional components known to bind to the estrogen receptor, namely, estratriol, 17β-aminoestrogen (AE) derivatives such as prolame and butolame, drugs such as tamoxifen, ICI-164384, raloxifene, genistein, 17β-estradiol, glucocorticoids, progesterone, estrogens, retinoids, fatty acid derivatives, phytoestrogens, etc., citations supporting his assertions, as well as citations referencing commercially available kits that identify specific receptor

binding compounds (e.g., Estrogen Receptor-alpha Competitor Assay Kit, Red; Estrogen Receptor-beta Competitor Assay Kit, Red (Invitrogen Corp., Carlsbad CA). The references included with the Buolamwini Declaration are:

A. Invitrogen Estrogen Receptor Competitor Assay Kits – Product Description

B. Each of cholecystokinin, neurotensin, somatostatin, and bombesin in Guide to Receptors and Channels, 1st Edition (2005 revision), Alexander et al., p. S23, S46, S56, S12, S1, and S2

C. PanVera Corporation, Postings, Winter 1998 – Product Description

D. J Neurochem 62, 1426-1431 (1994)

E. PerkinElmer Inc. - Product Description

F. J. Nuclear Medicine 37(6), 1014-1022 (1996)

G. J. Biomol Screen 5(2), 77-88 (2000)

H. Pharm. Res. 17, 1250-1258 (2000)

I. Endocrinology 131, 799-806 (1992)

Applicants also refute the Examiner's characterizations of the Erlanger Declaration as not on point. Previous rejections were based on applicants' lack of showing "how to make and/or use the full scope of the claimed invention" and that "the nature of the invention is chemical synthesis, which involves chemical reactions (Office Action 02/09/05, page 9). In response, Dr. Erlanger detailed how he, as one skilled in the art, would make the claimed formula by a detailed showing of how to chemically linking estradiol as only one example. The Examiner now characterizes Dr. Erlanger's explanation as "not on point", while applicants have attempted to be "on point" and respond fully to the Examiner's rejections.

Applicants also refute the Examiner's characterization of the Erlanger Declaration as "at odds" with not claiming any particular binding property. Applicants' consistent position is that the claimed invention is met by binding of the targeting moiety E which locates the compound at the target site. As one example, Dr. Erlanger stated that one skilled in the art would likely consider 1 μM for receptor affinity, and that one skilled in the art could empirically determine this without undue experimentation. This has been applicants' consistent position and is not "at odds" with previous assertions.

With respect to the pending rejections of claims 12-14 and 23-33 under §112 ¶2, and claims 12-14 and 23-33 under §112 ¶1, applicants have addressed these in the Buolamwini Declaration. Briefly, Dr. Buolamwini, a medicinal chemist with specific expertise in drug design, targeting, and structure/function activity relationships, has provided his opinion, reasons for his opinion, and references supporting reasons for his opinion, that that the claimed methods are sufficiently definite and enabled and that the claims meet the requirements for patentability under 35 U.S.C.§112 ¶¶1 and 2, which are the only outstanding rejections.

CONCLUSION

For the foregoing reasons, applicants submit that all the rejections have been overcome and that the application is in complete condition for allowance. Applicants respectfully request a Notice of Allowance.

Applicants submit the fee for a one-month extension of time and do not believe any other fee is due with this submission. Should any other fee or

surcharge be deemed necessary, the Examiner is authorized to charge fees or credit any overpayment to Deposit Account No. 23-3000.

The Examiner is invited to telephone applicants' undersigned representative if there are any questions.

Respectfully submitted,

WOOD, HERRON & EVANS, L.L.P.

By Beverly A. Lyman
Beverly A. Lyman
Reg. No. 41,961

2700 Carew Tower
441 Vine Street
Cincinnati, Ohio 45202
513 241 2324
513 421 7269 facsimile

Estrogen Receptor Competitor Assay Kits, Red

** Your account specific pricing will be displayed once an item has been added to your order.*

Product	Tech. Docs.	Cat. No.	Size	List Price*	Qty
ER-a Competitor Kit, Red		P3029	400 x 40 µL assay (s)	515.00	
ER-β Competitor Assay, Red		P3032	400 x 40 µL assay (s)	515.00	

For additional product info, click the associated Tech. Docs. icon. Add To Favorites Add To Order

Product Image(s)

Figure 1 - Competition data produced using the ER Competitor Assay Kits, Red

Table 1 - Z´-factor determination

Description:
Estrogen Receptor (ER) Competitor Assay Kits, Red provide a sensitive, efficient method for high-throughput screening of potential ER-alpha and ER-beta ligands using fluorescence polarization (FP). The ER Competitor Assay, Red kits contain human ERs and a novel, fluorescent estrogen ligand (Fluormone← EL Red) in a homogenous mix-and-read assay format. Using a longer excitation wavelength (530 nm) than that used for the Estrogen Receptor Competitor Assay, Green kits (485 nm) reduces the problem of intrinsic fluorescence found in some test compounds.

To assay: ER is added to the Fluormone™ EL Red ligand to form an ER/Fluormone™ EL Red complex. This complex is then added to individual test compounds in multiwell plates. If the test compounds do not compete with Fluormone™ EL Red binding to ER, the Fluormone™ EL Red ligand will tumble slowly during its fluorescence lifetime, resulting in a high polarization value. Competing test compounds will displace the Fluormone™ EL Red ligand from ER, leading to rapid tumbling and therefore a low olarization value. The change in polarization value in the presence of a test compound is used to determine relative affinity of that test compound for ER (Figure 1).

Contents and Storage:
The Estrogen Receptor Competitor Assay Kit, Red includes purified, active ER-α or ER-β protein, Fluormone™ EL Red ligand, and buffer. Store components as indicated in the assay protocol (-80°C, -20°C, or +4°C).

Reference(s):
1. Zhang, J.H. *et al.* (1999) *J. Biomol. Screen.* **4:** 67-73.

* Bulk quantities available.

EXHIBIT A

Cholecystokinin

Overview: Cholecystokinin receptors (nomenclature recommended by the NC-IUPHAR Subcommittee on CCK Receptors, Noble *et al.*, 1999) are activated by the endogenous peptides cholecystokinin (CCK)-4, CCK-8, CCK-33 and gastrin. There is evidence for species homologues of CCK_2 receptors distinguished by the relative affinities of the two stereoisomers of devazepide, *R*-L365260 and *S*-L365260, or by the differences in affinity of the agonist BC264 (Durieux *et al.*, 1992).

Nomenclature	**CCK_1**	**CCK_2**
Other names	CCK_A	CCK_B, CCK_B/gastrin
Ensembl ID	ENSG00000163394	ENSG00000110418
Principal transduction	$G_{q/11}/G_s$ (Wu *et al.*, 1997)	G_s
Rank order of potency	CCK-8 ≫ gastrin, des-CCK-8 > CCK-4	CCK-8 ≥ gastrin, des-CCK-8, CCK-4
Selective agonists	A71623, JMV180, GW5823	Desulfated CCK-8, gastrin, CCK-4, BC264, RB400
Selective antagonists	Devazepide (9.8), T0632 (9.6), SR27897 (9.2), IQM95333 (9.2), PD140548 (7.9–8.6), lorglumide (7.2)	YM022 (10.2), L740093 (10.0), GV150013 (9.3), RP73870 (9.3), L365260 (7.5–8.7), LY262691 (7.5)
Radioligands	[^{3}H]-Devazepide (0.2 nM)	[^{3}H]-Propionyl-BC264 (0.15 nM), [^{3}H]-PD140376 (0.2 nM), [^{3}H]-L365260 (2 nM), [^{3}H]- or [^{125}I]-gastrin (1 nM), [^{125}I]-PD142308 (0.25 nM)

A mitogenic gastrin receptor, which can be radiolabelled with [^{125}I]-gastrin-(1–17) and which appears to couple to the G_s family of G proteins, has been described on human colon cancer cells (Bold *et al.*, 1994) and other cell lines (e.g. pancreatic AR42J and Swiss 3T3 fibroblasts, Seva *et al.*, 1994; Singh *et al.*, 1995).

Abbreviations: **A71623,** Boc-Trp-Lys(*O*-toluylaminocarbonyl)-Asp-(*N*Me)Phe-NH_2; **BC264,** Tyr(SO_3H)-gNle-mGly-Trp-(NMe)Nle-Asp-Phe-NH_2; **GV150013,** (+)-*N*-(1-[1-adamantane-1-methyl]-2,4-dioxo-5-phenyl-2,3,4,5-tetrahydro-1*H*-1,5-benzodiazepin-3-yl)-*N'*-phenylurea; **GW5823,** 2-[3-(1*H*-indazol-3-ylmethyl)-2,4-dioxo-5-phenyl-2,3,4,5-tetrahydrobenzo[*b*][1,4]diazepin-1-yl]-*N*-isopropyl-*N*-(methyoxyphenyl)acetamide; **IQM95333,** (4α*s*,5*r*)-2-benzyl-5[*N*-(*tert*-butoxycarbonyl)-L-Trp]amino-1,3-dioxoperhydropyrido[1,2-*c*]pyrimidine; **JMV180,** Boc-Tyr(SO_3H)Ahx-Gly-Trp-Ahx-Asp^{2}phenylethyl ester; **L365260,** 3*r*(+)-*N*-(2,3-dihydro-1-methyl-2-oxo-5-phenyl-1*H*-1,4-benzodiazepin-3-yl)-*N'*-(3-methylphenyl)urea; **L740093,** *N*-([3*r*]-5-[3-azabicyclo{3.2.2}nonan-3-yl]-2,3-dihydro-1-methyl-2-oxo-1*H*-1,4-benzodiazepin-3-yl)-*N'*-(3-methylphenyl)urea; **LY262691,** *trans*-*N*-(4-bromophenyl)-3-oxo-4,5-diphenyl-1-pyrrazolidinecarboxamide(3.3.1.1^{3,7}); **PD140376,** L-3-([4-aminophenyl]methyl)-*N*-(α-methyl-*N*-[{tricyclo(3.3.1.1^{3,7})dec-2-yloxy}carbonyl]-D-Trp)-β-Ala; **PD140548,** *N*-(α-methyl-*N*-[{tricyclo(3.3.1.1^{3,7})dec-2-yloxy}carbonyl]-L-Trp)-D-3-(phenylmethyl)-β-Ala; **PD142308,** iodinated PD140548; **RB400,** HOOC-CH_2-CO-Trp-NMe(Nle)-Asp-Phe-NH_2; **RP73870,** ({[(*N*-methyoxy-3-phenyl)-*N*-(*N*-methyl-*N*-phenyl-carbamoylmethyl)-carbamoylmethyl]-3-ureido}-3-phenyl)-2-ethylsulfonate-(*rs*); **SR27897,** 1-([2-{4-(2-chlorophenyl)thiazole-2-yl}aminocarbonyl]indolyl)acetic acid; **T0632,** sodium (*s*)-3-(1-[2-fluorophenyl]-2,3-dihydro-3-[{3-isoquinolinyl}-carbonyl]amino-6-methoxy-2-oxo-1*H*-indole)propanoate; **YM022,** (*r*)-1-(2,3-dihydro-1-[2'-methylphenacyl]-2-oxo-5-phenyl-1*H*-1,4-benzodiazepin-3-yl)-3-(3-methylphenyl)urea

Further reading:

DE TULLIO, P., DELARGE, J. & PIROTTE, B. (2000). Therapeutic and chemical developments of cholecystokinin receptor ligands. *Expert. Opin. Investig. Drugs*, **9**, 129–146.

HERRANZ, R. (2003). Cholecystokinin antagonists: Pharmacological and therapeutic potential. *Med. Res. Rev.*, **23**, 559–605.

INUI, A. (2003). Neuropeptide gene polymorphisms and human behavioural disorders. *Nature Rev. Drug Discov.*, **2**, 986–998.

KOPIN, A.S., MCBRIDE, E.W., SCHAFFER, K. & BEINBORN, M. (2000). CCK receptor polymorphisms: an illustration of emerging themes in pharmacogenomics. *Trends Pharmacol. Sci.*, **21**, 346–353.

MORAN, T.H. (2000). Cholecystokinin and satiety: current perspectives. *Nutrition*, **16**, 858–865.

NOBLE, F. & ROQUES, B.P. (1999). CCK_B receptor: chemistry, molecular biology, biochemistry and pharmacology. *Prog. Neurobiol.*, **56**, 1–31.

NOBLE, F., WANK, S.A., CRAWLEY, J.N., BRADWEJN, J., SEROOGY, K.B., HAMON, M. & ROQUES, B.P. (1999). International Union of Pharmacology. XXI. Structure, distribution, and functions of cholecystokinin receptors. *Pharmacol. Rev.*, **51**, 745–781.

ROZENGURT, E. & WALSH, J. (2001). Gastrin, CCK, signaling, and cancer. *Annu. Rev. Physiol.*, **63**, 49–76.

References:

BOLD, R.J. *et al.* (1994) *Biochem. Biophys. Res. Commun.*, **202**, 1222–1226.

DURIEUX, C. *et al.* (1992) *Mol. Pharmacol.*, **41**, 1089–1095.

SEVA, C. *et al.* (1994) *Science*, **265**, 410–412.

SINGH, P. *et al.* (1995) *J. Biol. Chem.*, **270**, 8429–8438.

WU, V. *et al.* (1997) *J. Biol. Chem.*, **272**, 9032–9042.

Neurotensin

Overview: Neurotensin receptors (provisional nomenclature) are activated by the endogenous tridecapeptide neurotensin (pGlu-Leu-Tyr-Glu-Asn-Lys-Pro-Arg-Arg-Pro-Tyr-Ile-Leu) derived from a precursor (ENSG00000133636) which also generates neuromedin N, an agonist at the NTS2 receptor. A nonpeptide antagonist, SR142948A, shows high affinity (pk_i ~9) at both NTS1 and NTS2 receptors (Gully *et al.*, 1997). [^{3}H]-neurotensin and [^{125}I]-neurotensin may be used to label NTS1 and NTS2 receptors at 0.1–0.3 and 3–5 nM concentrations, respectively.

Nomenclature	NTS1	NTS2
Other names	High-affinity neurotensin receptor, NTRH, NTR-1, NT_1	Low-affinity neurotensin receptor, NTRL, NTR-1, NT_2
Ensembl ID	ENSG00000101188	ENSG00000169006
Principal transduction	$G_{q/11}$	$G_{q/11}$
Rank order of potency	Neurotensin > neuromedin N (Hermans *et al.*, 1997)	Neurotensin = neuromedin N (Mazella *et al.*, 1996)
Selective agonists	JMV449 (Souaze *et al.*, 1997)	Levocobastine (Mazella *et al.*, 1996)
Selective antagonists	SR48692 (7.5–8.2, Gully *et al.*, 1997)	—
Radioligands	[^{3}H]-SR48692 (3.4 nM, Labbe-Jullie *et al.*, 1995)	—

Neurotensin appears to be a low efficacy agonist at the NTS2 receptor (Vita *et al.*, 1998). An additional protein, provisionally termed NTS3 (also known as NTR3, gp95 and sortilin, ENSG00000134243) has recently been suggested to bind lipoprotein lipase and mediate it's degradation (Nielsen *et al.*, 1999). It has been reported to interact with the NTS1 receptor (Martin *et al.*, 2002) and has been implicated in hormone trafficking and/or neurotensin uptake.

Abbreviations: **JMV449,** *H*-LysΨ(CH_2NH)-Lys-Pro-Tyr-Ile-Leu; **SR142948A,** 2-([5-{2,6-dimethoxyphenyl}-1-{4-(*N*-[3-dimethylaminopropyl]-*N*-methylcarbamoyl)-2-isopropylphenyl}-1*H*-pyrazole-3-carbonyl]amino)adamantane-2-carboxylic acid hydrochloride; **SR48692,** 2-([1-{7-chloro-4-quinolinyl}-5-{2,6-dimethoxyphenyl}-pyrazol-3-yl]carboxylamino)tricyclo(3.3.1.1.[3.7])decan-2-carboxylic acid

Further reading:

BEROD, A. & ROSTENE, W. (2002). Neurotensin: an endogenous psychostimulant? *Curr. Opin. Pharmacol.*, **2,** 93–98.

BINDER, E.B., KINKEAD, B., OWENS, M.J. & NEMEROFF, C.B. (2001). Neurotensin and dopamine interactions. *Pharmacol. Rev.*, **53,** 453–486.

BOULES, M., FREDRICKSON, P. & RICHELSON, E. (2003). Current topics: brain penetrating neurotensin analog. *Life Sci.*, **73,** 2785–2792.

DOBNER, P.R., DEUTCH, A.Y. & FADEL, J. (2003). Neurotensin: dual roles in psychostimulant and antipsychotic drug responses. *Life Sci.*, **73,** 801–811.

KINKEAD, B. & NEMEROFF, C.B. (2002). Neurotensin: an endogenous antipsychotic? *Curr. Opin. Pharmacol.*, **2,** 99–103.

KINKEAD, B. & NEMEROFF, C.B. (2004). Neurotensin, schizophrenia, and antipsychotic drug action. *Int. Rev. Neurobiol.*, **59,** 327–349.

MCMAHON, B.M., BOULES, M., WARRINGTON, L. & RICHELSON, E. (2002). Neurotensin analogs indications for use as potential antipsychotic compounds. *Life Sci.*, **70,** 1101–1119.

RICHELSON, E., BOULES, M. & FREDRICKSON, P. (2003). Neurotensin agonists: possible drugs for treatment of psychostimulant abuse. *Life Sci.*, **73,** 679–690.

TYLER-MCMAHON, B.M., BOULES, M. & RICHELSON, E. (2000). Neurotensin: peptide for the next millennium. *Regul. Pept.*, **93,** 125–136.

VINCENT, J.P., MAZELLA, J. & KITABGI, P. (1999). Neurotensin and neurotensin receptors. *Trends Pharmacol. Sci.*, **20,** 302–309.

References:

GULLY, D. *et al.* (1997). *J. Pharmacol. Exp. Ther.*, **280,** 802–812.

HERMANS, E. *et al.* (1997). *Br. J. Pharmacol.*, **121,** 1817–1823.

LABBE-JULLIE, C. *et al.* (1995). *Mol. Pharmacol.*, **47,** 1050–1056.

MARTIN, S. *et al.* (2002). *Gastroenterology*, **123,** 1135–1143.

MARTIN, S. *et al.* (2003). *J. Neurosci.*, **23,** 1198–1205.

MAZELLA, J. *et al.* (1996). *J. Neurosci.*, **16,** 5613–5620.

NIELSEN, M.S. *et al.* (1999). *J. Biol. Chem.*, **274,** 8832–8836.

PETERSEN, C.M. *et al.* (1997). *J. Biol. Chem.*, **272,** 3599–3605.

SOUAZE, F. *et al.* (1997). *J. Biol. Chem.*, **272,** 10087–10094.

VITA, N. *et al.* (1998). *Eur. J. Pharmacol.*, **360,** 265–272.

Somatostatin

Overview: Somatostatin (somatotropin release inhibiting factor) is an abundant neuropeptide, which acts on five subtypes of somatostatin receptor (sst1 – sst5; nomenclature approved by the NC-IUPHAR Subcommittee on Somatostatin Receptors, see Hoyer *et al.*, 2000). Activation of these receptors produces a wide range of physiological effects throughout the body. The relationship of the cloned receptors to endogenously expressed receptors is not yet well established in some cases. Endogenous ligands for these receptors are somatostatin-14 (SRIF-14) and somatostatin-28 (SRIF-28). Cortistatin (CST-14) has also been suggested to be an endogenous ligand for somatostatin receptors (Delecea *et al.*, 2000).

Nomenclature	sst_1	sst_2	sst_3	sst_4	sst_5
Alternative names	SSTR1, $SRIF_2$, $SRIF_{2A}$	SSTR2, $SRIF_1$, $SRIF_{1A}$	SSTR3, $SRIF_1$, $SRIF_{1C}$	SSTR4, $SRIF_2$, $SRIF_{2B}$	SSTR5, $SRIF_1$, $SRIF_{1B}$
Ensembl ID	ENSG00000139874	ENSG00000180616	ENSG00000183473	ENSG00000132671	ENSG00000162009
Principal transduction	G_i	G_i	G_i	G_i	G_i
Selective agonists	des-Ala^{1,2,5}-[DTrp^8,Iamp^9] SRIF, L797591	Octreotide, seglitide BIM23027, L054522	L796778	NNC269100 L803087	BIM23268, BIM23052, L817818
Selective antagonists	—	Cyanamid 154806 (7.7–8.0)	—	—	BIM23056 (7.4–8.3)
Radioligands	—	[^{125}I]-[Tyr^3]octreotide (0.13 nM) [^{125}I]-BIM23027	—	—	[^{125}I]-[Tyr^3]octreotide (0.23 nM)

[^{125}I]-[Tyr^{11}]-SRIF-14, [^{125}I]-LTT-SRIF-28, [^{125}I]-CGP23996 and [^{125}I]-[Tyr^{10}]CST-14^6 may be used to label somatostatin receptors non-selectively; BIM23052 is said to be selective at rat but not human receptor (Patel & Srikant, 1994). A number of non-peptide subtype-selective agonists have been synthesised (see Rohrer *et al.*, 1998)

Abbreviations: **BIM23027,** *cyc*(N-Me-Ala-Tyr-D-Trp-Lys-Abu-Phe); **BIM23052,** DPhe-Phe-Phe-DTrp-Lys-Thr-Phe-Thr-NH_2; **BIM23056,** DPhe-Phe-Tyr-DTrp-Lys-Val-Phe-dNal-NH_2; **BIM23268,** *cyc*(Cys-Phe-Phe-D-Trp-Lys-Thr-Phe-Cys)-NH_2; **CGP23996,** *cyc*(Asn-Lys-Asn-Phe-Phe-Trp-Lys-Thr-Tyr-Thr-Ser); **Cyanamid 154806,** Ac-(4-NO_2-Phe)-*cyc*(D-Cys-Tyr-D-Trp-Lys-Thr-Cys)-D-Tyr-NH_2; **L797591,** (2R)-N-(6-amino-2,2,4-trimethylhexyl)-3-(1-naphthyl)-2-({[(2-phenylethyl)2-pyridin-2-ylethyl)amino]carbonyl}amino)propanamide; **L054522,** tert-butyl (bS)-b-methyl-N{[4-(2-oxo-2,3,-dihydro-1H-benzimidazol-1-yl)piperidin-1-yl]carbonyl}-D-tryptophyl-L-lysinate; **L796778,** methyl (2S)-6-amino-2-[((2R)-2-{[({(1S)-1-benzyl-2-[(4-nitrophenyl)amino]-2-oxoethyl}amino)carbonyl]amino}hexanoyl)amino]hexanoate; **L803087,** methyl (2S)-5-{[amino(imino)methyl]amino}-2-{[4-(5,7-difluoro-2-phenyl-1H-indol-3-yl)butanoyl]amino}pentanoate; **L817818,** (2R)-2-aminopropyl N2-{[2-(2-naphthyl)-1H-benzo[g]indo-3-yl]acetyl}-L-lysinat; **LTT-SRIF-28,** [Leu^8,DTrp^{22},DTyr^{25}]SRIF-28; **NNC269100,** 1-[3-[N-(5-Bromopyridin-2-yl)-N-(3,4-dichlorobenzyl)amino]propyl]-3-[3-(1H -imidazol-1-yl)propyl]thiourea

Further reading:

CSABA, Z. & DOURNAUD, P. (2001). Cellular biology of somatostatin receptors. *Neuropeptides*, **35**, 1–23.

DASGUPTA, P. (2004). Somatostatin analogues: Multiple roles in cellular proliferation, neoplasia, and angiogenesis. *Pharmacol. Ther.*, **102**, 61–85.

HANNON, J.P., NUNN, C., STOLZ, B., BRUNS, C., WECKBECKER, G., LEWIS, I., TROXLER, T., HURTH, K. & HOYER, D. (2002). Drug design at peptide receptors – somatostatin receptor ligands. *J. Mol. Neurosci.*, **18**, 15–27.

HOYER, D., EPELBAUM, J., FENIUK, W., HUMPHREY, P.P.A., MEYERHOF, W., O'CAROLL, A.M., PATEL, Y., REISINE, T., REUBI, J.C., SCHINDLER, M., SCHONBRUNN, A., TAYLOR, J.E. & VEZZANI, A. (2000). Somatostatin receptors, pp 354–364. In *The IUPHAR Compendium of Receptor Characterization and Classification, 2nd edition*, IUPHAR Media, London.

MOLLER, L.N., STIDSEN, C.E., HARTMANN, B. & HOLST, J.J. (2003). Somatostatin receptors. *Biochimica. Et. Biophysica. Acta-biomembranes*, **1616**, 1–84.

PATEL, Y.C. (1999). Somatostatin and its receptor family. *Front. Neuroendocrinol.*, **20**, 157–198.

PATEL, Y.C., GREENWOOD, M.T., PANETTA, R., DEMCHYSHYN, L., NIZNIK, H. & SRIKANT, C.B. (1995). The somatostatin receptor family. *Life Sci.*, **57**, 1249–1265.

RASHID, A.J., O'DOWD, B.F. & GEORGE, S.R. (2004). Minireview: Diversity and complexity of signaling through peptidergic G protein-coupled receptors. *Endocrinology*, **145**, 2645–2652.

REISINE, T. & BELL, G. (1995). Molecular properties of somatostatin receptors. *Neurosci.*, **67**, 777–790.

WECKBECKER, G., LEWIS, I., ALBERT, R., SCHMID, H.A., HOYER, D. & BRUNS, C. (2003). Opportunities in somatostatin research: Biological, chemical & therapeutic aspects. *Nature Reviews Drug Discovery.*, **2**, 999–1017.

References:

DELECEA, L. *et al.* (1996). *Nature*, **381**, 242–245.

PATEL, Y.C. & SRIKANT, C.B. (1994). *Endocrinology*, **135**, 2814–2817.

ROHRER, S.P. *et al.* (1998). *Science*, **282**, 737–740.

Bombesin

Overview: Bombesin receptors are activated by the endogenous ligands gastrin-releasing peptide (GRP), neuromedin B (NMB) and GRP-18–27 (previously named neuromedin C). Bombesin is a tetradecapeptide, originally derived from amphibians. These receptors couple, primarily, to the $G_{q/11}$ family of G proteins (but see also Jian *et al.*, 1999). Activation of BB1 and BB2 receptors causes a wide range of physiological actions, including the stimulation of tissue growth, smooth-muscle contraction, secretion and many central nervous system effects (Tokita *et al.*, 2002). A physiological role for the bb3 receptor has yet to be defined.

Nomenclature	**BB1**	**BB2**	**bb3**
Other names	NMB-R	GRP-R	BRS-3
Ensembl ID	ENSG00000135577	ENSG00000126010	ENSG00000102239
Principal transduction	$G_{q/11}$	$G_{q/11}$	$G_{q/11}$
Selective agonists	NMB	GRP	—
Selective antagonists	PD165929, DNal-*cyc*(Cys-Tyr-DTrp-Orn-Val)-Nal-NH_2, DNal-Cys-Tyr-DTrp-Lys-Val-Cys-Nal-NH_2	1-naphthoyl-[DAla^{24},DPro^{26},ψ26–27]GRP-20–27, kuwanon H, [DPhe^{6}]bombesin-6–13-ethylester, [DPhe^{6},Cpa^{14},ψ13–14]bombesin-6–14	—
Radioligands	[^{125}I]-BH-NMB, [^{125}I]-[Tyr^{4}]-bombesin	[^{125}I]-[DTyr^{6}]bombesin-6–13-methylester, [^{125}I]-GRP, [^{125}I]-[Tyr^{4}]bombesin	[^{125}I]-[Tyr^{6},βAla^{11},Phe^{13},Nle^{14}] bombesin-6–14

All three subtypes may be activated by [dPhe^{6}, βAla^{11}, Phe^{13}, Nle^{14}]bombesin-6–14 (Mantey *et al.*, 1997). One analogue, [D-Tyr^{6}, Apa-4Cl, Phe^{13}, Nle^{14}] bombesin-6–14 has more than 200 fold selectivity for bb3 receptors over BB1 and BB2. (Mantey *et al.*, 2004)

Abbreviation: PD165929, 2-[3-(2,6-diisopropylphenyl)-ureido]3-(1*H*-indol-3-yl)-2-methyl-*N*-(1-pyridin-2-yl-cyclohexylmethyl)-proprionate.

Further reading:

BATTEY, J. & WADA, E. (1991). Two distinct receptor subtypes for mammalian bombesin receptors. *Trends Neurosci.*, **14,** 524–528.

IWABUCHI, M., UI-TEI, K., YAMADA, K., MATSUDA, Y., SAKAI, Y., TANAKA, K. & OHKI-HAMAZAKI, H. (2003). Molecular cloning and characterisation of avian bombesin-like peptide receptors: new tools for investigating molecular basis of ligand selectivity. *Br. J. Pharmacol.*, **139,** 555–566.

JENSEN, R. & COY, D. (1991). Progress in the development of potent bombesin receptor antagonists. *Trends Pharmacol. Sci.*, **12,** 13–18.

KROOG, G.S., JENSEN, R.T. & BATTEY, J.F. (1995). Bombesin receptors. *Med. Res. Rev.*, **15,** 389–417.

MOODY, T.W., MANTEY, S.A., PRADHAN, T.K., SCHUMANN, M., NAKAGAWA, T., MARTINEZ, A., FUSELIER, J., COY, D.H. & JENSEN, R.T. (2004). Development of high affinity camptothecin-bombesin conjugates that have targeted cytotoxicity for bombesin receptor-containing tumor cells. *J. Biol. Chem.*, **279,** 23580–23589.

OHKI-HAMAZAKI, H. (2000). Neuromedin B. *Prog. In Neurobiol.*, **62,** 297–312.

TOKITA, K., HOCART, S.J., COY, D.H. & JENSEN, R.T. (2002). Molecular basis of the selectivity of gastrin-releasing peptide receptor for gastrin-releasing peptide. *Mol. Pharmacol.*, **61,** 1435–1443.

WEBER, D. (2003). Design of selective peptidomimetic agonists for the human orphan receptor BRS-3. *J. Med. Chem.*, **46,** 1918–1930.

References:

JIAN, X.Y. *et al.* (1999). *J. Biol. Chem.*, **274,** 11573–11581.

MANTEY, S.A. *et al.* (1997). *J. Biol. Chem.*, **272,** 26062–26071.

MANTEY, S.A. *et al.* (2004). *J. Pharmacol. Exp. Ther.*, **310,** 1161–1170.

Guide to Receptors and Channels, 1st Edition (2005 revision)

The great proliferation of drug targets in recent years has driven the need to organise and condense the information in a logical way. This is the underlying reason for this Guide to Receptors and Channels, distributed with the British Journal of Pharmacology and Nature Reviews Drug Discovery. Our intent is to produce an authoritative but user-friendly publication, which allows a rapid overview of the key properties of a wide range of established or potential pharmacological targets. The aim is to provide information succinctly so that a newcomer to a particular target group can identify the main elements "at a glance". It is not our goal to produce all-inclusive reviews of the targets presented; references to these are included in the Further Reading sections of the entries. The Guide to Receptors and Channels presents each entry, typically a circumscribed target class family, on a single page so as to allow easy access and rapid oversight.

Targets have been selected for inclusion where there is sufficient pharmacological information to allow clear definition or where, in our view, there is clear interest in this molecular class from the pharmacological community. Our philosophy has been to present data on human receptors wherever possible, both in terms of structural information and pharmacology. To this end, the Ensembl ID allows rapid access through a free online database (http://www.ensembl.org/) to several other species, including mouse and rat. From this database, links are also provided to structural information in a number of formats. Where structural or pharmacological information is not available for human targets, we have used data from other species. A priority in constructing these tables was to present agents which represent the most selective and which are available by donation or from commercial sources, now or in the near future.

The Guide is divided into seven sections, which comprise pharmacological targets of similar structure/function. These are 7TM receptors, transmitter-gated channels, ion channels, catalytic receptors, nuclear receptors, cell-surface transmitter transporters and second messenger metabolising enzymes.

The Editors of the Guide have compiled the individual records, taking advice from many Consultants (listed on page ii). With each record, an indication is given of the status of the nomenclature as proposed by Nomenclature Committees of the International Pharmacological Congress (NC-IUPHAR), published in Pharmacological Reviews. Where this guidance is lacking, advice from several prominent, independent experts has been obtained to produce an authoritative consensus, which attempts to fit in within the general guidelines from IUPHAR (Vanhoutte *et al.*, 1996). Tabulated data provide ready comparison of selective agents and we recommend that any citations to information in the guide be presented in the following format: e.g. Histamine receptors, in Guide to Receptors and Channels, radioligands within a family of targets and additional commentary highlights whether species differences or ligand metabolism are potential confounding factors. ALEXANDER, S.P.H., MATHIE, A. & PETERS, J.A. (2005). *British Journal of Pharmacology*, **144S**, 1–128.

The Editors

Stephen P.H. Alexander
School of Biomedical Sciences and Institute of Neuroscience,
University of Nottingham Medical School,
Nottingham NG7 2UH,
England
steve.alexander@nottingham.ac.uk

Alistair Mathie
Department of Biological Sciences,
Imperial College London,
Biophysics Section,
Blackett Laboratory,
South Kensington Campus,
London SW7 9AZ,
England
a.mathie@imperial.ac.uk

John A. Peters
Neuroscience Institute Division of Pathology and Neuroscience
University of Dundee
Dundee DD1 9SY,
Scotland
j.a.peters@dundee.ac.uk

Reference:

VANHOUTTE, P.M. *et al.* (1996). *Pharmacol. Rev.* **48**, 1–2.

We would like to thank Pfizer Global Research and Development for their generous support with this publication.

Prof. H.P. Rang *FRS*
Editor-in-Chief
British Journal of Pharmacology

Dr. Adam Smith
Publisher
Biopharma and Biobusiness

Consultants

N. ABUL-HUSN, *New York, U.S.A.*
M. ARAIKSINEN, *Helsinki, Finland*
J.R. ATACK, *Harlow, U.K.*
Y.S. BAKHLE, *London, U.K.*
D.J.K. BALFOUR, *Dundee, U.K.*
C. BARBERIS, *Montpellier, France*
E.L. BARKER, *West Lafayette, U.S.A.*
N.M. BARNES, *Birmingham, U.K.*
R. BATHGATE, *Melbourne, Australia*
P.M. BEART, *Melbourne, Australia*
D. BELELLI, *Dundee, U.K.*
A.J. BENNETT, *Nottingham, U.K.*
N.J.M BIRDSALL, *London, U.K.*
D. BISHOP-BAILEY, *London, U.K.*
N.G. BOWERY, *Verona, Italy*
G. CALO', *Ferrara, Italy*
S.L.F. CHAN, *Nottingham, U.K.*
M.V. CHAO, *New York, U.S.A.*
N. CHING, *Boston, U.S.A.*
J.J. CHUN, *La Jolla, U.S.A.*
J.E. CLARK, *Rahway, U.S.A.*
S.G. CULL-CANDY, *London, U.K.*
F.M. DAUTZENBERG, *Allschwil, Switzerland*
A.P. DAVENPORT, *Cambridge, U.K.*
G. DENT, *Keele, U.K.*
L.A. DEVI, *New York, U.S.A.*
D. DIFRANCESCO, *Milan, Italy*
R.J. DINGLEDINE, *Atlanta, U.S.A*
A.C. DOLPHIN, *London, U.K.*
M. DUBOCOVICH, *Chicago, U.S.A.*
K. EIDNE, *Nedlands, Australia*
G.A. FITZGERALD, *Philadelphia, U.S.A.*
T.M. FONG, *Rahway, U.S.A.*
C.D. FUNK, *Kingston, Canada*
A. GOLDIN, *Irvine, U.S.A.*
A.L. GUNDLACH, *Melbourne, Australia*
M.J. GUNTHORPE, *Harlow, U.K.*
J.R. HAMMOND, *London, Canada*
R.L. HAUGER, *San Diego, U.S.A.*
D.L. HAY, *Auckland, New Zealand*
S.J. HILL, *Nottingham, U.K.*
M. HOLLENBERG, *Calgary, Canada*
S. HOULE, *Calgary, Canada*
D. HOYER, *Basel, Switzerland*
S. ISHII, *Tokyo, Japan*
K.A. JACOBSON, *Bethesda, U.S.A.*
R. JENSEN, *Washington, U.S.A.*
R.L. JONES, *Glasgow, U.K.*
B.I. KANNER, *Jerusalem, Israel*
B.F. KING, *London, U.K.*
J.J. LAMBERT, *Dundee, U.K.*
M. LAZDUNSKI, *Valbonne, France*
R. LEURS, *Amsterdam, The Netherlands*
S.J. LOLAIT, *Bristol, U.K.*
R.J. LUKAS, *Phoenix, U.S.A*
S.C.R. LUMMIS, *Cambridge, U.K.*
J.J. MAGUIRE, *Cambridge, U.K.*
I.L. MARTIN, *Birmingham, U.K.*
A.J. MOORHOUSE, *Sydney, Australia*
C.A. McARDLE, *Bristol, U.K.*
M.C. MICHEL, *Amsterdam, The Netherlands*
V. MITOLO, *Bari, Italy*
P. MONK, *Sheffield, U.K.*
P.K. MOORE, *Singapore*
B. MOUILLAC, *Montpellier, France*
P.M. MURPHY, *Bethesda, U.S.A.*
B. NILIUS, *Leuven, Belgium*
R.A. NORTH, *Manchester, U.K.*
R.W. OLSEN, *Los Angeles, U.S.A.*
M.A. PANARA, *Bari, Italy*
R.G. PERTWEE, *Aberdeen, U.K.*
J. PINTOR, *Madrid, Spain*
D.R. POYNER, *Birmingham, U.K.*
V. RALEVIC, *Nottingham, U.K.*
E. RICHELSON, *Jacksonville, U.S.A.*
G. RUDNICK, *New Haven, U.S.A.*
S.I. SAID, *Stony Brook, U.S.A.*
A. SCHOUSBOE, *Copenhagen, Denmark*
S. SCHULZ, *Philadephia, U.S.A.*
C.N. SERHAN, *Boston, U.S.A.*
P.M. SEXTON, *Melbourne, Australia*
D.R. SIBLEY, *Bethesda, U.S.A.*
G. SINGH, *Cambridge, U.K.*
R. SITSAPESAN, *Bristol, U.K.*
T.G. SMART, *London, U.K.*
D.M. SMITH, *London, U.K.*
P.G. STRANGE, *Reading, U.K.*
R.J. SUMMERS, *Clayton, Australia*
H. SUNDARAM, *Newhouse, U.K.*
A. TOWNSEND-NICHOLSON, *London, U.K.*
R. VANDENBERG, *Sydney, Australia*
S.A. WALDMAN, *Philadelphia, U.S.A.*
S.M. WILSON, *Dundee, U.K.*

:ATION IN STUDYING ENDOCRINE DISRUPTION

receptor, including altered conformation, dimerization, and new interactions with other proteins. Recently, a second estrogen receptor, ER-β, has been cloned (Paech *et al.*, 1997). Studies indicate that the two receptors differ both in their affinities for ligand, and in their response to ligand binding. Fluorescence polarization provides an easy method for the rapid screening of compounds for estrogen receptor binding capacity, either in the search for endocrine disruptors or for new therapeutics for diseases such as breast cancer and osteoporosis.

A human recombinant estrogen receptor (hrER) produced with baculovirus in insect cells, and an intrinsically fluorescent estrogen (FES1, Hwang *et al.*, 1992) with high-affinity to ER-α, were employed in developing a competitive FP assay. The binding affinity of a panel of compounds was measured by their abilities to replace the FES1 in the FES1:hrER complex (Figure 1). The competitors are characterized by their IC_{50}s, that is the concentration of the compound necessary to displace 50% of the fluorescent estrogen from the complex (inflection point of the semi-logarithmic binding curve).

A similar FP competition assay was performed to determine the effects of increasing the amount of estradiol to an FES1:ER-β complex (Bolger *et al.*, 1998). The results using this second estrogen receptor are shown in Figure 2.

The applicability of the competition assays with the two human estrogen receptors can be extended to studies of androgen receptor, glucocorticoid receptor, and thyroid receptor. Indeed, the versatility of the technique has led beyond receptor-ligand studies to applications for antibody-antigen binding, DNA hybridization, DNA-protein binding and proteases, DNases or RNases.

Connie Rickey

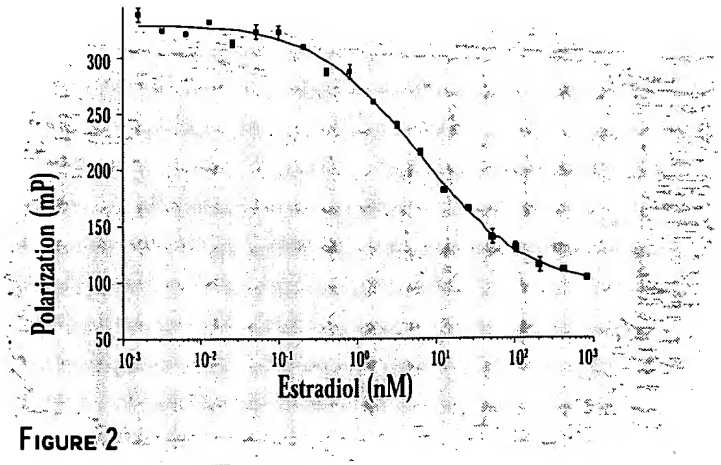

FIGURE 2

Estradiol Competition using ER-β and FES1. *The IC_{50} for estradiol was 6 nM, leading to a calculated K_D for the FES1:hrER-β binding of 0.15 nM. This compares favorably to the K_D observed in direct binding studies with [³H]estradiol and hrER-β (Clark* et al., *1992).*

REFERENCES

Bolger, R., Nestich, S., Wiese, T., Ervin, K., and Checovich, W., *Environ. Health Perspect.*, submitted.

Clark, J.H., Scrader, W.T., and O'Malley, B.W., Mechanisms of action of steroid hormones, in Textbook of Endocrinology, J. Wilson and D.W. Foster, eds, WB Saunders Company, Philadelphia, PA, pages 35 - 90 (1992).

Hwang, K.J., Carlson, K.E., Anstead, G.M., Katzenellenbogen, J.A., *Biochemistry*, **31**, 11536-11545 (1992).

Paech, K., Webb, P., Kuiper, G.J.M., Nilsson, S., Gustafsson, J.A., Kushner, P.J., and Scanlan, T.S., *Science*, **277**, 1508 – 1510 (1997).

EXHIBIT C

New Products

New Product Ordering Information:

DNA and RNA Labeling:

MIR 3100	*Label* IT™ Rhodamine Labeling Kit (for labeling 100 µg nucleic acid)	$299
MIR 3125	*Label* IT™ Rhodamine Labeling Kit-Trial Size (for labeling 25 µg nucleic acid)	$99
MIR 3200	*Label* IT™ Fluorescein Labeling Kit (for labeling 100 µg nucleic acid)	$299
MIR 3225	*Label* IT™ Fluorescein Labeling Kit-Trial Size (for labeling 25 µg nucleic acid)	$99
MIR 3300	*Label* IT™ Digoxin Labeling Kit (for labeling 100 µg nucleic acid)	$299
MIR 3325	*Label* IT™ Digoxin Labeling Kit-Trial Size (for labeling 25 µg nucleic acid)	$99
MIR 3400	*Label* IT™ Biotin Labeling Kit (for labeling 100 µg nucleic acid)	$299
MIR 3425	*Label* IT™ Biotin Labeling Kit-Trial Size (for labeling 25 µg nucleic acid)	$99

PCR and PCR-Related:

TAK 6608	Rat Cytochrome P450 Competitive RT-PCR Set, 20 tests	$165*
TAK 6607	Human β-Actin Competitive PCR Set, 20 reactions	$90*
TAK RR017	Competitive DNA Construction Kit, 10 reactions	$90*
TAK 6125	Competitive RNA Transcription Kit, 10 reactions	$90*
TAK RR024B	One Step RNA PCR Kit (AMV), 50 tests	$300
TAK 6122	RACE Core Set, 5'-Full, 10 reactions	$140*
TAK 6121	RACE Core Set, 3'-Full, 20 reactions	$110*
TAK RR112A	*Salmonella* One-Shot PCR Kit, 48 Assays	$380
TAK E406	LA PCR Buffer II (Mg^{++}-free), 30 ml	$50

*Sale prices apply until March 31, 1998

Apoptosis:

MBL 595	Anti-TRADD Antibody, polyclonal, 100 µg	$210
MBL 596	Anti-RIP Antibody, polyclonal, 100 µg	$210
MBL 597	Anti-TRAF 6 Antibody, polyclonal, 100 µg	$210
MBL M0283	Anti-TRAF1 Antibody, clone 3D4, 100 µg	$210
MBL M0293	Anti-TX (Caspase 4) Antibody, clone 4B9, 100 µg	$210
MBL M0303	Anti-Bag-1 Antibody, clone 4A2, 100 µg	$210
MBL 0313	Anti-TRADD Antibody, monoclonal, 100 µg	$210
MBL 0323	Anti-FLICE (Caspase 8) Antibody, clone 5F7, 100 µg	$210
MBL 0333	Anti-FADD Antibody, clone 1F7, 100 µg	$210
MBL 4700	MEBCYTO Apoptosis Detection Kit, Annexin-V-FITC, 100 tests	$400
MBL 5251	sFas ELISA Kit, 96 Assays	$490
TAK MK600	Apopladder Ex™, 24 tests	$170
TAK6623	Apoprimer Set, (Bcl-2 family), 20 Sets	$250

Cell Biology:

TAK M109, 127	Anti-P-Cadherin Antibodies, monoclonal, 100 µg	$270
TAK M110	Anti-N-Cadherin Antibody, clone NCD-1, 100 µg	$270
TAK M106, 107, 108, 126	Anti-E-Cadherin Antibodies, monoclonal, 100 µg	$270
MBL M0273	Anti-Msx2 Antibody, clone 2E12, 100 µg	$250
MBL 0011A	Anti-GSK3-β Antibody, monoclonal, 100 µg	$150
TAK MK400	Premix WST-1 Cell Proliferation Assay, 2,500 tests	$280
MBL 555	Anti-Phospho-RB (ser 780) Antibody, polyclonal, 100 µg	$250
MBL M0193	Anti-Nucleolin Antibody, clone 4E2, 100 µg	$250
MBL 5235	MESACUP cdc2 Kinase Assay Kit, 96 wells	$295
MBL 5236	HCK Gel for cdc2 Kit, 1 ml	$60

Other:

MBL M0243	Anti-GFP Antibody, clone 4C12, 100 µg	$175
MBL M0263	Anti-Leptin Antibody, clone 3F2, 100 µg	$250
TAK 2310A	RNase Inhibitor, 5,000U	$100
P2466	Human Estrogen Receptor-β (750 pmol)	please inquire
P2445	Anti-PKC 8 Antibody Panel, polyclonal, 250 µl each	$500
P2352	PKC Protein Panel (7 isoforms), 1 µg each	$250
P2213	Anti-ApoE Antibody, polyclonal, 400 µl	$160

Ask about TaKaRa's high-quality, economical restriction and modifying enzymes!

Competitive PCR Kits

RT PCR is a useful tool for detection of low abundance RNAs. However, this method does not allow accurate quantitation, because the amount of PCR product generated does not generally reflect the amount of RNA originally present in the sample. Competitive PCR is one of the approaches to allow accurate PCR quantitation.

TaKaRa has developed three kits to facilitate performance of competitive PCR: the Competitive DNA Construction Kit (for construction of competitive DNA templates), the Competitive RNA Transcription Kit (for generating RNA competitors by in vitro transcription) and the Human Beta-actin Competitive PCR Set (for correction for the amount of intact RNA in the original sample). A Competitive RNA PCR Manual is included in the purchase of any one of these kits.

3'- and 5'-Full RACE Core Sets

TaKaRa's 3'- and 5'- Full RACE Core Sets are designed for efficient generation of full-length cDNAs. The simple 5' Core Set uses inverse PCR to obtain unknown 5' mRNA sequences, and can be used for the cloning of mRNA sequences having cap sites at the 5'-end. The 3' Core Set uses a specially designed oligo-dT-3 sites adaptor primer for efficient reverse transcription from the 3' end of poly A+ mRNAs, and easy cloning. Both kits use AMV RT XL for maximum length of first-strand cDNAs, and are recommended for use with Takara's *Taq, ExTaq™,* and LA *Taq™* Polymerases.

Rat Cytochrome P450 Competitive RT-PCR Primer Set (Part #TAK 6608)

The TaKaRa Rat Cytochrome P450 Competitive RT-PCR Primer Set enables ***quick and selective quantification of rat cytochrome P450 expression levels.*** Results are obtained in only half a day. This kit consists of 9 specific sense and antisense primer mixes for amplifying male rat CYP1A1, 1A2, 2B1/2, 2C11, 2E1, 3A1, 3A2, 4A1, and one universal RNA competitor. This kit also includes a primer mix for amplifying cyclophilin, a housekeeping gene, allowing for the correction of differences in mRNA amounts among samples.

New Products

Label IT™ Nucleic Acid Labeling Kits

Mirus' *Label* IT™ Nucleic Acid Labeling Kits offer efficient one-step non-radioactive labeling of any DNA or RNA with a single reagent. The proprietary *Label* IT method covalently and non-destructively tags original substrate nucleic acids. In contrast to laborious and poorly controlled enzymatic reactions, *Label* IT reactions are simple, non-enzymatic, and result in very reproducible products and yields. In addition, the reactions can be scaled up in a single tube without loss of efficiency. Products can be used in any molecular biology application, FISH, or DNA or RNA transport studies. *Label* IT Kits are available for biotin, digoxin, rhodamine, and fluorescein labeling applications.

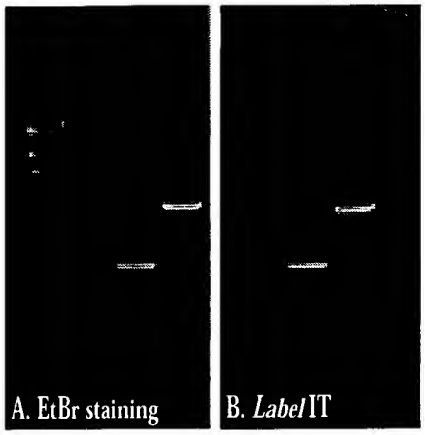

Identical linear ds DNA fragments, either unlabeled (A), or labeld with the Label IT ™ *Rhodamine* Labeling Kit (B), were analyzed by gel electrophoresis and visualized under UV illumination. Gel A was stained with EtBr; the labeled fragments on Gel B were visualized WITHOUT EtBr staining. This demonstrates the high labeling efficiency and non-destructiveness of the Label* IT *method.*

Human Estrogen Receptor-β (Part # P2466)

Available now, human recombinant Estrogen Receptor-β (hrERβ) joins our Estrogen Receptor-α and Vitamin D_3 Receptor in our growing family of human nuclear receptors. Like our other receptors, hrERβ is active and highly purified after baculovirus-mediated expression in insect cells. In equilibrium binding experiments, hrERβ bound tritiated estradiol with a K_D of approximately 0.3nM.

PKC Polyclonal Antibody Panel (Part #P2445)

By popular demand, we now offer our PKC antibodies in a convenient sample-pack format. Each of our antibodies is tested in immunoblots against our human recombinant PKCs. The panel includes 250µl of each of seven antibodies raised against PKC α, βI, βII, γ, ζ, ε, and δ. The antibodies were raised in rabbits.

PKC Protein Panel α, βI, βII, γ, ε, ζ, and δ (Part #P2352)

PanVera also offers our human recombinant PKC isoforms in a sample-pack format. Each isoform is expressed by a baculovirus-mediated system and purified to >95% while retaining activity. The panel contains 1µg each of PKC α, βI, βII, γ, ε, ζ, and δ. The cost of the panel is $250.

ApoE Polyclonal Antibody (Part #P2213)

PanVera's ApoE antibody is sensitive multi-use antibody that recognizes all three of PanVera's human recombinant ApoEs (E2, E3, and E4) and serum ApoE from human, rabbit, rat, mouse, and dog. While ideal of immunoblotting, the antibody has also been tested by use in direct ELISAs and immunoprecipitations. The antibody was raised in goats.

MAbs for Apoptosis Research

PanVera announces the availability of several new monoclonal antibodies for use in apoptosis research. These new antibodies, manufactured by Medical and Biological Laboratories (MBL) of Japan, include: anti-TRAF1, anti-TRAF6, anti-TX (Caspase 4), anti-TRADD, anti-FADD, anti-Bag-1, anti-RIP, and anti-FLICE (Caspase 8). The MBL line also includes antibodies to several other Bcl-family proteins, as well as the MEBCYTO (Annexin V) and MEBSTAIN (TUNEL) Apoptosis Detection Kits. Anti-Fas (mouse and human) apoptosis-inducing and -inhibiting antibodies, and sFas and Fas Ligand ELISA Kits are also available.

Q&A

PanVera offers several ApoE's. What is the difference between ApoE2, E3, and E4?

The three common isoforms of ApoE differ by a single amino acid substitution at two locations. ApoE2 (Cys112, Cys158), ApoE3 (Cys112, Arg158), ApoE4 (Arg112, Arg158). These differences are best visualized by two-dimensional gel electrophoresis - each isoform exhibiting a distinct pI. Each ApoE also exhibits multiple minor isoforms that each share the same amino acid sequence, but probably differ in terminal glycosylations and non-specific deaminations. These differences result in complicated multi-band isoform patterns on two-dimensional gels. All of these bands are considered to be authentic forms of ApoE and are found in any isolation of ApoE from human plasma. Indeed, the pattern of human ApoE secondary modifications by way of baculovirus-mediated expression is more similar to human plasma ApoE modifications than ApoE expressed in bacterial systems.

Do PanVera's ApoE's require special treatment prior to use?

PanVera's human recombinant ApoE's (hrApoE) can be used as they come, but many researchers prefer to reconstitute them in lipid particles. ApoE is an amphipathic protein and will quickly associate with lipid particles. The questions become 'which lipids should I use?', 'what size particles should I make?', and whether to make vessicles or liposomes. The answers depend on your research interest (cardiovascular or neuroscience). ApoE-containing lipoproteins in the CNS and circulation differ in lipid composition and bouyant density.

Do you have to add exogenous NADPH-P450 reductase to PanVera's Cytochrome P450 BACULOSOMES™ in order to get biotransformation activity?

No, not at all. Cytochrome P450 BACULOSOMES are prepared from insect cells infected with recombinant baculovirus containing a cDNA insert for a human P450 *AND* the NADPH-P450 reductase. Therefore, BACULOSOMES contain a complete, functional P450 enzyme system. The activity of these insect microsomes is generally higher than that seen in human liver microsomes (HLMs) and is due not only to the overexpression of the individual P450 enzyme but also to the stoichiometric excess of the NADPH-P450 reductase to the P450 enzyme. The opposite is true of HLMs where the NADPH-P450 reductase to P450 ratio is considerably lower and is believed to be the limiting factor of functional P450 activity. Cytochrome b_5 can also boost activity in those P450 systems known to be affected by its presence (i.e. 3A4).

PANVERA

POSTINGS

Published quarterly by
PanVera Corporation
545 Science Drive
Madison, WI 53711
USA
1-800-791-1400
E-mail: info@panvera.com
www.panvera.com
Phone 608-233-5050
Fax 608-233-3007

Winter 1998

Postings

Published quarterly by PanVera Corporation, Madison, Wisconsin

"The important thing in science is not so much to obtain new facts as to discover new ways of thinking about them."

Sir William Bragg

Welcome

Welcome to the first issue of PanVera's new newsletter – *Postings*. You will find scientific information that you can use in your everyday work as well as reports on new discoveries and products from PanVera. We hope *Postings* will be a publication you look forward to receiving. If you have questions, comments or contributions, please contact us at (608) 233-5050 or e-mail at info@panvera.com.

*Trans*IT® Transfection Reagents: High Efficiency and Low Toxicity

James E. Hagstrom, Lisa J. Hanson and Jon A. Wolff
Mirus Corporation

Introduction

The delivery of exogenous genes into cells in culture has become the primary means by which researchers study both gene product function and promoter and enhancer function. In many cases a reporter gene such as luciferase or beta-galactosidase is used to quantitatively assay gene expression. For these type of studies the efficiency of gene transfer into the recipient cells is usually the most critical parameter. In recent years cationic lipid mediated transfection has become the method of choice because of it's ease of use, reproducibility and relative efficiency. While the current generation of cationic lipids are able to transfect a variety cell lines efficiently, there are still problems such as cellular toxicity and transfection cost. Mirus *Trans*IT LT (Low Toxicity) reagents have been designed to minimize cellular toxicity while transfecting at the highest level of efficiency.

Principle

The mechanism by which cationic liposomes deliver DNA into the nucleus of cells is still poorly understood. It is now believed that the majority of cationic liposomes deliver DNA through the plasma membrane via an endocytosis pathway but exactly how the DNA escapes these endosomes and travels to the nucleus is unclear. In many cases the endosomal acidification that occurs during endosomal maturation triggers the DNA release and specific inhibitors that block this acidification process also inhibit transfection (Budker, *et al.*, 1996; Zhou and Huang, 1994).

Mirus *Trans*IT 100 cationic lipid transfection reagent is a pH sensitive reagent in that endosomal acidification is required for transfection. This reagent consists of a 1:1 mixture of the cationic lipid DPIm (Budker, *et al.*, 1996) and DOPE. Mirus *Trans*IT LT-1 and LT-2 reagents consist of a mixture of a 3:1 wt:wt ratio of protein and cationic polyamines. The LT-1 and LT-2 reagents are also believed to use the endosomal pathway for cellular entry but cause much lower cellular toxicity following transfection than conventional cationic liposomes. The mechanistic reasons for this are still unclear.

Results

High transfection efficiency:

To compare the transfection efficiency of the *Trans*IT LT-1 or LT-2 reagents with a leading competitor's cationic liposome reagents, we transfected a variety of common cell lines with the luciferase reporter plasmid pCILuc. After transfection the cells were incubated for 40 hours before being harvested and assayed for luciferase activity. The results indicate that either *Trans*IT LT-1 or LT-2 was more efficient than reagents from a leading competitor in

(continued on next page)

Figure 1

Comparative Transfection Efficiencies

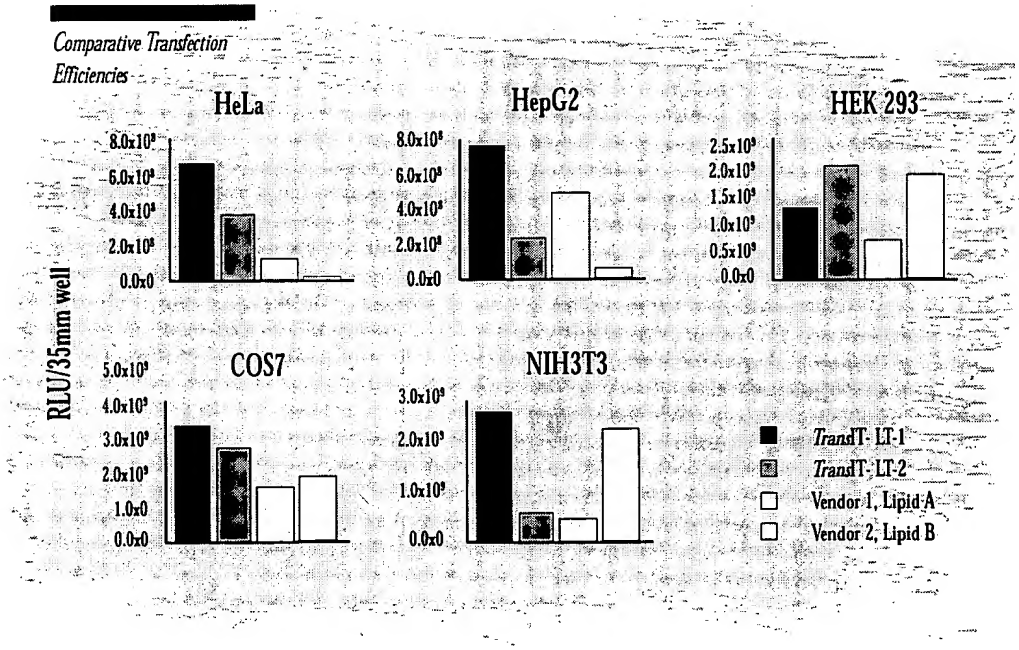

TransIT™ Transfection Reagents

(continued from front page)

5 common cell lines (HeLa, NIH3T3, COS-7, HEK293, HepG2) (see Figure 1). In four out of five cell lines *Trans*IT LT-1 was the better reagent based on luciferase activity but in one cell line (293) the *Trans*IT LT-2 had higher activity.

Low Cellular Toxicity:

Second generation cationic lipids (i.e. DOSPA/PE) are more efficient at transfecting a variety of cell lines than previous formulations (DOTMA/PE) but in most cases there has been a tradeoff with increased cellular toxicity (see Figure 2). Direct cellular toxicity is an obvious detriment to transfection but there are more subtle reasons for not wanting to alter the state of the cell with your transfection agent. Many transfection experiments are designed to study how the introduction of an exogenous gene affects the function of a naive cell so any effect from the transfection agent would be highly undesirable. While many insults are not lethal to a cell directly, they can activate a cascade of intracellular second messengers that can stimulate the expression of both endogenous cellular genes and exogenously introduced genes. Thus even sub-lethal insults are undesirable. In contrast to the current second generation cationic liposomes, *Trans*IT LT reagents are formulated with a combination of a non-toxic cellular protein and a small amount of a novel polyamine. This much reduced amount of polyamine, as compared to cationic lipid content in the current liposome formulations, is one possibility for the much reduced toxicity.

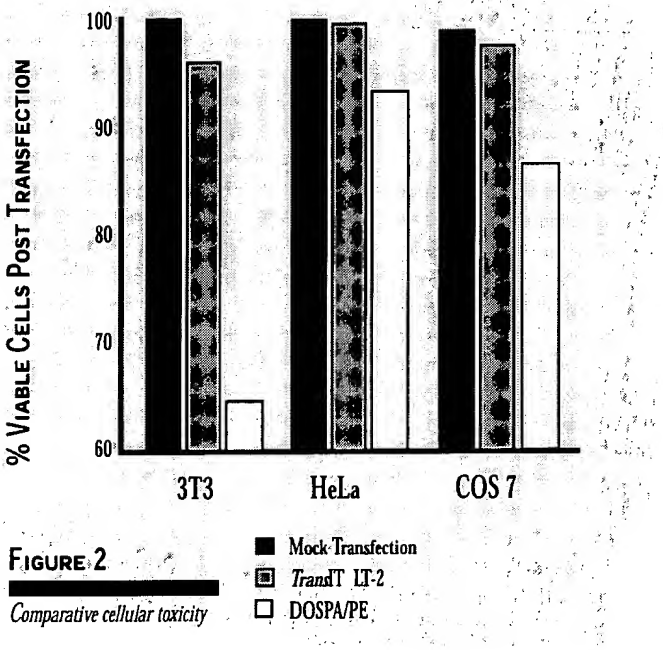

Figure 2
Comparative cellular toxicity

Materials and Methods
Complex Formation

Transfection competent complexes were prepared according to manufacturer's recommendations. Briefly, complexes were formed by mixing several different ratios of transfection reagent (*Trans*IT LT or cationic lipid) to plasmid DNA in 150 ul of Opti-MEM (Gibco BRL, Life Technologies, Inc., Grand Island, NY). Two micrograms of plasmid DNA (pCILuc) were used for each 35 mm well. pCILuc was constructed by removing the luciferase cassette (*Nhe*I-Luc-*Eco*R1) from pSPLuc+ (Promega, Madison WI) and ligating it into *Nhe-Eco*R1 digested pCI expression vector (Promega, Madison WI).

Transfections and Reporter Gene Assays

NIH3T3 (mouse fibroblast), HeLa (human cervical carcinoma), 293 (human embryonic kidney), HepG2 (human hepatoma) and COS7 cells (monkey kidney, SV40 T antigen transformed) were grown in Dulbecco's modified Eagle's medium (DMEM) supplemented with 10% fetal calf serum and split one day prior to transfection. At transfection, 50-60% confluent cultures were washed once with 2 ml Opti-MEM followed by addition of 2 ml of Opti-MEM to each 35mm well. Pre-formed complexes (2 micrograms pDNA/well in 150 µl Opti-MEM) were then added dropwise to each well and dishes were placed at 37°C in 5% CO_2. After a 4 hour incubation, complexes were removed and 2 ml of fresh growth medium was added.

Cells were harvested after 40-48 hours as previously described (Wolff, *et al.*, 1992; Wolff, *et al.*, 1992) and assayed for luciferase expression.

Measurements of Cellular Toxicity

NIH 3T3 cells were grown on glass coverslips in 35 mm wells prior to staining with the fluorescent dye propidium iodide (Molecular Probes). Ten micrograms of propidium iodide (1 mg/ml) was added to each well and the cultures were incubated at 37° C for another 15 min. The plates were removed and washed two times with PBS. The coverslips were then removed and mounted on glass slides using Gel/Mount (Biomeda Corp., Foster City, California). Using a Leitz Orthoplan fluorescent microscope, a total of five fields were randomly selected and the numbers of cells with nuclear red staining (propidium iodide) were noted. Nuclear staining with propidium iodide indicates a cell with a compromised plasma membrane and hence a non-viable cell. For each transfection reagent, the staining pattern in a total of over 300 cells (in the five fields) was noted.

James E. Hagstrom

References

Budker, V., Gurevich, V., Hagstrom, J.E., Bortzov, F., and Wolff, J.A., *Nature Biotechnol.*, **14**, 760-764 (1996).

Wolff, J.A., Ludtke, J.J., Acsadi, G., Williams, P., and Jani, A., *Molec. Genet.*, **1**, 363-369 (1992).

Wolff, J.A., Malone, R.W., Williams, P., Chong, W., Acsadi, G., Jani, A., and Felgner, P.L., *Science*, **247**, 1465-1468 (1990).

Zhou, X., and Huang, L., *Biochim. Biophys. Acta*, **1184**, 195-203 (1994).

PanVera POSTINGS

Post IT

Overloaded with Recombinant Protein Work.... Why Not Pharm It Out?

PanVera Corporation, the *Discovery Outsourcing Company*, provides customized assistance to pharmaceutical and diagnostic companies in recombinant protein expression/purification and assay development for HTS screening and process development. Our customers continually come back to us with more challenging projects because we save them time and money and free up their internal resources for more exploratory research. Our capabilities include

- Subcloning, construct and vector optimization
- Optimization and scale-up of expression
- Development and scale-up of purification methods
- Biochemical characterization and assay development

Our discovery outsourcing services let you expand existing development and production capacity *without an increase in staff and/or facilities.*

We view your success with recombinant proteins as our own. Call to learn how we can help: 800-791-1400

Excitation and Emission Maxima for Several Common Fluorophores

Fluorophore	Excitation Wavelengths, nm	Emission Wavelengths, nm
Dansyl Chloride	263, 368	578
1,5 IAEDANS	337	520
Pyrene	345	378
Fluorescamine	370	488
Hydroxycoumarin	385	445
Lucifer Yellow	425	540
NBD (4-chloro-7-nitrobenzo-2-oxa-1,3-diazole)	470	554
DTAF (Dichlorotriazinylamino-fluorescein dihydrochloride)	489	513
Fluorescein	492	520
TMR (Tetramethylrhodamine)	543	566
Cy3™	552	568
Lissamine Rhodamine B	570	590
Texas Red® (Sulforhodamine 101 acid chloride)	587	620
Cy5™	650	667

Cy is a trademark of Amersham International PLC. Texas Red is a registered trademark of Molecular Probes, Inc.

PANVERA

PanVera Corporation
545 Science Drive
Madison, WI 53711 USA
Phone 1-800-791-1400 or 608-233-9450
Fax 608-233-3007

TaKaRa RNA PCR SPECIALS!

Offers valid from Jan 1, 1998 to March 31, 1998.

Product Number	Description	Quantity	Standard Price	Sale Price!
TAK 6121	RACE Core Set, 3'-Full	20 reactions	$220	$110
TAK 6122	RACE Core Set, 5'-Full	10 reactions	$280	$140
TAK R019A	RNA PCR Kit, Version 2.1	50 reactions	$300	$250
TAK 6607	Human β-Actin Competitive PCR Set	20 reactions	$180	$90
TAK 6125	Competitive RNA Transcription Kit	10 transcriptions	$150	$90
TAK RR017	Competitive DNA Construction Kit	10 constructions	$150	$90
TAK RR023A	*Bca*BEST™ RNA PCR Kit	50 reactions	$270	$185
TAK 6608	Rat Cytochrome P450 Competitive RT-PCR Set	20 reactions	$250	$165
TAK RR012A	RNA LA PCR Kit, Verson 1.1	50 reactions	$500	$325

WHAT IS FP?

Fluorescence Polarization (FP) is an increasingly popular technique that can be used to observe molecular interactions at equilibrium, in a homogeneous format. The binding of a fluorescent molecule to another molecule can be quantified by its speed of rotation and FP is a measure of that speed or tumbling rate.

When plane-polarized light is used to excite a solution of fluorescent molecules, only those molecules whose excitation dipoles are in the same plane will become excited. If the molecules remain stationary during the period of excitation (4 nanoseconds for fluorescein) the emitted light will remain highly polarized. If the molecules tumble during the period of excitation the emitted light will be random and therefore depolarized.

FP is a measure of the tumbling rate of the fluorescent molecule and is directly related to its molecular volume. Therefore, an increase in the volume of a fluorescent molecule (due to receptor-ligand binding, antibody-antigen binding, DNA hybridization, or DNA-protein binding) or a decrease in molecular volume (due to dissociation or enzymatic degradation) can be measured directly by FP.

The observed FP value (see figure below) is a weighted average of the FP values of the individual bound and free molecules and is therefore a direct measure of the fraction bound. The data are manipulated in the same way as a conventional radioligand-binding assay. Polarization is plotted against receptor concentration to obtain the familiar saturation-binding isotherm.

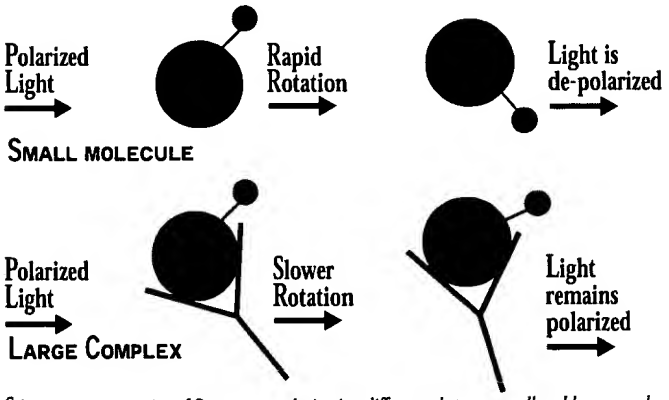

Schematic representation of fluorescence polarization differences between small and large complexes.

REFERENCES

GENERAL REVIEW

Perrin, F., *J. Phys. Radium*, 7, 390-401 (1926).

Checovich, W.J., Bolger, R.E., and Burke, T., Fluorescence Polarization – a new tool for cell and molecular biology, *Nature*, 375, 254 – 256 (1995).

Lundblad, J.R., Laurance, M., and Goodman, R.H., Fluorescence Polarization Analysis of Protein-DNA and Protein-Protein Interactions, *Molec. Endocrinol.*, 10, 607 – 612 (1996).

Fluorescence Polarization Applications Guide, 1998, PanVera Corporation.

PROTEASE ASSAYS

Bolger, R., Checovich, W., A New Protease Activity Assay Using Fluorescence Polarization, *BioTechniques*, 17, 585 – 589 (1994).

Levine, L.M., Michener, M.L., Toth, M.V., and Holwerda, B.C., Measurement of Specific Protease Activity Utilizing Fluorescence Polarization, *Anal. Biochem.*, 247, 83 – 88 (1997).

RNASE ASSAYS

Bolger, R., and Thompson, D., A quantitative RNase assay using fluorescence polarization, *Amer. Biotechnol. Lab.*, 12, 113 - 116 (1994).

USE OF FLUORESCENCE POL

Connie Rickey and Randy Bolger
PanVera Corporation

There has been increasing interest lately in characterizing environmental compounds for their effects as estrogenic agonists or antagonists. The classic estrogen receptor (ER-α) is a 66 kDa transcription factor that regulates expression of genes involved in tissue growth and differentiation. The binding of agonists activates ER-α, resulting in several changes in the

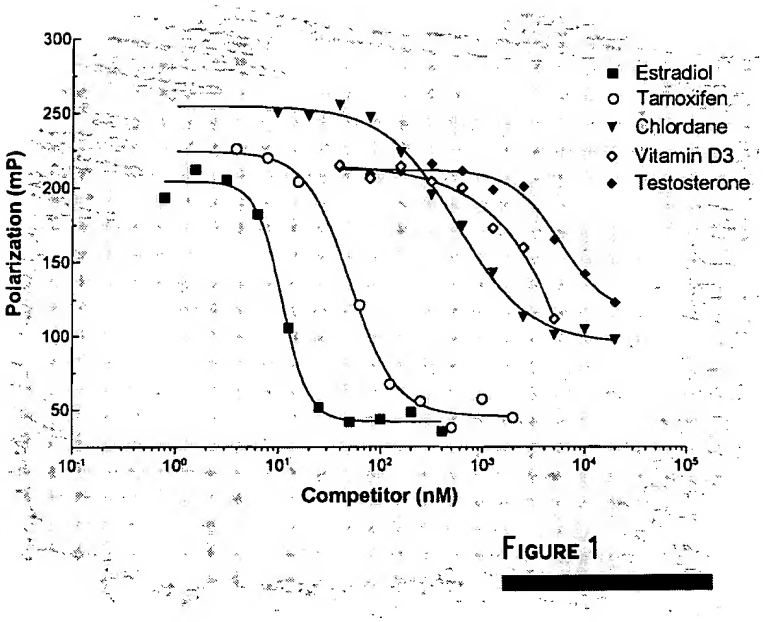

FIGURE 1

Fluorescent Estrogen Competition Assay. *Several compounds were investigated for their ability to compete with FES1 binding to purified ER. Competitors were serially diluted in buffer. FES1 and ER were then added to each tube to a final concentration of 1 nM and 5 nM, respectively. Polarization readings were taken with the Beacon® 2000 FP instrument (PanVera Corporation). Estradiol is the most potent competitor (IC_{50} = 8 nM), followed by tamoxifen (IC_{50} = 50 nM). Vitamin D3 and testosterone were both poor competitors, with IC_{50} values > 5 mM.*

Journal of Neurochemistry
Raven Press, Ltd., New York

Binding of Cholecystokinin-8 (CCK-8) Peptide Derivatives to CCK_A and CCK_B Receptors

Ute Schäfer, Rainer Harhammer, Monika Boomgaarden, Reinhard Sohr, Tilmann Ott, Peter Henklein, and *Heinrich Repke

*Institute of Pharmacology and Toxicology Medical Faculty (Charité), Humboldt University at Berlin, Berlin, F.R.G.; and *Department of Molecular Biology, Massachusetts General Hospital, Boston, Massachusetts, U.S.A.*

Abstract: The structural requirements for the selective binding of cholecystokinin-8 (CCK-8)-related peptides to peripheral (CCK_A) receptors are not sufficiently understood. In this study, the interaction of a series of newly shortened analogues of CCK-8 with both receptor subtypes was analyzed by displacement studies using [^{3}H]-CCK-8 and ^{125}I-Bolton–Hunter (BH)–CCK-8 as radioligands. The pentapeptide derivative of CCK-8, succinyl-Tyr (SO_3H)-Met-Gly-Trp-Met-phenethylamide, was found to bind selectively with high affinity to the CCK_A receptor. The replacement of Met^{28} and/or Met^{31} by norleucine and of L-Trp^{30} by its D-analogue had no significant effect on the binding properties of the peptide. Further C-terminal shortening resulted in a drastic loss of affinity and selectivity of the CCK receptor binding. **Key Words:** Cholecystokinin—Cholecystokinin-8 derivatives—Cholecystokinin receptors—Radioligand binding—Rat pancreas—Guinea pig cortex.
J. Neurochem. **62,** 1426–1431 (1994).

Cholecystokinin (CCK) is a 33-amino-acid intestinal peptide that plays an important physiological role in the control of pancreatic secretion and gallbladder and gut contraction (Jorpes and Mutt, 1973). Different fragments of the peptide have been described and exert hormonal effects in addition to those of the full-length CCK molecule (Larsson and Rehfeld, 1979). CCK-8 [H-Asp-Tyr(SO_3H)-Met-Gly-Trp-Met-Asp-Phe-NH_2], the C-terminal octapeptide of CCK, mimicks most of the peripheral effects of the full-length CCK molecule and also occurs in many areas of the brain (Crawley, 1985).

Today two different types of CCK receptors can be distinguished. CCK_A receptors are primarily found in peripheral organs and occur in particularly high concentrations in the pancreas. However, CCK_A receptors could also be detected in some areas of rat brain by autoradiography and radioligand binding studies (Hill and Woodruff, 1990; Hill et al., 1990). The predominant CCK receptor in the brain is the CCK_B receptor (Moran et al., 1986). Both receptor subtypes can be distinguished by different binding properties of CCK analogues (Innes and Snyder, 1980; Saito et al., 1980). For example, desulfated CCK-8, CCK-4 (the C-terminal tetrapeptide of CCK-8), and gastrin bind with low affinity to the CCK_A receptor but are high-affinity ligands of the CCK_B receptor subtype (Knight et al., 1984; Lin and Miller, 1985).

Different classes of CCK_A receptor antagonists, such as derivatives of cyclic nucleotides (Barlas et al., 1982), amino acid and glutamic acid derivatives (Hahne et al., 1981), and C-terminal CCK fragments (Spanarkel et al., 1983), have been described. However, most of these compounds are of limited use because of low affinity and/or selectivity of binding to CCK receptor subtypes. The most potent and selective CCK_A receptor antagonist described so far is the benzodiazepine derivative MK-329 (Chang and Lotti, 1986; Evans et al., 1986).

This study describes the interaction of various newly synthesized CCK-8-related peptide fragments with CCK_A receptors of rat pancreas and CCK_B receptors of guinea pig cortex to provide new information regarding the structural requirements for the selective interaction of CCK peptides with CCK_A receptors.

MATERIALS AND METHODS

Drugs and chemicals

CCK-8 and the derivatives were synthesized as previously described (Henklein et al., 1989; Boomgaarden et al., 1992). All compounds were purified by preparative HPLC, and their purity was checked by analytical HPLC (>95%). (For analytical data for compounds 18–21, see Table 2.) [^{3}H]-CCK-8 (specific activity, 76 Ci/mmol) and monoiodo ^{125}I-Bolton–Hunter (^{125}I-BH) reagent (specific activity, 2,000 Ci/mmol) were purchased from the Radiochemical Centre (Amersham, U.K.). The conjugation of ^{125}I-BH reagent to CCK-8 was carried out as previously described (Lin and Miller, 1985). MK-329 was obtained from Merck, Sharp & Dohme Research Laboratories (West Point, PA, U.S.A.).

Tissue preparation

The pancreas was prepared from male Wistar rats (weight 200–250 g) as described by Chang et al. (1984). The homoge-

Received May 11, 1993; revised manuscript received August 31, 1993; accepted August 31, 1993.

Address correspondence and reprint requests to Dr. U. Schäfer at Institute of Pharmacology and Toxicology Medical Faculty (Charité), Humboldt University, 10098 Berlin, PF 140, F.R.G.

Abbreviations used: BH, Bolton–Hunter; CCK, cholecystokinin; PEA, phenethylamide; Suc, succinyl.

nization was carried out in 10 volumes of 50 m*M* Tris-HCl (pH 7.4) with a glass–Teflon homogenizer. The homogenate was centrifuged at 12,000 *g* at 4°C for 30 min and suspended in 20 m*M* HEPES buffer (pH 6.5) containing 5 m*M* KCl, 5 m*M* $MgCl_2$, 1 m*M* EDTA, 360 m*M* NaCl, 0.01% bovine serum albumin, and 0.25 mg/ml of bacitracin.

Cerebral cortex from a guinea pig was dissected on ice, homogenized in 20 volumes of 50 m*M* Tris-HCl buffer (pH 7.4), and centrifuged as described above. The pellet was rehomogenized in HEPES (20 m*M*, pH 7.4) incubation buffer containing 5 m*M* KCl, 5 m*M* $MgCl_2$, 1 m*M* EGTA, 120 m*M* NaCl, 0.2% bovine serum albumin, and 0.062 mg/ml of bacitracin.

Binding assay

[^{3}H]CCK-8 binding. The binding assay mixture consisted of 50 μl of [^{3}H]CCK-8 (2 n*M* final concentration, except in saturation experiments), 100 μl of buffer with or without inhibitor, and 200 μl of homogenate of rat pancreas (1 mg of protein per filter). The samples were incubated for 90 min at 2°C (various intervals were used in kinetic experiments). Bound radioligand was rapidly separated from free radioligand by filtration through Whatman glass fiber filters (GF/A) using a 24-well cell harvester (Brandel, Gaithersburg, MD, U.S.A.). The filters were quickly rinsed three times each with 5 ml of ice-cold HEPES buffer (without bacitracin) in <8 s. Radioactivity was counted in a liquid scintillation spectrometer (LKB Wallac; counter efficiency >45%). The nonspecific binding, defined as binding of [^{3}H]CCK-8 in the presence of 1 μ*M* CCK-8, was 10–15%.

^{125}I-BH-CCK-8 binding. The binding assay mixture consisted of 100 μl of HEPES buffer containing ^{125}I-BH-CCK-8 (0.2 n*M* final concentration, except in saturation experiments), 100 μl of HEPES buffer with or without inhibitor, and 50 μl of homogenate of guinea pig cortex (1.5 mg of protein per filter). The samples were incubated for 90 min at room temperature. Bound radioligand was rapidly separated from free radioligand by filtration through Scatron filter mats (catalogue no. 11731) using a 12-well Scatron Combi cell harvester. The filters were washed with ~15 ml of ice-cold HEPES buffer (without bacitracin). The bound radioactivity was measured using a γ-counter (Wallac model 1275 Minigamma). The nonspecific binding was determined in the presence of 5 μ*M* CCK-8 (~30%). The protein concentration was determined according to the method of Lowry et al. (1951).

Data analysis

Data were analyzed by a modified version (H. Schnittler, H. Repke, and C. Liebmann, unpublished data) of the computer program developed by Tobler and Engel (1983). This method is based on a numeric approach. The computation of affinity spectra requires neither model selection (one or more binding sites) nor initial parameter estimation. The program of Tobler and Engel (1983) uses the untransformed binding data and computes the number of binding sites and their affinity and proportion and provides a statistical evaluation of the data (affinity spectra) that is based on χ^2 statistics.

RESULTS

Characterization of [^{3}H]CCK-8 and ^{125}I-BH-CCK-8 binding

The binding kinetics of [^{3}H]CCK-8 to CCK_A receptors of rat pancreas were performed at 2°C, because partial radioligand degradation was observed at room temperature and 37°C (data not shown). The equilibrium dissociation constant (K_D) was 5.8 n*M* for [^{3}H]-CCK-8 binding to CCK_A receptors of rat pancreas and 3.8 n*M* for ^{125}I-BH-CCK-8 binding to CCK_B receptors of guinea pig cortex (values were calculated from association and dissociation constants). Saturation studies analyzed with increasing concentrations of [^{3}H]CCK-8 (2.3–5,000 p*M*) for 90 min at 2°C or ^{125}I-BH-CCK-8 (1.8–3,660 p*M*) for 90 min at room temperature revealed a single binding site for both radioligands. A K_D of 4.7 n*M* and a B_{max} of 110 fmol/mg of protein were determined for specific [^{3}H]CCK-8 binding to pancreatic receptors. For specific ^{125}I-BH-CCK-8 binding to cortical receptors, a K_D of 1.5 n*M* and a B_{max} of 3.0 fmol/mg of protein were calculated.

For further characterization of the [^{3}H]CCK-8 binding, CCK-8 (compound 1) and the CCK_A receptor antagonist MK-329 were analyzed in displacement studies (Table 1). The C-terminal octapeptide, CCK-8, was a potent inhibitor of both [^{3}H]CCK-8 binding to rat pancreas and ^{125}I-BH-CCK-8 binding to guinea pig cerebral cortex. MK-329 was found to have a high affinity toward the [^{3}H]CCK-8 binding to rat pancreatic homogenate and a considerably lower affinity to the CCK_B receptor of guinea pig cerebral cortex. Both inhibitors interacted with a single binding site in both tissues (Fig. 1).

Binding of newly synthesized CCK-8-related peptides to CCK_A and CCK_B receptors

The binding of a series of CCK-8-related peptide analogues to CCK_A receptors of rat pancreas and to CCK_B receptors of guinea pig cortex (Table 1) was studied by displacement experiments. Homogenates of either tissue were incubated with radiolabeled CCK-8 in the presence of increasing concentrations of the unlabeled peptide derivatives. The half-maximal inhibitory concentration was calculated by a computer-assisted procedure as previously described (Tobler and Engel, 1983). Using this method for the analysis of the slope of the displacement curves, a single binding site was found throughout all experiments, indicating that neither of the tested compounds interacts with different receptor conformations or subtypes (Fig. 1). Some of the synthesized C-terminal and N-terminal derivatives of the CCK-8 sequence resulted in dramatically impaired affinity toward the CCK_A receptor (compounds 3, 5, 7, and 8; Table 1). Further shortening of the C-terminal sequence (compounds 9–17; Table 1) resulted in up to a 15-fold reduction in the affinity of binding to the CCK_A receptor as compared with the original CCK-8 molecule. The reduction of the binding affinity to the CCK_B receptor was ~200-fold, indicating that the C-terminal phenylalanine of the CCK-27–33 sequence contributes substantially to the interaction energy

TABLE 1. *Binding of shortened CCK-8 derivatives to CCK_A receptors of rat pancreas and CCK_B receptors of guinea pig cortex*

Inhibitor	K_i (n*M*) Pancreas (A)	Cortex (B)	$K_{i,A}/K_{i,B}$
1. Asp- Tyr(SO_3H)-Met-Gly- Trp-Met-Asp-Phe-NH_2	6.3 ± 0.5	7.9 ± 0.7	0.79
2. Suc- Tyr(SO_3H)-Met-Gly- Trp-Met-Asp-Phe-NH_2	6.3 ± 0.3	1.1 ± 0.1	5.70
3. PBA- Tyr(SO_3H)-Met-Gly- Trp-Met-Asp-Phe-NH_2	3,981 ± 210		
4. ADC- Tyr(SO_3H)-Met-Gly- Trp-Met-Asp-Phe-NH_2	7.9 ± 0.6		
5. Asp- Tyr(SO_3H)-Met-Gly- Trp-Met-Asp-Phe-PEA	1,585 ± 95		
6. Suc- Tyr(SO_3H)-Met-Gly- Trp-Met-Asp-Phe-PEA	50 ± 8.1		
7. Suc- Tyr(SO_3H)-Met-Gly- Trp-Met-Asp-Phe-BUT	631 ± 13		
8. Suc- Tyr(SO_3H)-Met-Gly- Trp-Met-Asp-Phe-ADA	1,995 ± 120		
9. Suc- Tyr(SO_3H)-Met-Gly- Trp-Met-Asp-PEA	79 ± 10	316 ± 34	0.26
10. Suc- Tyr(SO_3H)-Met-Gly- Trp-Met-Asp-DBA	1,259 ± 110		
11. Suc- Tyr(SO_3H)-Met-Gly- Trp-Met-Asp-DPA	128 ± 12		
12. Suc- Tyr(SO_3H)-Met-Gly- Trp-Met-Asp-DDA	251 ± 15		
13. Suc- Tyr(SO_3H)-Met-Gly- Trp-Met-Asp-ADA	794 ± 35		
14. Suc- Tyr(SO_3H)-Nle-Gly- Trp-Met-Glu-PEA	158 ± 10		
15. Suc- Tyr(SO_3H)-Met-Gly-D-Trp-Nle-Asp-PEA	36 ± 7.5	18,423 ± 1,435	0.003
16. Suc- Tyr(SO_3H)-Nle-Gly-D-Trp-Nle-Asp-PEA	50 ± 4.6	15,848 ± 1,224	0.003
17. Suc- Tyr(SO_3H)-Met-Gly-D-Trp-Met-Asp-PEA	130 ± 10	21,535 ± 3,443	0.006
18. Suc- Tyr(SO_3H)-Met-Gly- Trp-Met-PEA	13 ± 1.4	19,952 ± 2,845	0.0006
19. Suc- Tyr(SO_3H)-Met-Gly-D-Trp-Met-PEA	25 ± 2.5	16,300 ± 970	0.002
20. Suc- Tyr(SO_3H)-Met-Gly-D-Trp-Nle-PEA	10 ± 0.9	50,118 ± 4,590	0.0002
21. Suc- Tyr(SO_3H)-Nle-Gly-D-Trp-Nle-PEA	16 ± 1.2		
22. Suc- Tyr(SO_3H)-Met-Gly- Trp-PEA	1,280 ± 100	16,325 ± 1,090	0.08
23. Boc- Tyr(SO_3H)-Met-Gly- PEA	103,300 ± 5,000		
24. MK-329	2.5 ± 0.3	39,810 ± 3,570	0.00005

The half-maximal inhibition (IC_{50}) of radiolabeled CCK-8 was computed as previously described (Tobler and Engel, 1983). The inhibition constant (K_i) values were calculated from IC_{50} values according to the approximation of Cheng and Prusoff (1973). Data are mean ± SEM values from three to eight experiments. ADA, 1-adamantylamide; ADC, 1-adamantylcarbonyl; Boc, *tert*-butylcarbonyl; BUT, butylamide; DBA, dibutylamide; DDA, dodecylamide; DPA, dipentylamide; PBA, 4-phenylbutyric acid.

with the pharmacophore of this receptor type. Derivatives of the C-terminal amino acid of the CCK-27–32 sequence resulted in a further decrease of the binding affinity toward the CCK_A receptor (compounds 10–13; Table 1). The exchange of either one or both of the methionines within the CCK-27–32 fragment (compounds 14–16; Table 1) had no effect on the affinity of the corresponding peptide derivatives on the binding to the CCK_A receptor as compared with the original hexapeptide sequence. In contrast, the binding affinity to the CCK_B receptor decreased by nearly two orders of magnitude. The same effect was observed after replacement of L-tryptophan in position 30 by the corresponding D-amino acid (compound 17; Table 1). The compounds 14–17 can therefore be considered to be selective ligands of the CCK_A receptor.

A further increase in the selectivity of the interaction with CCK_A receptors was achieved by removing

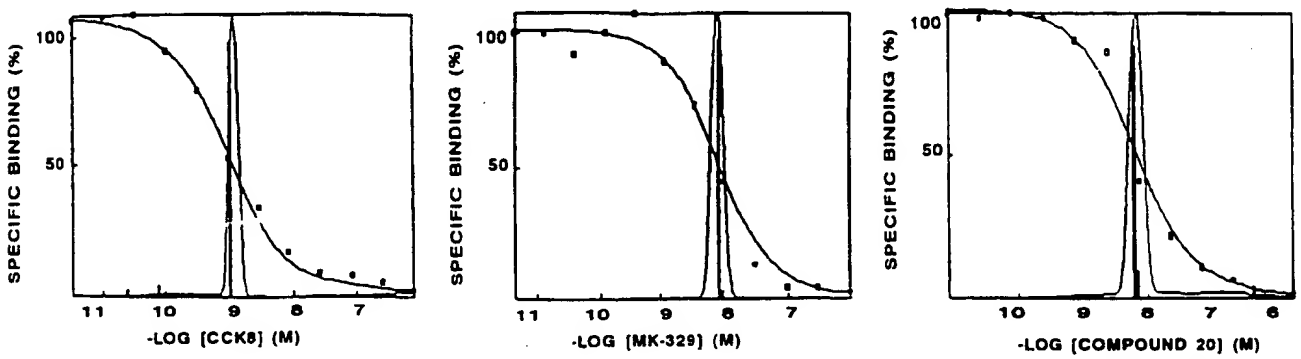

FIG. 1. Inhibition of specific [^{3}H]CCK-8 binding to CCK_A receptors of rat pancreas: CCK-8, MK-329, and compound 20 (see Table 1). The results are expressed relative to the specific radioligand binding in the absence of inhibitor. Computer-assisted data analysis (Tobler and Engel, 1983) shows one binding site. The position of the affinity bar represents the inhibition constant (K_i); the surrounding affinity spectrum is an expression of the goodness of fit based on χ^2 statistics.

TABLE 2. *Analytical data of synthesized CCK-27–31 pentapeptide analogues*

Compound	$(\alpha)_D$ (c = 0.5; DMF)	mp (°C)	t_R (HPLC) (min)	Analysis (CHN)
18. Suc-Tyr(SO_3H)-Met-Gly- Trp-Met PEA	149–152	−20.7	7.25	$C_{43}H_{55}N_7O_{12}S_3$
19. Suc-Tyr(SO_3H)-Met-Gly-D-Trp-Met-PEA	135–138	−16.9	7.38	$C_{43}H_{55}N_7O_{12}S_3$
20. Suc-Tyr(SO_3H)-Met-Gly-D-Trp-Nle-PEA	150–153	−9.2	9.43	$C_{44}H_{57}N_7O_{12}S_2$
21. Suc-Tyr(SO_3H)-Nle-Gly-D-Trp-Nle-PEA	153–154	NM	10.57	$C_{45}H_{59}N_7O_{12}S$

Analytical HPLC was performed on a Hewlett-Packard chromatograph using Hypersil ODS (particle size, 5 μm; 100 × 21 mm). The mobile phase was water with 0.1% trifluoracetic acid, 0.01% triethylamine (compound A), acetonitrile (compound B) at a flow rate of 0.5 ml/min and a linear gradient from 20% B to 60% B over 20 min. Optical rotations were measured on a Polamat A apparatus (Carl Zeiss Jena). Elemental analyses were within 0.4% of all calculated values. NM, not measured; DMF, dimethylformamide.

the C-terminal aspartic acid from the remaining CCK hexapeptide fragment (compound 18; Tables 1 and 2). This peptide fragment was found to bind with an affinity toward the CCK_A receptor that is similar to that of the complete CCK-8 molecule. The replacement of methionine by norleucine and of L-tryptophan by D-tryptophan (compounds 19–21; Tables 1 and 2 and Fig. 1) did not affect the binding of the pentapeptide to either the CCK_A or the CCK_B receptor. This result is in line with the effect of the same substitutions on the binding properties of the hexapeptide fragments (compounds 14, 16, and 17; Table 1).

C-Terminal shortening of the CCK-27–31 sequence resulted in a drastic loss of the binding affinity toward the CCK_A receptor (compounds 22 and 23; Table 1). It can therefore be concluded that the minimal selective CCK_A receptor recognition sequence is contained within the CCK-27–31 fragment.

DISCUSSION

The interaction of a series of newly synthesized CCK-8-related peptides with CCK_A receptors of rat pancreas and CCK_B receptors of guinea pig cerebral cortex was analyzed by displacement studies using the radioligands [^{3}H]CCK-8 and ^{125}I-BH-CCK-8. Peptide derivatives that bind selectively with high affinity to the CCK_A receptor could be obtained by amino acid substitutions within the succinyl (Suc)-CCK-27–31-phenethylamide (PEA) pentapeptide sequence.

To determine whether the radioligand binding assays reflect the selective binding of [^{3}H]CCK-8 to CCK_A receptors of rat pancreas and of ^{125}I-BH-CCK-8 to CCK_B receptors of guinea pig cerebral cortex, a series of methodologic experiments was performed. Data analysis of association and dissociation kinetics as well as Tobler plot analysis revealed a single and high-affinity binding site for both radioligands. Moreover, the potent and selective CCK_A receptor antagonist MK-329 (Chang and Lotti, 1986; Evans et al., 1986) was found to bind with high affinity to pancreatic homogenate, indicating that [^{3}H]CCK-8 interacts mainly with CCK_A receptors in this tissue.

It has previously been reported that N-terminal aspartic acid of CCK-8 (amino acids 26–33 of the complete CCK sequence) is not essential for the binding to either the CCK_A or the CCK_B receptor (Gardner et al., 1984). The N-terminal aspartic acid can be replaced by the Suc group without significant effects on biological activity (Yanaihara et al., 1985). This is in line with the findings of this study demonstrating that the replacement of the N-terminal aspartic acid of CCK-8 by both Suc and 1-adamantylcarbonyl groups had little effect on the affinity of the peptide derivatives toward the CCK_A receptor. Moreover, the results also confirm the high affinity of these Suc-CCK heptapeptides for the CCK_B receptor of guinea pig cortex. In contrast, the replacement of the N-terminal aspartic acid by 4-phenylbutyric acid resulted in a drastic loss of the ability of the peptide to bind to CCK_A receptors with high affinity. It can be concluded that there is presumably no high-affinity recognition between the N-terminal aspartic acid of the peptide and the receptor binding site.

Modifications of the C-terminal sequence of CCK-8 have also been described so far. In this study, it is demonstrated that the exchange of the amide group of the C-terminal phenylalanine with various substituted hydrophobic amide residues resulted in a substantial loss of the binding affinity of the resulting hepta- and hexapeptide derivatives (compounds 5, 7, and 8). This may be due either to steric hindrance of the peptide binding to the receptor pharmacophore or to an effect of these derivatives on the folding of the peptide in solution. The latter possibility has to be taken into account, as the loss of binding affinity could be nearly completely reversed by the simultaneous replacement of the N-terminal aspartic acid by the Suc group and the conjugation of the C-terminal phenylalanine with the β-PEA residue (compound 6). This is in line with previous studies (Martinez et al., 1986, 1988; Lignon et al., 1987; Galas et al., 1988) that have shown that even the C-terminal phenylalanine amide group of CCK-8 can be replaced by substituents of similar structure such as β-PEA or β-phenethyl ester residues without a significant effect on the binding affinity of the resulting peptide derivative toward CCK_A receptors. Moreover, Tilley et al. (1992) have demonstrated that various other hydrophobic

residues can replace the C-terminal phenylalanine of CCK-8 without a major impact on the binding affinity. We have extended the analysis of the structural requirement for substituents in this position and found that the substitution of the C-terminal phenylalanine amide requires either residues that resemble to the original amino acid in this position such as the PEA group or medium-size alkyl residues such as the dipentylamide group. Substitutions with molecules of larger or smaller size resulted in peptide derivatives with significantly impaired affinity toward the CCK_A receptor. The results presented in this study demonstrate that the aromatic ring in the position of the C-terminal phenylalanine could be replaced by an aliphatic residue of the appropriate size such as dipentylamide without a major effect on the affinity of the molecule toward the CCK_A receptor.

However, most of the C-terminal hexapeptides bind with similar high affinity to both the CCK_A and CCK_B receptor (Lignon et al., 1987; Martinez et al., 1988; Tilley et al., 1992). The most potent peptide derivative described to date is the *tert*-butyloxycarbonyl-CCK-27–32-phenethylester, which is characterized by the replacement of L-tryptophan by the D-stereoisomer and methionine in position 31 by norleucine (Lignon et al., 1987). It was the goal of this study to create peptide derivatives that bind selectively to CCK_A receptors. Recently, Boomgaarden et al. (1990, 1992) demonstrated that further C-terminal shortening of the CCK-8 sequence produced the highly active compound Suc-Tyr(SO_3H)-Met-Gly-Trp-Met-PEA, which is a selective antagonist on CCK_A receptors. Indeed, Suc-CCK-27–31-PEA analogues, which are characterized by the replacement of either one or both methionines by norleucine and/or by the replacement of L-tryptophan by the D-stereoisomer, were found to be high-affinity ligands of the CCK_A receptor. The compound with the highest receptor selectivity within this series was compound 20 [Suc-Tyr(SO_3H)-Met-Gly-D-Trp-Nle-PEA]. It is noteworthy that different combinations of the substitutions indicated above resulted in compounds with very similar receptor binding properties. Further C-terminal shortening of the above pentapeptide (compounds 22 and 23) resulted in drastic loss of binding affinity toward the CCK_A receptor, indicating that the described derivatives of Suc-CCK-27–31-PEA represent the optimal structure for the selective recognition of CCK_A receptors.

Acknowledgment: The authors wish to thank Astrid Arnswald and Waltraud Fischer for expert technical assistance and Rainer Halatsch for synthesizing ^{125}I-BH-CCK-8.

REFERENCES

Barlas N., Jensen R. T., Beinfeld M. C., and Gardner J. D. (1982) Cyclic nucleotide antagonists of cholecystokinin: structural requirements for interaction with the cholecystokinin receptor. *Am. J. Physiol.* **242**, G161–G167.

Boomgaarden M., Henklein P., Sohr R., Morgenstern R., Martinez J., and Ott T. (1990) Synthese und biologische Aktivität neuer Cholecystokinin (CCK)-Analoga mit vorrangig CCK_A rezeptorantagonistischer Wirkung. *Pharmazie* **45**, 377–378.

Boomgaarden M., Henklein P., Morgenstern R., Sohr R., Ott T., and Martinez J. (1992) Synthesis and biological activity of CCK peptides with antagonistic activity for CCK-A-receptor. *Eur. J. Med. Chem.* **27**, 955–959.

Chang R. S. L. and Lotti V. J. (1986) Biochemical and pharmacological characterization of a new extremely potent and selective nonpeptide cholecystokinin antagonist. *Proc. Natl. Acad. Sci. USA* **83**, 4923–4926.

Chang R. S. L., Lotti V. J., and Chen T. B. (1984) Inactivation of cholecystokinin receptors in rat pancreatic membranes by sulfhydryl reagents: protection by guanosine 5′-triphosphate (GTP) but not N^2O^2-dibutyryl guanosine 3′,5′-cyclic monophosphate (dibutyryl cGMP). *Biochem. Pharmacol.* **33**, 2334–2335.

Cheng J.-C. and Prusoff W. H. (1973) Relationship between the inhibition constant (K_i) and the concentration of inhibitor which causes 50 percent inhibition (IC_{50}) of an enzymatic reaction. *Biochem. Pharmacol.* **22**, 3099–3108.

Crawley J. N. (1985) Comparative distribution of cholecystokinin and other neuropeptides: why is this neuropeptide different from all other neuropeptides. *Ann. NY Acad. Sci.* **448**, 1–8.

Evans B. E., Bock M. G., Rittle K. E., Di Pardo R. M., Whitter W. L., Veber D. F., Anderson P. S., and Freidinger R. M. (1986) Design of potent, orally effective, nonpeptidal antagonists of the peptide hormone cholecystokinin. *Proc. Natl. Acad. Sci. USA* **83**, 4918–4922.

Galas M. C., Lignon M. F., Rodriguez M., Mendre C., Fulcrand P., Laur J., and Martinez J. (1988) Structure–activity relationship studies on cholecystokinin: analogues with partial agonist activity. *Am. J. Physiol.* **254**, G176–G182.

Gardner J. D., Knight M., Sutliff V. E., Tamminga C. A., and Jensen R. T. (1984) Derivatives of CCK-(26–32) as cholecystokinin receptor antagonists in guinea pig pancreatic acini. *Am. J. Physiol.* **246**, G292–G295.

Hahne W. F., Jensen R. T., Lemp G. F., and Gardner J. D. (1981) Proglumide and benzotript: members of a different class of cholecystokinin receptor antagonists. *Proc. Natl. Acad. Sci. USA* **78**, 6304–6308.

Henklein P., Boomgarden M., Penke B., Morgenstern R., and Ott T. (1989) Synthesis and biological activity of new CCK antagonists. *Pharmazie* **44**, 61.

Hill D. R. and Woodruff G. N. (1990) Differentiation of central cholecystokinin receptor binding sites using the non-peptide antagonists MK-329 and L-365,260. *Brain Res.* **526**, 276–283.

Hill D. R., Shaw T. M., Graham W., and Woodruff G. N. (1990) Autoradiographical detection of cholecystokinin-A receptors in primate brain using [^{125}I]Bolton Hunter–CCK-8 and [^{3}H]-MK-329. *J. Neurosci.* **10**, 1070–1081.

Innes R. B. and Snyder S. (1980) Distinct cholecystokinin receptors in brain and pancreas. *Proc. Natl. Acad. Sci. USA* **77**, 6917–6921.

Jorpes J. E. and Mutt V. (1973) *Secretin, Cholecystokinin, Pancreozymin and Gastrin*, pp. 1–144. Springer-Verlag, Berlin.

Knight M., Tamminga C. A., Steardo L., Bock M. E., Barone P., and Chase T. N. (1984) Cholecystokinin-octapeptide fragments: binding to brain cholecystokinin receptors. *Eur. J. Pharmacol.* **105**, 49–55.

Larsson L.-I. and Rehfeld J. F. (1979) Localization and molecular heterogeneity of cholecystokinin in the central and peripheral nervous system. *Brain Res.* **165**, 201–218.

Lignon M.-F., Galas M.-C., Rodriguez M., Laur J., Aumelas A., and Martinez J. (1987) A synthetic peptide derivative that is a cholecystokinin receptor antagonist. *J. Biol. Chem.* **262**, 7226–7231.

Lin C. W. and Miller T. (1985) Characterization of cholecystokinin receptor sites in guinea pig cortical membranes using [^{125}I]-Bolton Hunter-cholecystokinin octapeptide. *J. Pharmacol. Exp. Ther.* **232**, 775–780.

Lowry O. H., Rosebrough N. J., Farr A. L., and Randall R. J. (1951)

Protein measurement with the Folin phenol reagent. *J. Biol. Chem.* **193,** 265–275.

Martinez J., Rodriguez M., Bali J. P., and Laur J. (1986) Phenylethylamide derivatives of the C-terminal tetrapeptide of gastrin. *Int. J. Pept. Protein Res.* **28,** 529–535.

Martinez J., Rodriguez M., Lignon M.-F., and Galas M.-C. (1988) Selective cholecystokinin receptor antagonists, in *Cholecystokinin Antagonists* (Wang R. Y. and Schönfeld R., eds), pp. 29–51. Alan R. Liss, New York.

Moran T. H., Robinson P. H., Goldrich M. S., and McHugh P. R. (1986) Two brain cholecystokinin receptors: implications for behavioral actions. *Brain Res.* **362,** 175–179.

Saito A., Sankaran H., Goldine I. D., and Williams J. A. (1980) Cholecystokinin receptors in the brain: characterization and distribution. *Science* **208,** 1155–1156.

Spanarkel M., Martinez J., Briet C., Jensen R. T., and Gardner J. D. (1983) Cholecystokinin-27–32-amide. *J. Biol. Chem.* **258,** 6746–6749.

Tilley J. W., Danho W., Shiuey S.-J., Kulesha I., Sarabu R., Swistok J., Makofske R., Olson G. L., Chiang E., Rusiecki V. K., Wagner R., Michalewsky J., Triscari J., Nelson D., Chiruzzo F. Y., and Weatherford S. (1992) Structure activity of C-terminal modified analogs of Ac-CCK-7. *Int. J. Pept. Protein Res.* **39,** 322–336.

Tobler H. J. and Engel G. (1883) Affinity spectra: a novel way for the evaluation of equilibrium binding experiments. *Naunyn Schmiedebergs Arch. Pharmacol.* **322,** 183–192.

Yanaihara C., Sugiura N., Kashimoto K., Kondo M., Kawamura M., Naruse S., Yasni A. and Yanaihara N. (1985) Dissociation of pancreozymin (PZ) activity from cholecystokinin (CCK) activity by N^{α}-carboxyacyl CCK-7 and CCK-8 analogues with a substituted glycine. *Biomed. Res.* **6,** 111–115.

Binding Assays: Receptor Binding Assays, GTP Binding Assays and Immunoassays

Any type of binding assay can be run on your VICTOR³ using PerkinElmer's exclusive DELFIA technology. DELFIA technology is a heterogeneous time-resolved fluorometric assay method in which an enhancement step assures high sensitivity and a wide response range for immunoassays and other types of binding assays. This robust, easy-to-use platform provides an excellent alternative to either ELISA or RIA, eliminating assay steps or the use of radioactivity.

Your VICTOR³ and our sensitive DELFIA technology also provide a powerful non-isotopic alternative for demanding receptor ligand binding assays. With detection limits as low as 1 attomole of Europium-labeled compound per well, DELFIA technology lets you use recombinant and endogenous receptor membranes, even those with low expression levels.

DELFIA Ligands

PerkinElmer offers a range of Europium-labeled ligands for setting up DELFIA receptor-ligand binding assays. You can design your assays using our SignalScreen® or Membrane Target System (MTS) cloned receptors and AcroWell™ Filter Plates. For easy assay set-up, use DELFIA L*R Wash Solution and DELFIA L*R Binding Buffer. After incubation, unbound ligand is removed by filtration then signal is enhanced using DELFIA Enhancement Solution.

You can also set up your assays using adherent cell lines on cell culture plates, such as PerkinElmer's Isoplate™ microplates, or as solid phase assays using streptavidin-coated microplates and biotinylated wheat germ agglutinin. However you choose to set up your receptor ligand binding assays, VICTOR³ lets you count them quickly and reliably.

Products

Bombesin, Eu-labeled, 150 pmol
AD0227

Bombesin, Eu-labeled, 600 pmol
AD0228

EGF, Eu-labeled, 350 pmol
AD0217

EGF, Eu-labeled, 1,400 pmol
AD0218

Galanin, Eu-labeled, 200 pmol
AD0215

Galanin, Eu-labeled, 850 pmol
AD0216

Interleukin-2, Eu-labeled, 650 pmol
CR401-650

Interleukin-4, Eu-labeled, 60 pmol
CR403-060

Interleukin-5, Eu-labeled, 400 pmol
CR402-400

Interleukin-8, Eu-labeled, 160 pmol
AD0213

Interleukin-8, Eu-labeled, 700 pmol
AD0214

Motilin, Eu-labeled, 60 pmol
AD0208

Motilin, Eu-labeled, 240 pmol
AD0209

NDP-αMSH, Eu-labeled, 200 pmol
AD0225

NDP-αMSH, Eu-labeled, 800 pmol
AD0226

Neurotensin, Eu-labeled, 200 pmol
AD0219

Neurotensin, Eu-labeled, 750 pmol
AD0220

Neurokinin A, Eu-labeled, 300 pmol
AD0221

Neurokinin A, Eu-labeled, 1,200 pmol
AD0222

Substance P, Eu-labeled, 200 pmol
AD0223

Substance P, Eu-labeled, 800 pmol
AD0224

TNFα, Eu-labeled, 600 pmol
CR400-600

DELFIA Enhancement Solution, 50 mL
1244-104

DELFIA Enhancement Solution, 250 mL
1244-105

DELFIA Enhancement Solution, 1,000 mL
4001-001

DELFIA L*R Wash Solution Concentrate (25X), 250 mL
CR135-250

DELFIA L*R Binding Buffer Concentrate, 250 mL
CR134-250

AcroWell Filter Plate, 10 plates
P5020

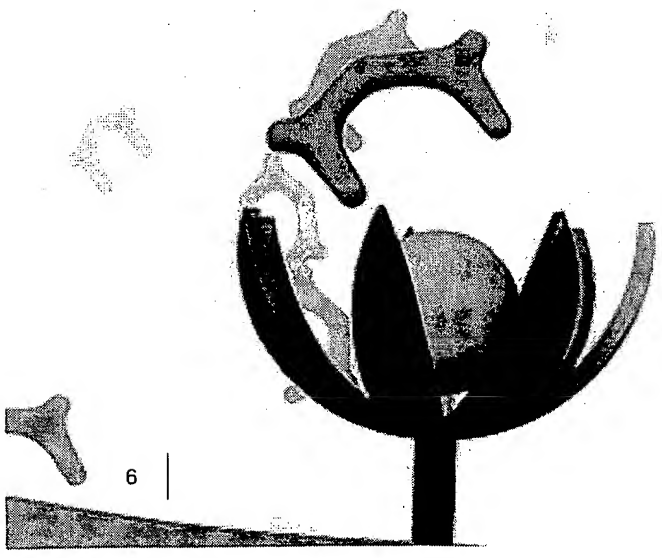

EXHIBIT E

DELFIA Neurotensin Receptor Binding Kit

This kit contains all the necessary components to perform a neurotensin receptor binding filtration assay, including DELFIA Eu-labeled neurotensin, unlabeled human neurotensin, human neurotensin NT1 receptor, DELFIA L*R Binding Buffer (10X), DELFIA L*R Wash Solution (25X), Enhancement Solution, and AcroWell Filter Plates (2 x 96-well plates).

DELFIA Eu-labeled neurotensin and the ligand specific receptor are incubated on an AcroWell Filter Plate after which the unbound labeled ligand is removed by filtration. Europium is dissociated from the bound ligand by using DELFIA Enhancement Solution.

Products

DELFIA Neurotensin Receptor Binding Kit, 2 x 96 wells
AD0257

DELFIA GTP Binding Kit

VICTOR³ works well for other signal transduction assays too. Our DELFIA GTP Binding Kit lets you optimize the conditions for screening novel agonists against a GPCR of interest. The kit is based on GDP-GTP exchange on G-protein subunits followed by GPCR activation by agonists. All GPCR membrane preparations need different conditions for GTP binding. The kit provides the instructions and tools for optimizing these conditions.

Products

DELFIA GTP Binding Kit, 10 x 96 wells
AD167

DELFIA GTP Reagents, GTP-Eu (1.65 nmol) and GTPγS (275 nmol) for 960 wells
AD0260

DELFIA GTP Reagents, Components for GTP Binding Buffer and Wash Solution for 960 wells
AD0261

DELFIA cAMP Assay Kit

Our sensitive, nonisotopic immunoassay for the quantitative determination of cAMP is designed for cell culture, plasma, or urine samples. The assay can be run on the VICTOR³ with three different protocols, basic, simple, and high sensitivity. The basic and high sensitivity protocols involve adherent cells. In the simple protocol, the determination is from cells in suspension, and all the steps from sample preparation to measurement of fluorescence are preformed on a DELFIA microplate. The sensitivity of the 384-well kit is at least 0.1 ng/well (0.28 pmol/well) when using the simple assay protocol. When using the high sensitivity protocol the sensitivity is at least 0.1 pg/well (0.28 fmol/well).

DELFIA cAMP Assay Kit, 10 x 384 wells
4004-0010

DELFIA cAMP Assay Kit, 2 x 384 wells
CR92-102

DELFIA cAMP Assay Kit, 10 x 96 wells
4003-0010

DELFIA cAMP Assay Kit, 2 x 96 wells
CR89-102

DELFIA Reagents

Running RIAs or ELISAs? Convert your existing assays to DELFIA and realize the added safety, performance, and convenience of DELFIA technology.

Visit our DELFIA literature page at http://las.perkinelmer.com/content/featured/DELFIAliterature.html and download our Applications Guides for details about reagents and procedures for converting your assays.

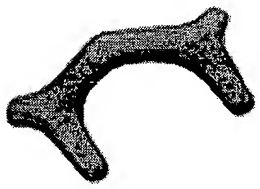

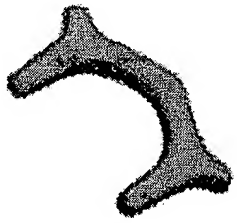

Kinetic Assays

TruPoint Beta-Secretase Assay Kit[384]

Products

TruPoint Beta-Secretase Assay Kit[384], 1536 assays
AD0258

TruPoint Beta-Secretase Assay Kit[384], 15360 assays
AD0259

β-secretase (also referred to as BACE1, BACE, Asp2 protease, Memapsin-2 or β-site APP cleaving enzyme) is an aspartic protease that has been identified as a key enzyme in deposition of β-amyloid (Aβ) found in plaques involved in Alzheimer's disease.

The TruPoint Beta-Secretase Assay Kit[384] measures BACE1 enzyme activity. Based on proprietary SignalClimb technology, TruPoint Beta-Secretase reagents can be used in sensitive, robust and homogeneous time-resolved fluorescence β-secretase assays. Assay conditions have been optimized for compound screening and in the detection of BACE1 enzyme even in biological materials.

The homogeneous TruPoint platform utilizes the SignalClimb technology based on the close proximity of two labels. One is a fluorescent lanthanide chelate and the other is a suitable organic quencher molecule. In this assay, the TruPoint BACE1 substrate is a ten amino acids long peptide, with a fluorescent europium (Eu) chelate coupled to one end and a quencher of europium fluorescence (QSY® 7) to the other end via lysine. If the sample contains BACE1 activity, the europium chelate and the quencher will be separated as the substrate is cleaved. The Eu-signal increases and it can be measured on a VICTOR³ with the TRF-option.

Complementary Microplates

For complementary microplates please refer to our Microplate Overview Guide (007097_01) which can be found at www.perkinelmer.com/microplates.

Get the most out of your VICTOR³!

Why not run all the applications you can on your versatile VICTOR³? For more details about any of these assays or assistance with other applications, call us at 1-800-762-4000 or visit our website at www.perkinelmer.com.

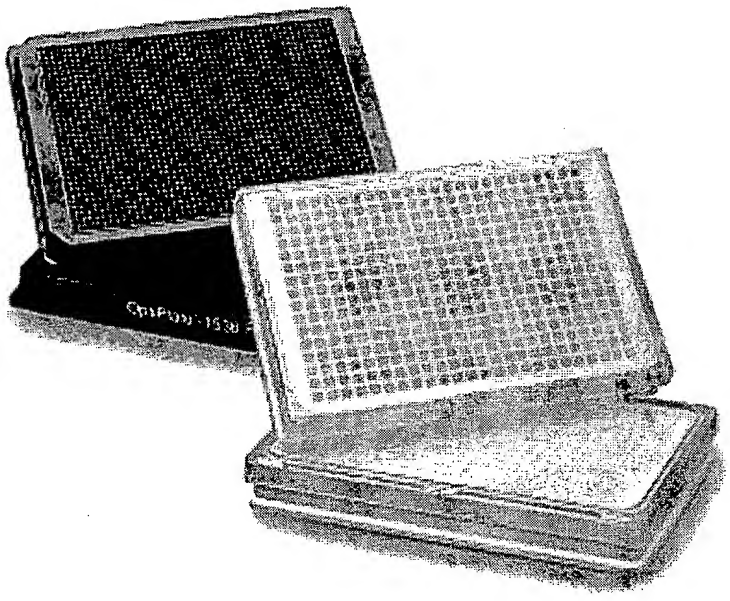

PerkinElmer Life and
Analytical Sciences
710 Bridgeport Avenue
Shelton, CT 06484-4794 USA
Phone: (800) 762-4000 or
(+1) 203-925-4602
www.perkinelmer.com

PerkinElmer®
precisely.

For a complete listing of our global offices, visit www.perkinelmer.com/lasoffices

007221_01 Printed in USA

The VICTOR^3 Multilabel Plate Reader

All you need for any application

is sitting right on your bench.

PerkinElmer®
precisely.

Get the Most Out of Your VICTOR$^{3}_{TM}$!

You purchased a Wallac VICTOR$^{3}_{TM}$ Multilabel Plate Reader from PerkinElmer because it's the most flexible, versatile and reliable plate reader available today. But are you really getting the most from it?

You may be using your VICTOR^{3} for just a few applications. But did you know it can handle a **wide range of applications** in many assay formats? You may be able to **do much more** with your VICTOR^{3} than you are now!

PerkinElmer can help you **use your VICTOR^{3} to its full potential** with our assay systems and reagents optimized for use on your VICTOR^{3} reader.

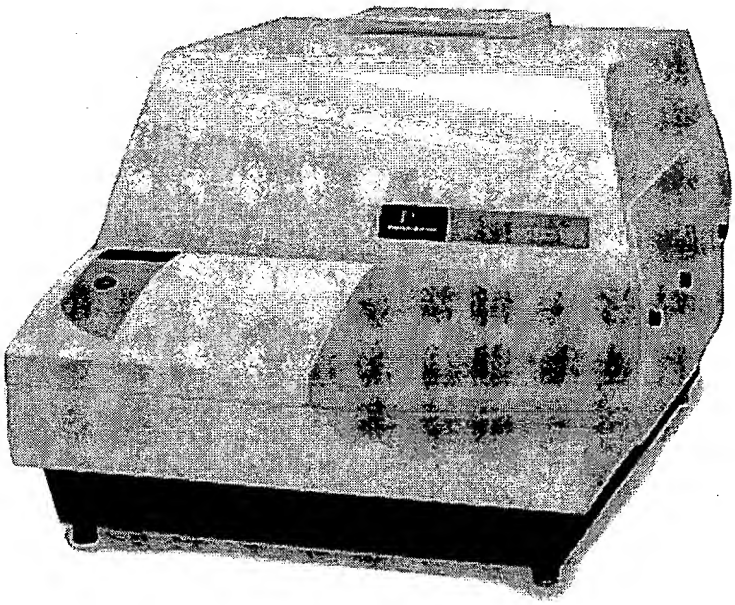

Versatile VICTOR^3 handles all your

Cell-based Assays: Cell Proliferation and Cytotoxicity Assays

For those whose interests lie in cellular processes, PerkinElmer offers fully optimized luminescence and time-resolved fluorescence assay systems for the quantitative evaluation of cell proliferation and cytotoxicity. These systems provide a choice of assay conditions and throughput sure to suit your needs. The broad range of PerkinElmer cell-based assays your VICTOR^3 can perform are described below.

ATPlite™ Luminescence ATP Detection Assay System

Here is a two-step mix-and-measure assay that provides high sensitivity and excellent linearity for ATP monitoring in cultured mammalian cells. The simplicity and speed of this assay make it an excellent tool to assess the cytocidal, cytostatic and proliferative effects of a wide range of drugs, biological response modifiers and biological compounds.

The system's long Constant-Quanta™ glow signal produces a long-lived glow type signal with a half-life of greater than five hours. You can run several microplates at the same time and more samples in a single experiment.

Products

ATP**lite** Assay Kit*, 300 points
6016943

ATP**lite** Assay Kit*, 1,000 points
6016941

* Assay points per kit based on 96-well microplates.

ATPlite 1step™ Luminescence ATP Detection Assay System

Need an easy high throughput solution? The one-step addition, short equilibrium time and high light output of the ATPlite 1step assay make it ideal for continuous process systems such as in-line systems.

This sensitive assay is simple and reproducible requiring only one reagent addition step and no separation steps. The luminescent signal is read within 30 minutes after adding the reagent, but the high light output allows a short counting time on the VICTOR^3, increasing the number of samples you can process.

Products

ATP**lite 1step** Assay Kit, 10 mL
6016736

ATP**lite 1step** Assay Kit, 100 mL
6016731

ATP**lite 1step** Assay Kit, 1,000 mL
6016739

research applications.

DELFIA Cell Proliferation Assay Kit

Products
DELFIA Cell Proliferation Kit,
10 x 96 wells
AD0200

This popular assay is a time-resolved fluoroimmunoassay using PerkinElmer's exclusive DELFIA® technology, a heterogeneous time-resolved fluorometric assay (TRF) method. The assay is based on the incorporation of BrdU into newly synthesized DNA strands of proliferating cells cultured in microplates. (Incorporated BrdU is detected using a europium-labeled monoclonal antibody.)

The fluorescence measured is proportional to the DNA synthesis in the cell population of each well. You can run this assay on your VICTOR³ for the direct assessment of cell numbers, and also assay for cytotoxic effects as an endpoint measurement. The assay can be used with adherent cells as well as with cells in suspension. It is an ideal, non-isotopic substitute for ^{3}H-Thymidine uptake assays in combination with your VICTOR³.

DELFIA Cytotoxicity Reagent Pack

Products
DELFIA EuTDA Cytotoxicity Reagents
Pack, 10 x 96 wells
AD0116

Cell death can be analyzed on your VICTOR³ using DELFIA technology to study cell membrane lysis, providing sensitivity similar to ^{51}Cr-release assays. The DELFIA Cytotoxicity Reagent Pack contains all of the reagents necessary to perform the assay with your VICTOR³. Reagents are also sold separately.

The method is based on loading target cells with an acetoxymethyl ester of a fluorescence enhancing ligand (BATDA). The ligand penetrates the cell membrane quickly where ester bonds are hydrolyzed to form a hydrophilic ligand (TDA) which no longer passes through the membrane. After cytolysis the ligand is released and introduced to a Europium solution. The Europium and the ligand form a highly fluorescent and stable chelate (EuTDA). The measured signal correlates directly with the amount of cells that have been lysed. There is no physical or chemical treatment of the cell membrane and the ligand is quickly accumulated in the target cells. This facilitates excellent recovery of the labeled cells.

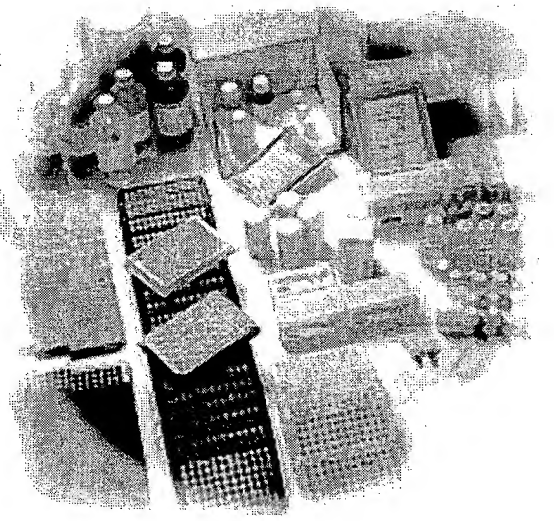

TruPoint™ Caspase Kits

Cysteine proteases called caspases play a central role in the initiation of the apoptotic cascades. Through our TruPoint™ platform, PerkinElmer offers several caspase assay systems that allow you to evaluate apoptotic cell death using your VICTOR³ reader.

Our homogeneous TruPoint platform is a unique combination of two technologies. One is time-resolved fluorometry (TRF) for signal detection and measurement. The other is our SignalClimb™ technology, which provides high quenching efficiency and purity of quenched peptides. The result is an increased signal for extra sensitive caspase assays with high Z' factors.

TruPoint systems are available for caspase-3, caspase-6, and caspase-8. Each of these assays effectively measures caspase activity from apoptotic cell lysates or purified enzymes.

Products

TruPoint Caspase-3 Assay Kit, 2 x 384 wells
AD0125

TruPoint Caspase-3 Assay Kit, 50 x 384 wells
AD0126

TruPoint Caspase-6 Assay Kit, 2 x 384 wells
AD0146

TruPoint Caspase-6 Assay Kit, 50 x 384 wells
AD0147

TruPoint Caspase-8 Assay Kit, 2 x 384 wells
AD0148

TruPoint Caspase-8 Assay Kit, 50 x 384 wells
AD0149

TruPoint Caspase-3 Assay Kit^{96}, 3 x 96 wells
AD0245

TruPoint Caspase-3 Assay Kit^{96} w/o plates, 288 assays
AD0246

Selection Guide: Cell Proliferation and Cytotoxicity Assays on VICTOR³

Assay Requirements	Recommended Product
Continuous process systems Simple and fast ATP readings	ATPlite 1step Assay System
High sensitivity ATP readings	ATPlite Assay System
Sensitive and reliable measurement of DNA synthesis Eliminate use of radioactivity	DELFIA Cell Proliferation Kit
Sensitive and reliable measurement of cell lysis Eliminate use of radioactivity	DELFIA Cytotoxicity Assay Reagents
Sensitive and reliable evaluation of apoptotic cell death	TruPoint Caspase-3 Kit

Reporter Gene Assays

Our easy-to-use "**lite**" family of luminescence assay systems extends to gene reporter assays too. These homogeneous mix-and-measure assays simplify the testing process and provide high sensitivity over a wide dynamic range. Plus, they provide the flexibility suited to your lab's processing and throughput needs. Both systems can be formatted in 96, 384 or 1536 wells, all easily handled by your VICTOR³.

britelite™ Luminescence Reporter Gene Assay System

britelite™ is an ultra-high sensitivity reporter gene assay that provides an extremely strong signal for remarkably accurate and thorough firefly luciferase readings. The assay detects and clearly highlights a wide range of luciferase content levels making it ideal for continuous process systems.

Note: Assay volume is dependent on microplate density. Bulk quantity assay kits are also available. Please contact your PerkinElmer representative for additional details.

Products

britelite Assay Kit, 10 mL
6016976

britelite Assay Kit, 100 mL
6016971

britelite Assay Kit, 1,000 mL
6016979

steadylite HTS™ Luminescence Reporter Gene Assay System

steadylite HTS™ is a long-lived high-sensitivity reporter gene assay specifically designed for large-batched processing. steadylite HTS delivers a signal half-life of 4 to 5 hours, allowing time to run additional tests while waiting to measure processed plates.

Note: Assay volume is dependent on microplate density. Bulk quantity assay kits are also available. Please contact your PerkinElmer representative for additional details.

Products

steadylite HTS Assay Kit, 10 mL
6016986

steadylite HTS Assay Kit, 100 mL
6016981

steadylite HTS Assay Kit, 1,000 mL
6016989

Selection Guide: Reporter Gene Assays on VICTOR³

Assay Requirements	Recommended Product
Continuous processing High sensitivity	britelite
Large batch processing Moderate sensitivity	steadylite HTS

Preclinical Evaluation of Technetium-99m-Labeled Somatostatin Receptor-Binding Peptides

Shankar Vallabhajosula, Brian R. Moyer, John Lister-James, Bill J. McBride, Helena Lipszyc, Hiram Lee, Diago Bastidas and Richard T. Dean

Division of Nuclear Medicine, Department of Radiology, The Mount Sinai Medical Center, New York, New York; and Diatide, Inc., Londonderry, New Hampshire

We report here the results of studies on the in vitro receptor binding affinity, in vivo tumor uptake and biodistribution of two ^{99m}Tc-labeled peptides. **Methods:** Peptides P587 and P829 were synthesized by N-α-Fmoc peptide chemistry, purified by reversed-phase HPLC and characterized by fast-atom bombardment mass spectrometry. The peptides were labeled with ^{99m}Tc by ligand exchange from ^{99m}Tc-glucoheptonate. In vitro somatostatin receptors (SSTR)-binding affinities of P587, P829 and their oxorhenium complexes, [DTPA]octreotide and In-[DTPA]octreotide were determined in an inhibition assay using AR42J rat pancreatic tumor cell membranes and ^{125}I-[Tyr^3]somatostatin-14 as the probe. In vivo single- and dual-tracer studies of ^{99m}Tc peptides and ^{111}In-[DTPA]octreotide were carried out using Lewis rats bearing CA20948 rat pancreatic tumor implants. **Results:** Technetium-99m-P587 and ^{99m}Tc-P829 of high-specific activity (>60 Ci (2.2 TBq)/mmole) were prepared in >90% radiochemical yield. P587 and P829 had a Ki = 2.5 n*M* and 10 n*M*, respectively. [ReO]P587 and [ReO]P829, representing the ^{99m}Tc complexes, had Ki = 0.15 n*M* and 0.32 n*M*, respectively. In comparison, [DTPA]octreotide and In-[DTPA]octreotide had Ki = 1.6 and 1.2 n*M*, respectively. In vivo tumor uptake of ^{99m}Tc-P587 and ^{99m}Tc-P829 was high (4.1 and 4.9%ID/g at 90 min postinjection compared to 2.9% for ^{111}In-[DTPA]octreotide). Tumor/blood and tumor/muscle ratios at 90 min postinjection were 6 and 33 for ^{99m}Tc-P587, 21 and 68 for ^{99m}Tc-P829, and 22 and 64 for ^{111}In-[DTPA]octreotide. **Conclusion:** The high SSTR-binding affinity and high, receptor-specific and saturable in vivo tumor uptake indicate that ^{99m}Tc-P587 and ^{99m}Tc-P829 are promising radiotracers for the clinical detection of SSTR-expressing tumors and other tissues by ^{99m}Tc gamma scintigraphy.

Key Words: tumor imaging; somatostatin receptor imaging; technetium-99m; peptide; receptor binding

J Nucl Med 1996; 37:1016–1022

Natural somatostatin, also known as somatotropin release inhibiting factor (SRIF or SRIF-14), is a cyclic tetradecapeptide (Table 1) which is produced by the hypothalamus and pancreas and which, through binding to specific receptors and possibly through subsequent induced reduction in cellular cyclic AMP, inhibits the secretion of many hormones and growth factors (*2,3*). Receptors for SRIF have been found in the central nervous system, pituitary, pancreas and in the mucosa of the gastrointestinal tract. Five subtypes of human SRIF receptors, conventionally termed somatostatin-type receptors or SSTRs, hence SSTR1, SSTR2, SSTR3, SSTR4 and SSTR5, have been cloned (*4–7*).

Most neuroendocrine tumors and their metastases express SSTRs to a much greater extent than do normal tissues (*8–11*). The types of tumors which have been found to express SSTRs include tumors of the amine-precursor-uptake-and-decarboxylation (APUD) cell system (APUDomas) such as small-cell lung cancer, endocrine pancreatic tumors, metastatic carcinoids, growth hormone-producing pituitary adenomas, paragangliomas, lymphomas (mainly Hodgkins), astrocytomas and meningiomas as well as some colorectal, breast and prostate cancers (as determined by ^{125}I-[Tyr^3]octreotide autoradiography (*9*)). SSTR2 appears to be the predominant SSTR sub-type expressed by these tumors (*10,11*).

SSTR-expressing tumors can be treated with SRIF or synthetic analogs to either reduce hypersecretion of hormones or inhibit tumor growth, or both (*8*). However, because SRIF undergoes rapid in vivo enzymatic degradation, SRIF analogs which are more resistant to in vivo degradation have been prepared (*12–16*). Octreotide (Sandostatin®; SMS 201-995) (Table 1) is a synthetic SRIF analog which is currently in clinical use for treating the hypersecretion of hormones symptomatic of gastroenteropancreatic (GEP) tumors, and acromegaly and is approved in the US for treatment of carcinoid tumors and VIPomas (*12*).

Lamberts and Krenning et al. (*1,8,17,18*) and Kvols et al. (*19*) have shown the radiolabeled octreotide derivatives, ^{123}I-[Tyr^3]octreotide and ^{111}In-[DTPA]octreotide, to be very useful for detecting small neuroendocrine tumors and metastases not detected by conventional means and for identifying tumors that respond to therapeutic doses of octreotide. Nevertheless, a ^{99m}Tc-labeled SSTR-binding radiotracer is highly desirable for routine nuclear medicine studies because ^{99m}Tc is considerably less expensive than ^{111}In and because ^{99m}Tc provides a greater photon flux, and hence better quality images, per unit of absorbed radiation dose.

We have developed a number of unique, high-affinity SSTR-binding peptides which can be radiolabeled readily with ^{99m}Tc with retention and, in many cases, enhancement of SSTR-binding affinity (*20*). Of these, ^{99m}Tc-P587 and ^{99m}Tc-P829 were selected for clinical studies and we describe their preclinical evaluation.

MATERIALS AND METHODS

Peptide Synthesis

Peptides P587, P829, octreotide and [DTPA]octreotide (see Table 1 for sequences) were synthesized at Diatide, Inc. (Londonderry, NH) using both solution and solid-phase peptide synthesis techniques and N-α-Fmoc chemistry. Details of the syntheses will appear elsewhere. The peptides were purified by preparative C_{18} reversed-phase HPLC using a Delta-Pak C_{18}, 15 μm, 300 Å, 47 × 300-mm column and 0.1% trifluoroacetic acid in water (0.1% TFA/H_2O) modified with 0.1% trifluoroacetic acid in 90% acetonitrile/10% water (0.1% TFA/(90% CH_3CN/H_2O)) as eluents, and then lyophilized. The purified peptides were lyophilized and their purity and identity were confirmed by analytical C_{18} reversed-

Received Jan. 19, 1995; revision accepted Nov. 3, 1995.

For correspondence or reprints contact: Shankar Vallabhajosula, PhD, Associate Professor of Radiology, Mount Sinai Medical Center, One Gustave L. Levy Pl., New York, NY 10029.

TABLE 1
Peptide Sequences*

Somatostatin: Ala-Gly-Cys-Lys-Asn-Phe-Phe-Trp-Lys-Thr-Phe-Thr-Ser-Cys
P587: cyclo-(N-Me)Phe-Tyr-(D-Trp)-Lys-Val-Hcy(CH_2CO-Gly-Gly-Cys-Lys-NH_2)
P829: cyclo-(N-Me)Phe-Tyr-(D-Trp)-Lys-Val-Hcy(CH_2CO-(β-Dap)-Lys-Cys-Lys-NH_2)
octreotide: (D-Phe)-Cys-Phe-(D-Trp)-Lys-Thr-Cys-Thr(ol)
[DTPA]octreotide: [DTPA]-(D-Phe)-Cys-Phe-(D-Trp)-Lys-Thr-Cys-Thr(ol)

*Cys ... Cys underline indicates cyclic disulfide; cyclo and underline indicates cyclic peptide.
Ala = L-alanine, Asn = L-asparagine, Cys = L-cysteine, β-Dap = β-(L-1,2-diaminopropionic acid), DTPA = diethylenetriaminepentaacetic acid, Gly = glycine, Hcy = L-homocysteine, Lys = L-lysine, (N-Me)Phe = N-α-methyl-L-phenylalanine, Phe = L-phenylalanine, D-Phe = D-phenylalanine, Ser = L-serine, Thr = L-threonine, Thr(ol) = L-threoninol, Trp = L-tryptophan, D-Trp = D-tryptophan, Tyr = L-tyrosine, Val = L-valine.

phase HPLC, C_{18}, 5 μm, 300 Å, 3.9 × 150-mm column and binary gradient elution with 0.1% TFA/H_2O as Solvent A and 0.1% TFA/(90% CH_3CN/H_2O) as Solvent B) and fast-atom bombardment mass spectrometry.

Peptide Metal Complexes

The oxorhenium complexes of P587 ([ReO]P587) and P829 ([ReO]P829) were prepared by ligand exchange using $Bu_4NReOBr_4$ (*21*) in DMF, followed by purification by preparative HPLC and confirmation of composition by electrospray mass spectrometry (ESMS). Indium-[DTPA]octreotide was prepared from In-chloride dissolved in 0.1 m citrate buffer at pH 5 and [DTPA]octreotide followed by purification by preparative HPLC and confirmation of composition by ESMS.

Preparation of Technetium-99m-Labeled Peptides

P587 and P829 were labeled with ^{99m}Tc by ligand exchange from ^{99m}Tc-glucoheptonate. P587 was dissolved to 1 mg/ml in 50% aqueous ethanol and P829 was dissolved to 1 mg/ml in normal saline. One quarter of a Glucoscan™ Kit (DuPont Pharma, N. Billerica, MA) that had been reconstituted with 1 ml ^{99m}Tc generator eluate (200–300 mCi; 7.4–11.1 GBq), was added to peptide solution. In the case of P587 the solution was heated at 100°C for 15 min. For P829, the reaction mixture was allowed to incubate at room temperature for 20 min. The radiochemical purity of the ^{99m}Tc-peptide complexes was determined by ITLC (ITLC-SG, Gelman Sciences, Ann Arbor, MI) developed in saturated saline (^{99m}Tc-peptide immobile, $^{99m}TcO_4$ and ^{99m}Tc-glucoheptonate mobile), ITLC-SG developed in 5:3:1.5 pyridine: acetic acid: water (^{99m}Tc-peptide, $^{99m}TcO_4$ and ^{99m}Tc-glucoheptonate mobile) and analytical reversed-phase HPLC, performed using an HPLC equipped with an in-line gamma detector linked to an integrating recorder, a Delta-Pak C_{18}, 5 μm, 300 Å, 3.9 × 150-mm column eluted at 1.2 ml/min with a gradient of 0.1% TFA/H_2O modified with 0.1% TFA/(90% CH_3CN/H_2O).

Preparation of Indium-111-[DTPA]Octreotide

Indium-111-[DTPA]octreotide was prepared by reacting ^{111}In-$InCl_3$ (1-2 mCi, 37-74 MBq) in 0.2 m HCl (1 ml) containing 25 mg trisodium citrate with 10 μg [DTPA]octreotide for 30 min at room temperature. The radiochemical purity of the ^{111}In-[DTPA]octreotide was determined by ITLC-SG developed in 0.1 m citrate buffer at pH 5.0.

In Vitro Assay

Peptides P587, P829 and [DTPA]octreotide and their metal complexes [ReO]P587, [ReO]P829 and In-[DTPA]octreotide were assayed in vitro for SSTR binding affinity by J.E. Taylor of Biomeasure, Inc., using AR42J rat pancreatic carcinoma cell membranes (expressing predominantly SSTR2 (*10*)) and ^{125}I-[Tyr^{11}]SRIF-14 as the probe. Briefly, AR42J cells were cultured in Dulbecco's Minimum Essential Medium supplemented with 10% fetal bovine serum and 8 mm L-glutamine maintained in a humidified 5% CO_2 atmosphere at 37°C in T-flasks. Harvested cells were homogenized in cold Tris buffer and the homogenate was centrifuged at 39,000 × g for 10 min at 4°C. The pellet was washed once using the same buffer then suspended in ice-cold 10 mm Tris HCl. Equal aliquots of cell membrane were incubated with ^{125}I-[Tyr-11]SRIF-14 (0.05 nm; 750,000 cpm/ml; 2000 Ci/mmole) and peptide at a final concentration of 10^{-11} to 10^{-6} m in 50 mm HEPES, pH 7.4 containing 1% bovine serum albumin, fraction V, 5 mm $MgCl_2$, Trasylol (200 KIU/ml), bacitracin (0.02 mg/ml) and phenylmethylsulfonyl fluoride (0.02 mg/ml) for 25 min at 30°C. Using a filtration manifold, the mixture was then filtered through a polyethylenimine-washed GF/C filter, and the residue was washed three times with 5 ml ice-cold buffer. The pellet/filter and filtrate/washings were counted in a well- counter to give the fractions of radioactivity bound and free. To assess nonspecific binding, the assay was run in the presence of 200 nm SRIF-14. Analysis of the data gave inhibition constants (Ki) via Hill plots (*22*).

Animal Model

The animal tumor model was essentially that described by Lamberts and Krenning et al. (*23*) and was prepared by A. Bogden, Biomeasure, Inc. CA20948 rat pancreatic tumor brei (0.05 to 0.1 ml) was inoculated into the subcutaneous space of the lateral aspect of the right thighs of 6-wk-old, male Lewis rats (175–225 g). The tumors were allowed to grow to approximately 0.5 to 2 g (2–3 wk) before serial passaging. The tumor-bearing animals used for the in vivo studies were from the fourth to the eleventh passage and carried 0.2 to 2 g (mean 1.2 ± 0.7 g) tumors. The tumors had a stable SSTR density of 80–100 fmole/mg tumor cell protein (assayed using ^{125}I-[Tyr^{11}]SRIF-14) through passages 4 to 9.

For studies of in vivo specificity of radiotracer localization in the tumors, selected animals were given a subcutaneous SSTR-blocking dose of 4 mg/kg octreotide 30 min prior to injection of the radiotracer. This protocol has been shown by Lamberts and Krenning et al. to result in a lowering of ^{111}In-[DTPA]octreotide tumor uptake by 40% (*23*).

In Vivo Tumor Uptake and Kinetics Studies

In all studies, CA20948 tumor-bearing Lewis rats were restrained and injected via the dorsal tail vein with radiolabeled peptides in a 0.2–0.4-ml volume containing 0.20 mCi (7.4 Mbq) of ^{99m}Tc-labeled P587 or P829 (2–8 μg) peptide and/or 0.10 mCi (3.7 MBq) of ^{111}In-[DTPA]octreotide (0.3–1 μg). For imaging studies, the animals were sedated with a mixture of ketamine and xylazine and whole-body images were obtained using a gamma camera (Technicare, Omega 500) fitted with a high-resolution collimator. Images were acquired for 5 min and the data were stored in 128 × 128-image matrix on a Summit image computer system.

Twenty-four Hour Pharmacokinetic Study. Fifteen tumor-bearing rats were injected with ^{99m}Tc-P587 and three animals each were sacrificed at 0.5, 1.5, 3, 6 and 24 hr. Selected tissue samples were excised, weighed and, along with an aliquot of the injected dose, were counted in a gamma well-counter set to count in the ^{99m}Tc window. The results were expressed as percent injected dose per gram (% ID/g) of tissue.

Dual-Tracer Comparison of Technetium-99m-P587 and Indium-111-[DTPA]Octreotide and In Vivo Receptor Specificity Study. Nine of 22 CA20948 tumor-bearing rats were injected subcutaneously with an SSTR-blocking dose of 4 mg/kg octreotide 30 min prior to injection of the radiotracers. All animals were injected with

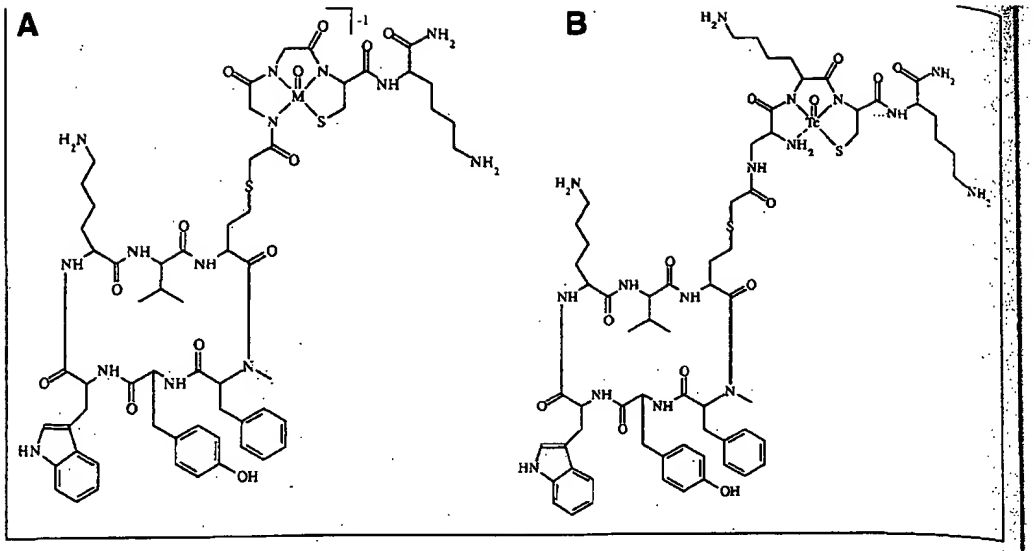

FIGURE 1. Proposed oxotechnetium/oxorhenium complexes of (A) P587 and (B) P829.

^{99m}Tc-P587 followed approximately 1 min later by ^{111}In-[DTPA]octreotide. At 30, 60 and 90 min, three SSTR-blocked and three nonblocked animals were killed by cervical dislocation and selected necropsy was performed. At 180 min the remaining four nonblocked animals were also killed and necropsied. Harvested tissue samples were weighed and, along with aliquots of both injected doses, were counted in a gamma well-counter set to count in both ^{99m}Tc and ^{111}In windows. Technetium-99m counts were corrected for ^{111}In spillover and 3 days later the samples were recounted for ^{111}In only. At 30, 60, 90 and 180 min selected animals also were imaged.

Dual-Tracer Comparison of Technetium-99m-P829 and Indium-111-[DTPA]Octreotide. The tumor uptake of ^{99m}Tc-P829 was compared with ^{111}In-DTPA-octreotide in a dual-tracer study using an additional five tumor-bearing rats. All animals were injected with ^{99m}Tc-P829 followed approximately 1 min later by ^{111}In-[DTPA]octreotide. The animals were killed at 90 min postinjection and % ID/g of tumor, blood, muscle, pancreas and gastrointestinal tract were determined as before for ^{99m}Tc and ^{111}In tracers.

Saturability Study. To assess the effect of specific activity on tumor uptake, ^{99m}Tc-P587 was studied in six groups of three tumor-bearing rats each. The animals were co-injected with either 0, 25, 100, 300, 600, 1000 or 4000 μg/kg of P587 peptide added to the standard dose of ^{99m}Tc-P587 (0.2 mCi; 7.4 MBq; 4 μg peptide). The animals were sacrificed at 90 min postinjection and % ID/g of tumor, blood, muscle, pancreas and gastrointestinal tract were determined as before. A similar study was performed with ^{99m}Tc-P829.

Biodistribution of Technetium-99m Peptides

The biodistributions of ^{99m}Tc-P587 and ^{99m}Tc-P829 were studied noninvasively in normal rabbits by gamma-camera imaging over a period of 4 hr. For the first 1 hr, serial static images (5 min per frame) were acquired and subsequent images were obtained at 2, 3 and 4 hr.

RESULTS

P587 peptide, P829 peptide, [DTPA]octreotide, [ReO]P587, [ReO]P829 and In-[DTPA]octreotide were all prepared and purified to >90% purity by HPLC analysis. The amino acid sequences of all of the peptides are shown in Table 1. The structures for P587 and P829 are shown in Figure 1. The proposed structures of the oxotechnetium and oxorhenium complexes of P587 and P829 are shown in Figures 1A and B, respectively. Selected analytical data are shown in Table 2.

The ^{99m}Tc-labeling of P587 and P829 were routinely obtained in >90% radiochemical yield and of >90% radiochemical purity by ITLC and HPLC analysis. No HPLC purification was required. Residual pertechnetate was <1% and ^{99m}Tc species immobile on ITLC analysis (^{99m}Tc-microcolloid or reduced, hydrolysed ^{99m}Tc) was <3%. HPLC analysis of ^{99m}Tc-P587 showed two, closely eluting radioactive components as expected for syn- and anti-oxotechnetium complexes of the -Gly-Gly-Cys-chelating sequence. HPLC analysis of ^{99m}Tc-P829 showed a single species. The ^{99m}Tc-labeled peptides were routinely prepared of high specific activity (50 mCi (2 GBq)/mg peptide; 60 Ci (2.2 TBq)/mmole peptide) but even higher specific activity (1000 Ci (37 TBq)/mmole P587) was readily achievable without significant loss of radiochemical yield. As discussed below, the effective specific activity was likely even higher.

[ReO]P587 was isolated as a mixture of two closely eluting components by HPLC analysis, presumed to be the expected two isomeric complexes. FABMS analysis showed only MH^+ peaks at m/z = 1458 corresponding to the expected mass (P587 − 4H + ReO + H^+) and 1258 corresponding to P587 itself. [ReO]P829 was isolated as a single peak by HPLC analysis. The HPLC analysis of oxorhenium complexes and ^{99m}Tc-labeled peptides showed that the corresponding rhenium and technetium complexes had virtually identical retention times (see Table 2). These data support the use of the oxorhenium complex(es) as a nonradioactive surrogate for ^{99m}Tc-peptides.

TABLE 2
Peptide and Peptide-Metal Complex Data

Peptide	Calc. MW	MH±(FABMS)	HPLC R_t (min)	
P587	1257.7	1258	7.2[1]	
[ReO]P587	1455.7	1458		14.6[4]
^{99m}Tc-P587	—	—		14.7, 14.9[4]
P829	1357.7	1358	5.8[3]	
[ReO]P829	1556.9	1558		12.2[1]
^{99m}Tc-P829	—	—		12.3[1]
[DTPA]octreotide	1392.6	1394	7.1[1]	
In-[DTPA]octreotide	1504.4*	1507	9.4[2]	

*Assumed formula: [DTPA]octreotide + In − 3H

HPLC elution conditions: (a) 0 to 100% Solvent B in 10 min (Delta-Pak column); (b) 10 to 60% Solvent B in 10 min (Delta-Pak column); (c) 20–50% Solvent B in 10 min (NovaPak column).

TABLE 3
Inhibition Constants for Peptides and Metal Complexes Iodine-125-[Tyr.[11]]SRIF-14/AR42J Rat Pancreatic Cell Membrane Assay

Peptide	Inhibition constant, Ki (nM) Peptide	Metal-peptide complex	Ratio*
P587	2.5	0.15[a]	20
P829	10	0.32[a]	30
DTPA-octreotide	1.6	1.20[b]	1

*Ratio of Ki of peptide to peptide-metal complex (to one significant figure).
a = [ReO]peptide complex; b = In-DTPA-octreotide.

The in vitro inhibition constants obtained for P587 peptide, P829 peptide and their corresponding oxorhenium complexes and [DTPA]octreotide, and In-[DTPA]octreotide are shown in Table 3. It is noted that [ReO]P587 has a Ki approximately 20 times lower than that of P587 peptide and [ReO]P829 has a Ki 30 times lower than that of P829 peptide. This indicates that the rhenium complexes (and by inference, the ^{99m}Tc complexes) have a SSTR binding affinities that are an order of magnitude higher than those of the parent peptides. In-[DTPA]octreotide and [DTPA]octreotide did not share this property.

Kinetics of Tumor Uptake

Tumor and selected tissue uptake data of ^{99m}Tc-P587 over the course of the 24-hr pharmacokinetic study are presented in Table 4. Technetium-99m-P587 showed rapid, high tumor uptake, maximizing to 5.0 %ID/g at 3 hr, and only slow (68% of maximum remaining at 6 hr) clearance of radioactivity from the tumor over 24 hr. Tumor-to-blood ratio increased throughout the study, reflecting the initial tumor retention and subsequent much faster clearance of radiotracer from the blood than from the tumor. Tumor-to-muscle increased to 6 hr then showed insignificant change over 24 hr.

Tumor Uptake of Technetium-99m-P587 and Technetium-99m-P829 and Comparison with Indium-111-[DTPA]Octreotide

Data from the ^{99m}Tc-P587 and ^{111}In-[DTPA]octreotide dual-tracer study are presented in Table 5. The tumor uptake of both radiotracers was high and although not significantly different over the course of the 3-hr study, in general ^{99m}Tc-P587 and ^{99m}Tc-P829 gave higher tumor uptake than did ^{111}In-[DTPA]octreotide. Although ^{111}In-[DTPA]octreotide had faster blood clearance than ^{99m}Tc-P587 resulting in higher tumor-to-blood and tumor-to-muscle ratios for ^{111}In-[DTPA]octreotide, the ratios of 6.3 and 29, respectively, obtained with ^{99m}Tc-P587 at 90 min were more than sufficient to predict good imaging.

Data from the ^{99m}Tc-P829 and ^{111}In-[DTPA]octreotide dual-tracer study are presented in Table 6. Technetium-99m-P829 also showed high tumor uptake which was higher than that of ^{111}In-[DTPA]octreotide. Moreover, the blood clearance of ^{99m}Tc-P829 was faster than that of ^{99m}Tc-P587 resulting in tumor-to-blood and tumor-to-muscle ratios which were essentially equivalent to those of ^{111}In-[DTPA]octreotide.

The studies in SSTR-blocked animals (Table 5) showed that the tumor uptake of ^{99m}Tc-P587 was reduced by 86% (at 90 min) in SSTR-blocked versus nonblocked animals. Indium-111-[DTPA]octreotide tumor uptake was similarly reduced by 94%. Blood levels did not change significantly and therefore tumor-to-blood and tumor-to-muscle ratios were concomitantly reduced in SSTR-blocked animals. Notably pancreatic uptake was substantially diminished in blocked animals, indicating that the pancreatic uptake was also substantially receptor-mediated.

As a negative control, a much weaker affinity peptide P443 ([DTPA]-(D-Phe)-(4-chlorophenylalanyl)-Tyr-(D-Trp)-Lys-Thr-Phe-Thr-(ε-Lys)-Gly-Cys-NH_2) having a Ki of 7.9 nm as the oxorhenium complex, was also studied in CA20948 tumor-bearing rats. At 90 min postinjection, ^{99m}Tc-P443 gave only 0.42 %ID/g in the tumor and tumor-to-blood and tumor-to-muscle ratios of 0.9 and 2.7, respectively.

Tumor Uptake of Technetium-99m-Peptides: Imaging Studies

Representative gamma camera images (anterior view) of CA20948 tumor-bearing rats 90 min after injection with ^{99m}Tc-P587 are presented in Figure 2. The radiotracer uptake in the tumor in the right hind leg of each animal is clearly seen. Also seen are kidneys and bladder and some gastrointestinal tract uptake. The images show the obvious difference in tumor uptake in an SSTR-blocked animal (left image) and a non-SSTR-blocked animal (right image). Gamma camera images of ^{99m}Tc-P829 in two animals are shown in Figure 3. Again the high tumor uptake of the ^{99m}Tc-labeled peptide is clearly seen.

Effect of Specific Activity on the Tumor Uptake of the Technetium-99m-Peptides

The effect of increasing the amount of co-injected P587 peptide on ^{99m}Tc-P587 tumor uptake is shown in Figure 4A. P587 peptide was added to a standard preparation of ^{99m}Tc-P587 (0.2 mCi; 7.4 MBq; 5 μg P587 peptide), effectively lowering the specific activity. Tumor uptake decreased substantially when >100 μg P587 peptide was co-injected. Thus 100 μg co-injected P587 resulted in a 50% decrease in tumor uptake. Pancreatic uptake was also reduced by increasing amounts of co-injected P587 peptide. Similarly, the effect of decreasing specific activity on the uptake of ^{99m}Tc-P829 by tumor and pancreas is shown in Figure 4B. Blood, muscle and gastrointestinal tract uptake did not change significantly in either the ^{99m}Tc-P587 or ^{99m}Tc-P829 study.

Biodistribution of Technetium-99m-P587 versus Technetium-99m-P829

The gamma-camera images showing the relative distribution of ^{99m}Tc-P587 and ^{99m}Tc-P829 in normal rabbits are presented in Figure 5. The images show that ^{99m}Tc-P587 has substantial

TABLE 4
Technetium-99m-P587 Pharmacokinetic Study in CA20948 Tumor-Bearing Rats*

Time (hr)	%ID/g Tumor	Blood	Muscle	Tumor: Blood	Tumor: Muscle	%ID GI Tract
1.5	4.0 ± 0.64	0.67 ± 0.048	0.13 ± 0.0067	6.0 ± 0.80	30 ± 4.5	45 ± 1.9
3	5.0 ± 0.066	0.35 ± 0.013	0.076 ± 0.0070	14 ± 0.49	66 ± 6.7	49 ± 2.6
6	3.4 ± 0.59	0.075 ± 0.013	0.029 ± 0.0045	46 ± 8.7	120 ± 4.6	60 ± 17
24	0.80 ± 0.13	0.011 ± 0.0011	0.0084 ± 0.0023	69 ± 5.0	97 ± 12	31 ± 11

*Three animals per time point; mean ± s.d.

TABLE 5
Technetium-99m-P587 and Indium-111-[DTPA]Octreotide Dual-Tracer Study in CA 20948 Tumor-Bearing Rats Data from SSTR-Blocked and Nonblocked Animals*

Time (min)		%ID/g			Tumor:	Tumor:	%ID	
		Tumor	Blood	Muscle	Blood	Muscle	Pancreas	GI Tract
				^{99m}Tc-P587				
30	n	3.8 ± 0.18	1.4 ± 0.45	0.36 ± 0.055	2.3 ± 0.030	11 ± 1.0	3.0 ± 0.23	22 ± 1.7
	b	0.69 ± 0.050	1.5 ± 0.29	0.27 ± 0.070	0.48 ± 0.060	2.6 ± 0.6	0.66 ± 0.38	16 ± 2.5
60	n	2.7 ± 0.68	0.93 ± 0.23	0.19 ± 0.028	3.0 ± 0.61	15 ± 2.6	3.2 ± 0.50	25 ± 3.8
	b	0.70 ± 0.052	1.2 ± 0.18	0.25 ± 0.053	0.61 ± 0.060	2.9 ± 0.49	0.32 ± 0.004	27 ± 5.3
90	n	4.1 ± 0.56	0.64 ± 0.030	0.14 ± 0.010	6.3 ± 1.0	29 ± 2.9	3.2 ± 0.060	33 ± 0.8
	b	0.57 ± 0.08	0.74 ± 0.10	0.14 ± 0.025	0.77 ± 0.080	4.1 ± 0.45	0.27 ± 0.030	35 ± 2.2
180	n	3.0 ± 0.66	0.27 ± 0.030	0.050 ± 0.008	11 ± 2.6	61 ± 14	3.1 ± 0.49	36 ± 3.3
				^{111}In-[DTPA]octreotide				
30	n	3.1 ± 0.72	0.76 ± 0.13	0.29 ± 0.22	4.3 ± 1.6	16 ± 10	2.1 ± 0.91	5.6 ± 1.3
	b	0.62 ± 0.17	0.92 ± 0.38	0.27 ± 0.11	0.71 ± 0.11	2.5 ± 1.0	0.38 ± 0.15	5.1 ± 1.0
60	n	3.1 ± 0.46	0.27 ± 0.040	0.071 ± 0.004	12 ± 0.13	43 ± 4.0	2.4 ± 0.080	5.5 ± 0.23
	b	0.33 ± 0.030	0.31 ± 0.050	0.010 ± 0.015	1.1 ± 0.080	3.3 ± 0.54	0.18 ± 0.11	3.2 ± 0.66
90	n	2.9 ± 1.8	0.13 ± 0.070	0.045 ± 0.024	22 ± 3	64 ± 4.3	2.1 ± 0.92	6.5 ± 0.53
	b	0.18 ± 0.017	0.10 ± 0.004	0.031 ± 0.004	1.8 ± 0.19	5.9 ± 0.61	0.075 ± 0.02	2.8 ± 0.06
180	n	2.7 ± 0.57	0.024 ± 0.004	0.014 ± 0.006	120 ± 39	240 ± 120	2.6 ± 0.12	7.0 ± 0.39

*n = 3 for each group except four in 180-min group; mean ± s.d.
† n = nonblocked; b = SSTR-blocked with 4 mg/kg octreotide s.c. 30 min before dosing.

uptake in the gastrointestinal tract compared to ^{99m}Tc-P829 which is cleared mostly by the kidneys. A quantitative analysis of the images at 1 hr indicated that about 40% of ^{99m}Tc-P587 activity was in the gastrointestinal tract, 25% in the urinary bladder and only 6% in the kidneys. In contrast, 30% of ^{99m}Tc-P829 activity was in the kidneys, 20% in the urinary bladder and less than 5% in the gastrointestinal tract.

DISCUSSION

The presence of the disulfide bridge of octreotide means that labeling this molecule with ^{99m}Tc is problematic because the reducing agent (usually stannous ion) used in ^{99m}Tc labeling can reduce (open) the disulfide bond with consequent considerable loss of receptor-binding affinity. Macke et al. (*24*) has recently reported a ^{99m}Tc-labeled PnAO conjugate of octreotide. They reported, however, using essentially the same tumor model as we have used, only 0.38% ID/g in the tumor, a tumor-to-blood ratio <1 and only 30% reduction of tumor uptake in SSTR-blocked versus unblocked animals. In contrast, very high tumor uptake (4–5% ID/g), tumor-to-blood (6–21) and tumor-to-muscle ratios (21–68) were seen with ^{99m}Tc-labeled P587 and P829. In addition, 85% reduction in tumor uptake in SSTR-blocked animals was seen with ^{99m}Tc-P587 and both ^{99m}Tc-P587 and ^{99m}Tc-P829 tumor uptake was 80–90% by co-injection of large amounts of the respective peptides. These differences suggest that the ^{99m}Tc-labeled PnAO conjugate of Macke et al. did not retain high receptor-binding affinity and gave mainly nonspecific tumor uptake in vivo.

Inspection of the literature reveals that in order to maintain high SSTR-binding affinity, the pharmacophore of an SSTR ligand needs to be conformationally constrained (*25*). Expressly in order to avoid the incompatibility of having a disulfide in a molecule that is to be radiolabeled with ^{99m}Tc under reducing conditions, we designed peptide P587 and P829 to hold the pharmacophore, that is the key four SSTR-binding amino acid residues -Tyr-(D-Trp)-Lys-Val-, in a cyclic configuration that was not susceptible to reductive cleavage. The sequence -Gly-Gly-Cys- of P587, which constitutes a triamide-thiol chelator which would be expected to form a kinetically stable oxotechnetium (+5) complex (*26*), was appended to the thiol group of the side-chain of a the noncritical homocysteine residue of the molecule. The result was that P587 peptide had an in vitro inhibition constant (Ki) of 2.5 nm, showing it to be a high-affinity ligand for the SSTR. Similarly, with P829 comprises the same SSTR binding cyclic peptide with the novel monoamine, bisamide, monothiol chelating sequence -(β-Dap)-Lys-Cys- appended to the homocysteine side-chain. The Ki for P829 was 10 nm but the oxorhenium complex had a Ki of 0.32 nm.

In order to assess the SSTR-binding affinity of the ^{99m}Tc complex of P587 and ^{99m}Tc-P829, we chose to use the oxorhenium (+5) complexes of these two peptides as a ^{99m}Tc

TABLE 6
Technetium-99m-P829 and Indium-111-[DTPA]Octreotide Dual-Tracer Study in CA 20948 Tumor-Bearing Rats (90-Minute Data)*

%ID/g			Tumor:	Tumor:	%ID	
Tumor	Blood	Muscle	Blood	Muscle	Pancreas	GI Tract
			^{99m}Tc-P829			
4.8 ± 1.1	0.29 ± 0.14	0.078 ± 0.015	21 ± 11	68 ± 26	2.4 ± 0.34	8.4 ± 0.5
			^{111}In-[DTPA]octreotide			
2.8 ± 0.43	0.10 ± 0.024	0.048 ± 0.044	29 ± 5.9	90 ± 57	1.6 ± 0.10	5.0 ± 0.50

*n = 3 for each group.

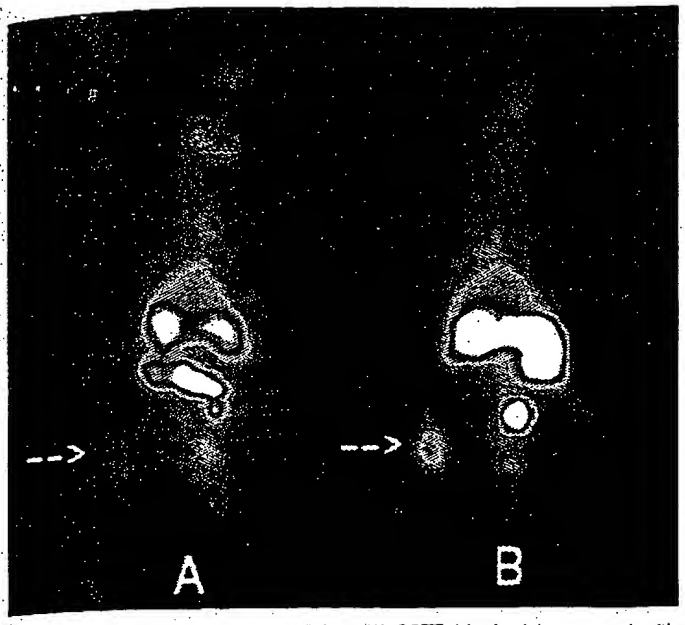

FIGURE 2. Technetium-99m-P587 in a (A) SSTR-blocked (pretreated with octreotide 4 mg/kg) and (B) a nonblocked CA20948 tumor-bearing rat at 90 min postinjection (anterior).

complex surrogate so as to avoid having to use the long-lived isotope ^{99m}Tc in the receptor-binding assay. It has been well-established that technetium and rhenium form configurationally equivalent, albeit not identical, oxometal (+5) complexes of triamide-thiol and bisamide-bisthiol ligands (*27*). As the results show, [ReO]P587 and [ReO]P829 have an even higher SSTR-binding affinity than the parent peptides. The higher affinity of the labeled peptides has important consequences in regard to specific activity. That is that co-injected peptides (P587 or P829) will compete poorly with the ^{99m}Tc-peptide complexes for the somatostatin receptors. Thus a readily achievable specific activity of 1000 Ci/mmole based on total injected P587 may be effectively an order of magnitude higher. In contrast the Kis of [DTPA]octreotide (1.6 nM) and In-[DTPA]octreotide (1.2 nm) which were similar to the previously reported values (*28*), showed that the unlabeled [DTPA]octreotide will compete equally with the ^{111}In-[DTPA]octreotide for the SSTRs.

The in vivo studies in CA20948 tumor-bearing rats showed

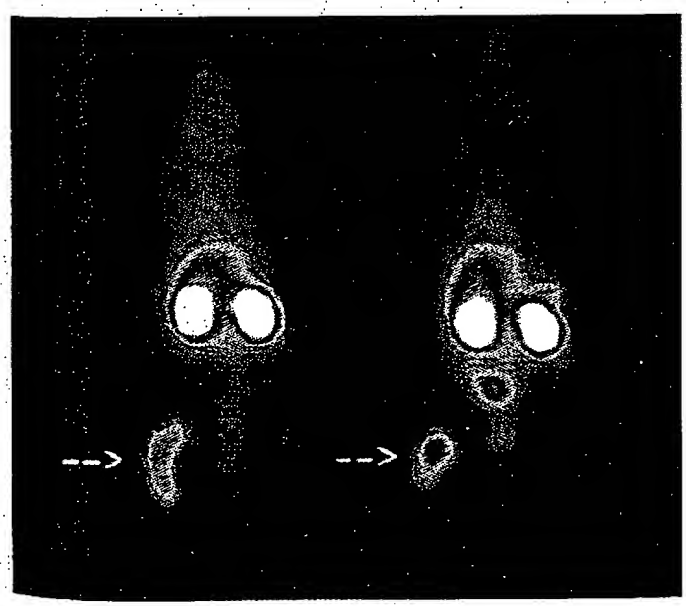

FIGURE 3. Technetium-99m-P829 in CA20948 two tumor-bearing rats (at 90 min postinjection, anterior views).

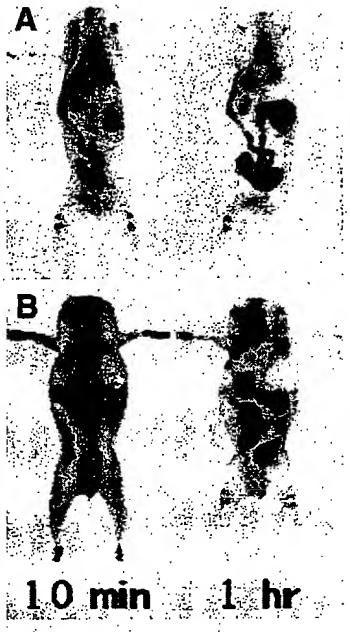

FIGURE 5. Gamma-camera images showing the relative distribution of (A) ^{99m}Tc-P587 and (B) ^{99m}Tc-P829 in normal rabbits at 10 min and 1 hr postinjection.

that the tumor uptake of ^{99m}Tc-P587 and ^{99m}Tc-P829 is at least, and perhaps a little higher than, that of ^{111}In-[DTPA]octreotide, that the tumor uptake of the labeled peptides is specific (blocked by octreotide) and that the tumor uptake of ^{99m}Tc-P587 and ^{99m}Tc-P829 is saturable (diminished by large amounts of co-injected parent peptide).

Regarding the biodistribution of ^{99m}Tc-P587 in normal animals, the biphasic nature of the blood clearance suggested hepatobiliary recycling which was supported by the observed progressive uptake from 15 min to 5 hr in the gastrointestinal tract. Significant reabsorption is probable since less than 6% ID remained in the large intestine at 5 hr and less than 5% ID remained in the entire gastrointestinal tract at 24 hr. Interestingly, the tumor-bearing animals showed greater and more persistent gastrointestinal uptake than did the normal animals. It is noted that as rats do not have gall bladders, biliary secretion is continuous as opposed to being controlled in other species including humans. Thus the gastrointestinal tract uptake seen maximally at from 3 to 6 hr in the rat may occur much later in the human leaving an early window in which the abdomen would be relatively clear of nonspecific radiotracer uptake. The retention of a fraction of the dose in the kidneys indicates proximal tubular reabsorption as has been observed for ^{111}In-[DTPA]octreotide. The primary route of excretion was the renal system as expected for a small peptide and as desirable for a radiopharmaceutical of this type. In comparison, the biodistribution of ^{99m}Tc-P829 showed almost no gastrointestinal uptake, with predominantly renal excretion.

These preclinical results have now been verified in initial clinical studies (*29*) with both agents in which SSTR-expressing tumors were detected as early as 5 min postinjection. Because it has showed both high tumor uptake and low gastrointestinal uptake, ^{99m}Tc-P829 has been selected for clinical studies.

CONCLUSION

Both ^{99m}Tc-P587 and ^{99m}Tc-P829 have been shown to have high SSTR-binding affinity and high, receptor-specific and saturable in vivo tumor uptake, and biodistribution characteristics favorable to early imaging. These observations support the clinical investigation of ^{99m}Tc-P587 and ^{99m}Tc-P829 as radiotracers for the detection of SSTR-expressing tumors and other tissues by gamma scintigraphy.

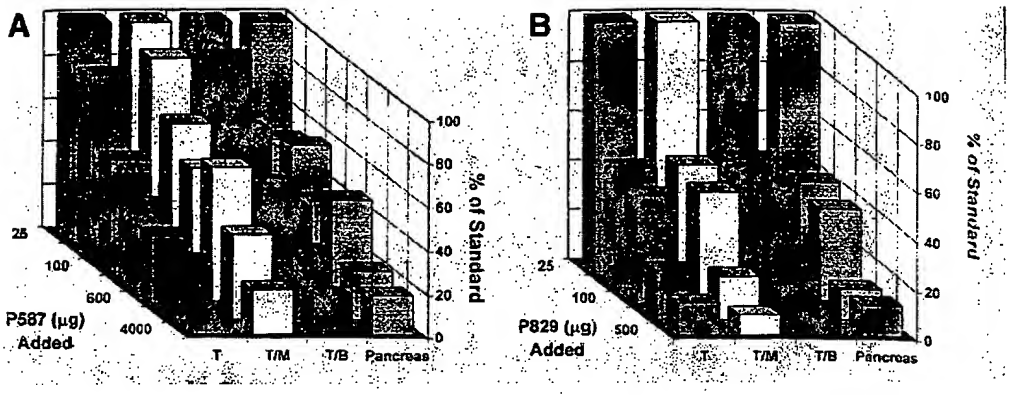

FIGURE 4. Effect of increasing amounts of co-injected cold peptide on the tumor uptake of ^{99m}Tc-peptides in CA20948 tumor-bearing rats. (A) ^{99m}Tc-P587 (top) and (B) ^{99m}Tc-P829. Tumor % ID/g (T), tumor:muscle (T/M), tumor:blood (T/B) and %ID in pancreas were plotted as percent of value observed with a standard (no additional cold peptide) ^{99m}Tc-peptide preparation.

ACKNOWLEDGMENTS

We thank Dr. John E. Taylor, of Biomeasure, Inc., for performing the in vitro assays and Dr. Arthur E. Bogden, also of Biomeasure, Inc., for preparing the animal model.

REFERENCES

1. Krenning EP, Kwekkeboom DW, Bakker WH, et al. Somatostatin receptor scintigraphy with [^{111}In-DTPA-D-Phe^1]- and [^{123}I-Tyr^3]-octreotide: the Rotterdam experience with more than 1000 patients. *Eur J Nucl Med* 1993;20:716–731.
2. Brazeau P, Vale W, Burgus R, et al. Hypothalamic polypeptide that inhibits the secretion of immunoreactive pituitary growth hormone. *Science* 1973;179:77–79.
3. Vale W, Brazeau P, Rivier C, et al. Somatostatin. *Recent Prog Horm Res* 1975;31: 365–397.
4. Yamada Y, Post SR, Wang K, et al. Cloning and functional characterization of a family of human and mouse somatostatin receptors expressed in brain, gastrointestinal tract and kidney. *Proc Natl Acad Sci USA* 1992;89:251–255.
5. Rens-Domiano S, Law SF, Yamada Y, et al. Pharmacological properties of two cloned somatostatin receptors. *Mol Pharmacol* 1992;42:28–34.
6. Raynor K, Murphy WA, Coy DH, et al. Cloned somatostatin receptors: identification of subtype-selective peptides and demonstration of high affinity binding of linear peptides. *Mol Pharmacol* 1993;43:838–844.
7. Raynor K, O'Carroll A-M, Kong H, et al. Characterization of cloned somatostatin receptors SSTR4 and SSTR5. *Mol Pharmacol* 1993;44:385–392.
8. Lamberts SWJ, Krenning EP, Reubi J-C. The role of somatostatin and its analogs in the diagnosis and treatment of tumors. *Endocrine Rev* 1991;12:450–482.
9. Reubi J-C, Krenning E, Lamberts SWJ, Kvols L. Somatostatin receptors in malignant tissues. *J Steroid Biochem Molec Biol* 1990;37:1073–1077.
10. Eden PA, Taylor JE. Somatostatin receptor subtype gene expression in human and rodent tumors. *Life Sci* 1993;53:85–90.
11. Reubi JC, Schaer JC, Waser B, Mengod G. Expression and localization of somatostatin receptor SSTR1, SSTR2 and SSTR3 messenger RNAs in primary human tumors using in situ hybridization. *Cancer Res* 1994;54:3455–3459.
12. Bauer W, Briner U, Doepfner W, et al. SMS 201-995: a very potent and selective octapeptide analog of somatostatin with prolonged action. *Life Sci* 1982;31:1133–1140.
13. Pless J, Bauer W, Briner U, et al. Chemistry and pharmacology of SMS 201-995, a long-acting octapeptide analog of somatostatin. In: Molinatti GM, Martinin L, Elsevier, eds. *Endocrinology '85*. New York, NY: 1986:319–333.
14. Murphy W, Lance VA, Moreau S, et al. Inhibition of rat prostate tumor growth by an octapeptide analog of somatostatin. *Life Sci* 1987;40:2515–2522
15. Veber DF, Saperstein R, Nutt RF, et al. *Science* 1984;34:1371.
16. Veber DF, Saperstein R, Nutt RF, et al. A super active cyclic peptide analog of somatostatin. *Life Sci* 1984;34:1371–1378.
17. Bakker WH, Kreening EP, Breeman WAP, et al. In vivo use of a radiolabeled somatostatin analog: dynamics, metabolism and binding to somatostatin receptor-positive tumors in man. *J Nucl Med* 1991;32:1184–1189.
18. Krenning EP, Bakker WH, Kooij PPM, et al. Somatostatin receptor scintigraphy with In-111-DTPA-D-Phe-1-octreotide in man: metabolism, dosimetry and comparison with I-123-Tyr-3-octreotide. *J Nucl Med* 1992;33:652–658.
19. Kvols LK, Brown ML, O'Connor MK, et al. Evaluation of a radiolabeled somatostatin analog (I-123 octreotide) in the detection and localization of carcinoid and islet cell tumors. *Radiology* 1993;187:129–133.
20. Lister-James J, McBride WJ, Moyer BR, et al. A structure-activity-relationship (SAR) study of somatostatin receptor-binding peptides radiolabeled with Tc-99m. *J Nucl Med* 1994;35:257P.
21. Cotton FA, Lippard SJ. Chemical and structural studies of the rhenium(V) oxyhalide complexes. I. Complexes from rhenium(III) bromide. *Inorg Chem* 1966;5:9–16.
22. Bylund DB, Yamamura HI. Methods for receptor binding. In: Yamamura HI, et al. eds. *Methods in neurotransmitter receptor analysis* New York, NY: Raven Press; 1990:1–35.
23. Bakker WH, Krenning EP, Reubi JC, et al. In vivo application of [^{111}In-DTPA-D-Phe^1]-octreotide for the detection of somatostatin receptor-positive tumors in rats. *Life Sci* 1991;49:593–1601.
24. Maina T, Stolz B, Albert H, et al. Synthesis, radiochemistry and biological evaluation of a new somatostatin analog (SDZ 219-387) labeled with technetium-99m *Eur J Nucl Med* 1994;21:437–444.
25. Huang Z, He Y-B, Raynor K, et al. Main chain and side chain chiral methylated somatostatin analogs: syntheses and conformational analyses. *J Am Chem Soc* 1992;114:9390–9401.
26. Fritzberg AR, Kasina S, Eshima D, Johnson DL. Synthesis and biological evaluation of technetium-99m MAG_3 as a hippuran replacement. *J Nucl Med* 1986;27:111–116.
27. Rao TN, Adhikesavalu D, Camerman A, Fritzberg AR. Technetium (V) and rhenium (V) complexes of 2,3-bis(mercaptoacetamido)propanoate. Chelate ring stereochemistry and influence on chemical and biological properties. *J Am Chem Soc* 1990;112: 5798–5804.
28. Bakker WH, Albert R, Bruns C, et al. [^{111}In-DTPA-D-Phe^1]-octreotide, a potential radiopharmaceutical for imaging of somatostatin receptor-positive tumors: synthesis, radiolabeling and in vitro validation. *Life Sci* 1991;49:1583–1591.
29. Lastoria S, Muto P, Acampa S, et al. Imaging of human tumors expressing somatostatin receptors with a novel synthetic peptide P587 labeled with ^{99m}Tc *Radiology* 1994;193P:300.

JOURNAL OF BIOMOLECULAR SCREENING
Volume 5, Number 2, 2000

Development of High Throughput Screening Assays Using Fluorescence Polarization: Nuclear Receptor-Ligand–Binding and Kinase*/Phosphatase Assays

GREGORY J. PARKER, TONG LIN LAW, FRANCIS J. LENOCH, and RANDALL E. BOLGER

ABSTRACT

Fluorescence polarization (FP) has been used to develop high throughput screening (HTS) assays for nuclear receptor-ligand displacement and kinase inhibition. FP is a solution-based, homogeneous technique requiring no immobilization or separation of reaction components. The FP-based estrogen receptor (ER) assay is based on the competition of fluorescein-labeled estradiol and estrogen-like compounds for binding to ER. These studies determined the K_d for this interaction to be 3 nM for ERα and 2 nM for ERβ; IC_{50} values for 17β-estradiol, tamoxifen, 4-OH-tamoxifen, and diethylstibestrol were determined to be 5.6, 189, 26, and 3.5 nM, respectively. In a screen of 50 lead compounds from a transcriptional activation screen, 21 compounds had IC_{50} values below 10 μM, with one having an almost 100-fold higher affinity for ERβ over ERα. These data show that an FP-based competitive binding assay can be used to screen diverse compounds with a broad range of binding affinities for ERs. The FP-based protein-tyrosine kinase (PTK) assay uses fluorescein-labeled phosphopeptides bound to anti-phosphotyrosine antibodies. Phosphopeptides generated by a kinase compete for this binding. In c-Src kinase reactions, polarization decreased with time as reaction products displaced the fluorescein-labeled phosphopeptide from the anti-phosphotyrosine antibodies. The experimentally determined IC_{50} of AG 1478 was 400 pM, while Genistein did not inhibit the epidermal growth factor receptor at similar concentrations. Like the FP-based PTK assay, the protein kinase C (PKC) assay utilizes competition. PKC isoforms had different turnover rates for the peptide substrate. The IC_{50} for staurosporine was less than 10 nM for all PKC isoforms. Tyrosine phosphatase assays use direct binding rather than competition. Increasing concentrations of T-cell protein–tyrosine phosphatase (TC PTP) increased the rate of dephosphorylation. This change in polarization was dependent on TC PTP and was inhibited by 50 μM Na_3VO_4. The IC_{50} of Na_3VO_4 was 4 nM for TC PTP. These data demonstrate that a FP-based assay can detect kinase and phosphatase activity. Homogeneous, fluorescent techniques such as FP are now methods of choice for screening many types of drug targets. New HTS instrumentation and assay methods like these make FP a technology easily incorporated into HTS.

INTRODUCTION

THE TREMENDOUS CHALLENGE facing the high throughput screening (HTS) scientist today is to screen more compounds against more targets using more quantitative and robust methods, without spending more money. Genomics efforts have flooded drug discovery with potential new drug targets.[1] New parallel combinatorial synthesis methods are providing more compounds that in turn must be screened for activity.[2] The process for identifying new lead compounds has to become more efficient. In order to increase the efficiency of HTS, new screening methods must be faster, cheaper, and more quantitative. Assays need to be miniaturized to decrease reagent costs and consumption of compound libraries. New assay formats must be homogeneous, requiring no separation of reaction components. Fluorescence methods are rapidly becoming the primary detection format in HTS[3] because they now approach the sensitivity of radioactive methods and are amenable to homogeneous, miniaturized formats. This report focuses on fluorescence polarization (FP) and how this technique is being used to improve HTS assays today.

PanVera Corporation, Madison, WI.
*Patent pending, PanVera Corporation.

EXHIBIT G

Theory of fluorescence polarization

FP is used to study molecular interactions by monitoring changes in the apparent size of fluorescently labeled or inherently fluorescent molecules.[4–6] When a small fluorescent molecule (tracer) is excited with plane-polarized light, the emitted light is largely depolarized because the molecule rotates rapidly in solution during the fluorescence lifetime (the time between excitation and emission). However, if the tracer is bound to a larger receptor, thereby increasing its effective molecular volume, its rotation is slowed sufficiently to emit light in the same plane in which it was excited. The bound and free states of the tracer each have an intrinsic FP value, a high value for the bound state and a low value for the free state. The measured polarization is a weighted average of the two values, thus providing a direct measure of the fraction of tracer bound to receptor. An increase in molecular volume resulting from receptor-ligand,[7] DNA-protein,[8,9] or peptide-protein[10] binding or a decrease in molecular volume resulting from dissociation or enzymatic degradation[11,12] can be followed by FP.

FP enables the researcher to view molecular binding events in solution. It is a truly homogeneous technique in that no separation of bound and free species is necessary. Methods requiring separation are not only more time consuming, but they disturb the reaction equilibrium and therefore prevent accurate qualification of binding. Other fluorescence techniques are homogeneous, such as fluorescence resonance energy transfer (FRET) and homogeneous time-resolved fluorescence[3] (HTRF®; Packard Instrument Company, Meriden, CT). However, these techniques require multiple labeling reactions instead of one as in FP. Also, because the readout for FRET and HTRF is fluorescence intensity, there is a higher probability for artifacts from quenching and exogenous fluorescence. FP is a ratiometric measurement and therefore less sensitive to these sources of interference.

Assay development using fluorescence polarization

FP is best suited to observe the binding of small fluorescent molecules (<10 kDa) to larger proteins. The smaller the fluorescent molecule, the larger the dynamic range of the assay. Fluorescent labeling of peptides and DNA oligos is straightforward and can even be performed during synthesis. Labeling other small molecules is sometimes more involved, often requiring multiple attempts using a range of chemistries at multiple sites on the molecule. FP differs from other binding assay formats in that it detects the fraction bound of the small, fluorescent molecule (tracer) instead of the large molecule (receptor). Thus it requires saturating the tracer with receptor instead of the inverse approach used in most binding experiments. For this reason, FP requires large amounts of relatively pure protein. Two assay formats that have been particularly well suited to FP are receptor-ligand–binding assays and enzyme assays where the product can be quantified by competitive immunoassay. This article describes the development of two such assays: a ligand displacement assay for estrogen receptors (ERs) α and β, and competitive immunoassays for protein-tyrosine kinases (PTKs) and protein kinase C (PKC) family members.

Ligand displacement assays for estrogen receptors

Estrogen receptors (ERα and ERβ) are transcription factors that regulate the expression of genes involved in tissue growth and differentiation in diverse target tissues, including reproductive, skeletal, cardiovascular, and mammary tissue.[13–16] Estrogen acts by binding to ER, resulting in the transcriptional control of a variety of genes in target cells. Pharmacologists are looking for new estrogens and antiestrogens to treat a host of disorders such as breast cancer, Alzheimer's disease, cardiovascular disease, osteoporosis, type II diabetes, and urinary incontinence.[17]

Historically, estrogen activity has been assessed using *in vivo* assays, including whole animal[18] or cell-based assays such as proliferation in a breast carcinoma cell line[19] and induction of reporter gene expression from an estrogen-response element transfected into yeast or mammalian cells.[20] These require extensive manipulations of animals or live cells and response times of several hours to days. The time and extensive labor required for the *in vivo* method preclude their use in HTS.

In contrast, molecular ligand-binding assays are faster, more precise, and less labor intensive than *in vivo* assays because they are performed *in vitro* with isolated components. Molecular assays are not limited by toxicity or cell permeability of the test compounds, factors that limit the type of compounds and concentrations that can be tested in a cell-based assay. To develop ligand-binding assays more suited to a HTS format, investigators have begun using various types of FlashPlate™ (NEN® Life Science Products, Boston, MA) or scintillation proximity assays (SPA, Amersham Pharmacia Biotech AB, Uppsala, Sweden). Receptor and the scintillant are bound to a solid phase to ensure that only the receptor-bound labeled estrogen, and not the excess free ligand, is close enough to excite the scintillant.[21] These approaches require no separation of bound and free ligand, but still rely on the use of radioisotopes and immobilization of the receptor, which could cause disadvantageous conformational changes. These shortcomings prevent the widespread adaptation of current ligand-binding assays to HTS formats.

The FP-based ER assay is a homogeneous, fluorescent assay requiring no immobilization and is well suited for HTS. Fluorescein-labeled estradiol and estrogen-like compounds compete for binding to the estrogen receptor. When there are no competing compounds present, the fluorescein-labeled estradiol will be bound by the estrogen receptor, resulting in a high FP value. However, in the presence of estrogen-like competitors, the fluorescein-labeled estradiol is displaced from the estrogen receptor, resulting in a decreased FP value. Because the observed FP value is a weighted average of the FP values of the individual bound and free tracer and therefore is a direct measure of the fraction bound, polarization may be plotted against the logarithm of the compound concentration to determine the IC_{50} for the compound under the assay conditions tested. Figure 1 illustrates these principles.

Protein-tyrosine kinases assays

PTKs catalyze the transfer of a high-energy phosphoryl group from ATP to the hydroxyl group of a tyrosine, whereas tyrosine phosphatases cleave the phosphate from phosphotyrosine. Phosphorylation appears to be the "master" biochemical

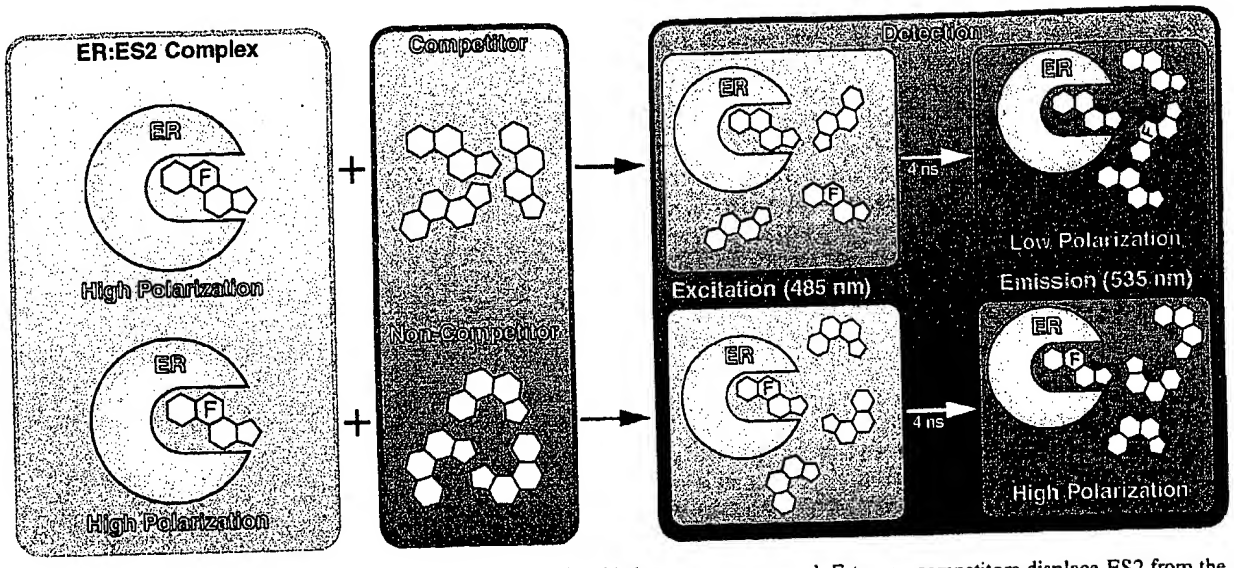

FIG. 1. In the ER competitor assays, an ER-ES2 complex is added to a test compound. Estrogen competitors displace ES2 from the ER-ES2 complex, causing ES2 to tumble rapidly during its 4-ns fluorescence lifetime, resulting in a reduced FP value. Noncompetitors will not displace the ES2 from the ER-ES2 complex, so the FP value remains high. The shift in polarization in the presence of test compounds is used to determine the relative affinity of test compounds for ERα or ERβ.

reaction in signal transduction, and it has been estimated that at least one third of the proteins in the average mammalian cell are phosphorylated.[22] The regulated and reversible phosphorylation of tyrosines is critical to the normal regulation of many biological mechanisms, including cell growth, proliferation, differentiation, motility, transcription, synaptic function, and metabolism.[22–24]

There have been more than 95 PTKs and 55 tyrosine phosphatase genes found in humans.[23] Defects in these signal transduction pathways can result in a number of human diseases, including cancer.[22,24] For example, in the case of the epidermal growth factor (EGF) receptor, overexpression and mutation have been associated with some of the most incurable cancers, including glial and pancreatic tumors.[26–27] The development of anticancer agents based on the inhibition of EGF binding to the receptor, however, has had limited success.[28] Efforts to screen for new tyrosine kinase inhibitors have been hindered by the lack of robust, high throughput tyrosine kinase assays.

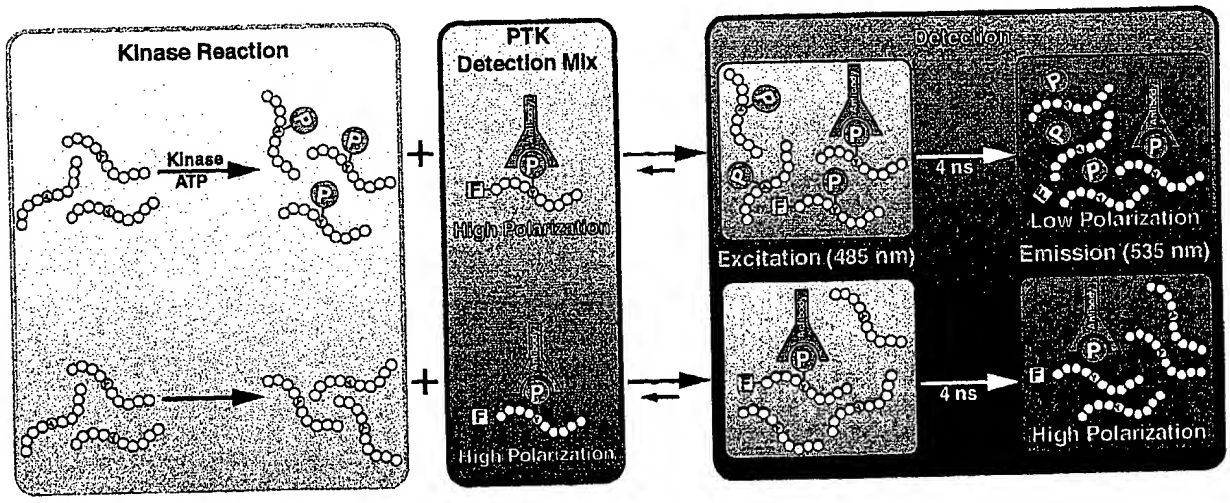

FIG. 2. This figure captures the general theme of the FP-based competitive immunoassay for PTK activity. In the top reaction, the addition of a tyrosine kinase and ATP leads to the phosphorylation (P) of the peptide substrate on a tyrosine residue (Y). After the reaction is quenched, the PTK Detection Mix, which has a high polarization and contains an anti-pY Ab (Antibody) bound to a fluorescein-labeled (F) phosphopeptide tracer, is added and the system reaches equilibrium. In the detection phase of the experiment, the tracer is displaced from the anti-pY Ab by kinase reaction products, causing the tracer to tumble rapidly during its 4 ns fluorescence lifetime, resulting in a low FP signal. When no kinase reaction products are present, the tracer-antibody complex remains intact, with no change in the high FP value.

Current tyrosine kinase assay formats include ELISA- and radioimmunoassay-based methods. These methods require immobilization of reaction components on plates, as well as multiple separation and washing steps, making them difficult to implement in HTS. Although radioactive methods are very sensitive, they create significant radioactive waste. Newer homogeneous methods now in use include SPA[29] and HTRF.[30] SPA is a radioactive technique requiring immobilization, and HTRF requires labeling and characterizing multiple assay components.

The FP-based PTK assay is a homogeneous, fluorescent assay requiring no immobilization that is well suited for HTS. A fluorescein-labeled phosphopeptide (tracer) and any unlabeled phosphopeptides generated during a kinase reaction compete for binding to anti-phosphotyrosine antibodies (anti-pY Ab). When there are no kinase reaction products present, the tracer will be bound by the anti-pY Ab, resulting in a high FP value. However, after a PTK reaction has occurred, reaction products displace the tracer from the anti-pY Ab, resulting in a decreased FP value. The observed FP value is a weighted average of the FP values of the individual bound and free tracer and therefore is a direct measure of the fraction bound. If sufficient competitor phosphopeptide is generated during the PTK reaction, the tracer will be totally displaced from the anti-pY Ab and the emitted light will be totally depolarized. Thus the change in FP value is directly related to the amount of the PTK activity. These principles are diagrammed in Figure 2. Measurements can be made in real time, allowing the observed enzymatic activity to be monitored both kinetically or in an endpoint assay format.

The general principles described here can also be applied to a tyrosine phosphatase assay, which, like the kinase assay, can be monitored as either a kinetic or an endpoint assay. Phosphatase assays are slightly different from the competition-based PTK assays described earlier in that reaction progress is monitored using direct binding rather than competition. Because the tracer is dephosphorylated by a phosphatase, it can no longer be bound by the anti-pY Ab, increasing the free fraction and decreasing the polarization of the sample.

Protein kinase C assay

The phosphorylation of serine and threonine residues in proteins by PKC family members is critical to the normal regulation of many biological mechanisms, including the modulation of membrane structure, receptor desensitization, transcriptional control, cell growth and differentiation, and the mediation of immune response. PKCs also play a role in memory, learning, other long-term functions, and various pathological processes.[31–33] A number of studies have suggested that inappropriate activation of PKCs can contribute to cancer, inflammation, viral infection, immune and central nervous system disorders, cardiovascular malfunction, vascular complications of diabetes, and insulin resistance.[34] Therefore, identifying PKC inhibitors is essential to developing new therapies for these diseases.

Like the FP-based PTK assay, the principle behind the PKC assay is competition. Fluorescein-labeled phosphopeptide tracers and any unlabeled phosphopeptide products generated during a PKC reaction will compete with each other for binding to anti-phosphoserine antibodies. In a reaction mixture containing no phosphopeptide products, a significant portion of the fluorescent tracer will be bound by the antibody, resulting in a high polarization value. However, in a reaction mixture containing phosphopeptide products, some of the tracer will be displaced from the antibody and the emission signal will become depolarized. Therefore, the change in polarization is directly related to the amount of PKC activity in a reaction.

MATERIALS AND METHODS

FP-based ligand displacement assay for ERα and ERβ

The results of direct binding studies of a fluorescent estradiol to ERα or ERβ using the FP method are presented in Figure 3. The assay consists of recombinant, human ERα or ERβ (PanVera Corporation, Madison, WI), and a fluorescein-labeled estradiol, Fluormone™ ES2 (PanVera Corporation). Using a 96-well plate (DYNEX, Chantilly, VA) and Estrogen Screening Buffer (PanVera Corporation) as the diluent, a constant amount of ES2 was titrated with increasing concentrations of ERα or ERβ. The FP value was measured at each receptor concentration on a Polarion instrument (TECAN, Research Triangle Park, NC) using 483-nM excitation and 536-nM emission filters. These data were then used to determine the equilibrium binding constants.

Displacement of bound ES2 by estrogen ligands. Four compounds, 17β-estradiol, tamoxifen, its active metabolite 4-OH-tamoxifen, and diethylstilbestrol (DES), were obtained and tested for their ability to displace ES2 from an ERα- or ERβ-

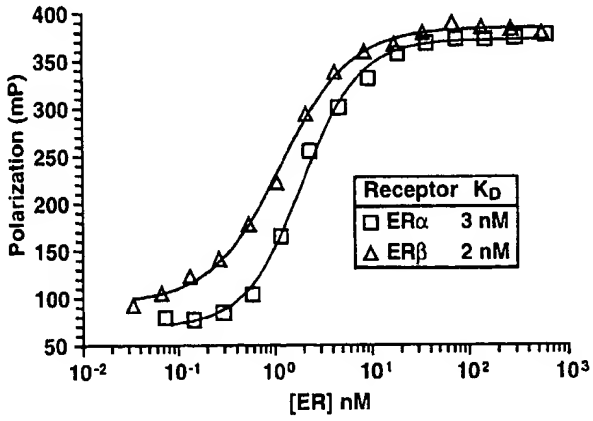

FIG. 3. A saturation-binding isotherm was generated in triplicate for ERα and ERβ binding to ES2. Both ERα and ERβ were diluted in buffer (100 mM potassium phosphate [pH 7.4] containing 100 μg/ml bovine gamma globulin [BGG]) to a final volume of 100 μl on a 96-well plate. ES2 was then added to each well to a final concentration of 1 nM. The plate was mixed and incubated at room temperature for 2 h. The polarization (mP, mean ± 1 standard deviation) was plotted against an increasing concentration of ER and the equilibrium binding constant (K_d) was calculated using nonlinear least squares analysis using Prism software. K_d values determined for ERα and ERβ were 3 nM and 2 nM, respectively.

ES2 complex. Because the large receptor-ligand complex tumbles slowly and has a high FP value, increasing concentrations of a competing ligand displace ES2 from ER. Free ES2 molecules are then able to tumble more rapidly and therefore have a low FP value. Because the measured polarization is the weighted average of the bound and free ES2 molecules, it can be directly used to calculate percent inhibition. All compounds were prepared as a 10 mM stock in DMSO (PanVera Corporation). In triplicate, tamoxifen (Sigma Chemical Co., St. Louis, MO), 4-OH-tamoxifen (Sigma), DES (Steraloids, Newport, RI), and 17β-estradiol (Sigma) were serially diluted in bovine gamma globulin/phosphate buffer (PanVera Corporation) on a 96-well plate (DYNEX). A mixture of either ERα or ERβ (PanVera Corporation) and Fluormone™ ES2 (PanVera Corporation) was added to the diluted inhibitors. The final concentration of ES2 in all wells was 1 nM. For ERα experiments, the final concentration of the receptor was 13 nM, while in ERβ experiments, the receptor was at a final concentration of 10 nM. The plate was then incubated at room temperature for 2 h. The polarization was measured on a TECAN Polarion using the recommended fluorescein filter set. The polarization (in millipolarization [mP]) was plotted against increasing concentrations of the test compounds. IC_{50} values were calculated using Prism® (GraphPad Software, Inc., San Diego, CA), a nonlinear least squares curve-fitting program.

ER competitor assays for HTS. As a feasibility study (and using techniques and reagents identical to those in the previous section), we tested 43 of our pharmaceutical collaborator's lead compounds from an ER-responsive gene reporter assay. Each plate tested contained several controls, including 17β-estradiol and DES. Our aim was to identify compounds selective for either ERα or ERβ.

Protein-tyrosine kinase assay

Reagent development for the FP-based PTK assay. The two critical components in the FP PTK assay are a fluorescent phosphopeptide tracer and an anti-pY Ab. In general, the antibody should bind the tracer with high affinity and exhibit a large shift in polarization between the bound and free tracer. High-affinity anti-pY antibodies enable use of lower concentrations in an assay. This is critical for both assay sensitivity and cost containment, considering both the cost of commercially available antibodies and the cost-per-well demands of HTS groups. Also, the anti-pY Ab used must be able to bind to both the tracer and phosphopeptide reaction products with similar affinity. For these assays, the tracer was synthesized by Genosys (The Woodlands, TX) and was optimized for maximum polarization shift, which included changing the sequence and length of the peptide, which was derived from a naturally occurring source. Further modifications could have included altering the fluorophore position or coupling chemistry. The goal was to maximize the dynamic range of the assay (polarization shift from bound to free tracer) without sacrificing affinity.

Kinetic and endpoint PTK assays. The PTK kinase assay was used to measure kinase activity of c-Src kinase (Signase, Houston, TX) in an endpoint mode. In a 96-well plate (DYNEX), parallel kinase reactions were run at room temperature for a maximum of 10 min in a final volume of 40 μl under the following conditions: 50 mM HEPES (pH 7.4), 6 mM $MgCl_2$, 0.1 ng/μl c-Src, 1.25 mM ATP, and 0.125 mg/μl poly(Glu, Tyr) 4:1 substrate (Sigma). Just after the addition of ATP to start the reaction and every 2 min after that, 10 μl of 100 mM EDTA was added to quench the reaction. After all of the reactions were quenched, 50 μl of the PTK Detection Mix (PanVera Corporation), which contains the F-phosphopeptide tracer–anti-pY Ab complex, was added to each well and the reaction was incubated for 5 min. The FP signal was then read at room temperature on a TECAN Polarion. Twenty hours later the polarization was read again to test the stability of a quenched PTK assay after the addition of the tracer–anti-pY Ab complex.

The activity of c-Src (Signase) was also assayed in the kinetic mode of the FP instrument by measuring the polarization signal in 1 min intervals over the duration of a 1-h experiment. In a 96-well plate (DYNEX), five separate kinase reactions were run at room temperature in a final volume of 100 μl. All reactions contained 50 μl of the PTK Detection Mix. The first three reactions contained either 1, 5, or 10 ng of c-Src (equal to 0.01, 0.05, and 0.1 ng/μl, respectively) with the following the reaction conditions: 50 mM HEPES (pH 7.4), 6 mM $MgCl_2$, 1.25 mM ATP, and 0.125 mg/μl poly(Glu, Tyr) 4:1 substrate (Sigma). Two control reactions were also run; one did not receive ATP, while the second did not receive the poly(Glu, Tyr) 4:1 substrate. ATP was added last to start each reaction.

Inhibition of EGF receptor by two compounds. By adding unknown compounds to the kinase reaction, inhibitors or activators can be screened and IC_{50} values established. Inhibition of the EGF receptor (PanVera Corporation) by two different compounds was examined. Compound AG 1478 has a published IC_{50} in the nanomolar range, while Genistein inhibits EGF receptor at micromolar concentrations. Both compounds were obtained from Calbiochem (San Diego, CA). In a black, round-bottom, 96-well plate (DYNEX), EGF receptor (PanVera Corporation) was preincubated with 2-fold serial dilutions of the inhibitors for 5 min; ATP was then added to start the reactions. Final conditions were 20 mM HEPES (pH 7.4), 5 mM $MgCl_2$, 2 mM $MnCl_2$, 50 μM Na_3VO_4, 1 nM EGF receptor, 1 mM ATP, 1% DMSO, and 1 mg/ml poly(Glu, Tyr) 4:1 (Sigma) substrate. The reaction was run for 2 h at room temperature and quenched with 20 mM EDTA. An equal volume of the PTK Detection Mix (PanVera Corporation) was added and the reaction was incubated for 5 min. The results were read at room temperature on a TECAN Polarion, and nonlinear regression analysis was performed on a semi-log plot of the data to determine the IC_{50} of each compound.

Protein-tyrosine phosphatase essay

The enzymatic activity of T-cell protein-tyrosine phosphatase (TC PTP) was measured in a dose-dependent manner by incubating different concentrations of TC PTP (New England Biolabs, Beverly, MA), from 0.05 U/μl to 0.0005 U/μl, with 50 μl of the PTK Detection Mix (PanVera Corporation) in a final volume of 100 μl. Two control assays were performed: one did not receive TC PTP, while the other was supplemented with 50 μM Na_3VO_4 (Sigma), a potent phosphatase inhibitor.

Inhibition of TC PTP by sodium vanadate. The IC_{50} values for Na_3VO_4 and TC PTP were determined in the following manner. In a 96-well plate (DYNEX), Na_3VO_4 (Sigma) was serially diluted 2-fold into 24 wells from a starting concentration of 500 nM in a volume of 50 μl. TC PTP was then added to each well so that the final concentration of the enzyme would be 0.005 U/μl per assay. To start the reaction, 50 μl of the PTK Detection Mix (PanVera Corporation) was added, and each reaction was incubated for 15 min. At the end of the incubation, 10 μl of 550 μM Na_3VO_4 was added to quench all of the reactions, and the polarization for each sample was measured on a TECAN Polarion. Nonlinear regression analysis of a semi-log plot of the data was used to analyze these data.

Protein kinase C assay

Reagent development for the FP-based PKC assay. The PKC assay requires two main reagents and four general steps. The reagents are very similar to those of the PTK assay. A fluorescein-labeled phosphoserine-containing peptide and an antibody that recognizes this phosphopeptide are required. For this assay to work, the tracer must be competitively displaced from the antibody by unlabeled phosphopeptides or phosphoproteins.

When performing the assay, the kinase, lipids, calcium, magnesium, fluorescent tracer, peptide substrate, and potential PKC inhibitor are combined. Next, ATP is added to start the reaction. Following an incubation period, a quench/detection mixture containing EDTA and anti-phosphoserine antibody is added to stop the kinase reaction and initiate the competition for antibody binding. Finally, polarization values are measured to determine the extent of PKC activity in the reaction.

Measuring the enzymatic activity of seven PKC isoforms. Using this basic experimental procedure, a dilution series of seven PKC isoforms (PanVera Corporation) were tested to determine the amount of each isoform required to achieve the necessary turnover in a 90-min reaction. The final amount of each PKC isoform ranged from 10 pg to 20 ng per well. After a 5-min incubation with additional PKC reaction components, ATP was added to initiate the reactions. Final reaction conditions (for a 50-μl total reaction volume) were 20 mM HEPES (pH 7.4), 10 mM $MgCl_2$, 100 μM $CaCl_2$, 0.1 mg/ml phosphatidylserine, 0.02 mg/ml diacylglycerol, 2 μM peptide substrate, 2× PKC fluorescent phosphopeptide tracer, 50 μM sodium vanadate, and 10 μM ATP.

After a 90-min incubation at room temperature, 50 μl of a quench/detection mixture (containing 130 mM EDTA and anti-phosphoserine antibodies) was added to each well to stop the reaction and initiate the competition for antibody binding. Following an additional 30-min incubation at room temperature, the FP of each well was measured on a TECAN Polarion.

Inhibition of PKC isoforms by staurosporine. Staurosporine IC_{50} values were determined for six PKC isoforms using the amount of each isoform required for sufficient reaction turnover. In a round-bottom, 96-well plate, PKC isoforms (15 ng PKCα, 300 ng PKCβI, 300 ng PKCβII, 17 ng PKCγ, 117 ng PKCδ, and 65 ng PKCϵ) were individually incubated with serial dilutions of staurosporine (Calbiochem) for 5 min at room temperature. ATP was then added to start the reactions. Final reaction conditions (for 50-μl total reaction volumes) were 20 mM HEPES (pH 7.4), 10 mM $MgCl_2$, 100 μM $CaCl_2$, 0.1 mg/ml phosphatidylserine, 0.02 mg/ml diacylglycerol, 2 μM peptide substrate, 2× PKC fluorescent phosphopeptide tracer, 50 μM sodium vanadate, 0.02% NP40, and 10 μM ATP. After a 90-min incubation at room temperature, 50 μl of a quench/detection mixture (containing 130 mM EDTA and the anti-phosphoserine antibody) was added to stop each reaction and initiate the competition for antibody binding. Results were measured on a TECAN Polarion, and nonlinear regression analysis was performed on a semi-log plot of the data.

RESULTS

Estrogen receptor assays

The FP value was measured at each receptor concentration and was used to calculate the equilibrium binding constants for each receptor. Using the log of the receptor concentration and polarization (mP), nonlinear regression analysis determined the K_d to be 3 nM for ERα and 2 nM for ERβ (Fig. 3).

IC_{50} values for 17β-estradiol, tamoxifen, 4-OH-tamoxifen, and DES, calculated using a nonlinear least squares curve-fit-

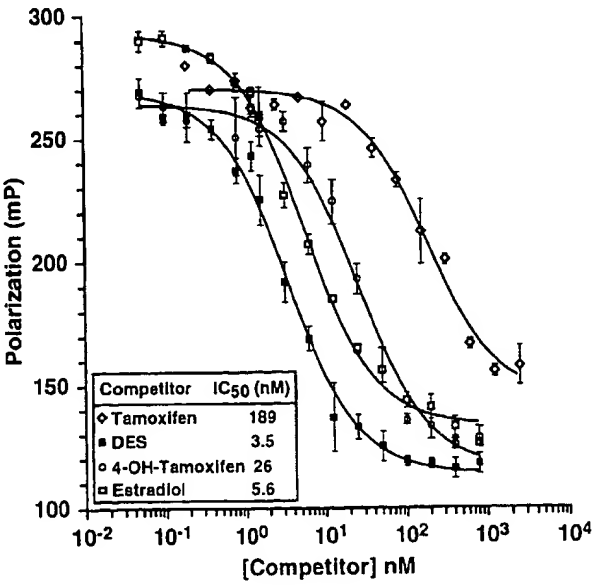

FIG. 4. The affinities of a panel of known estrogen ligands for ERβ were determined by their ability to displace the fluorescent ligand ES2 from ERβ using the FP-based competition assay. All compounds were prepared as a 10 mM stock in DMSO. Tamoxifen, its active metabolite 4-OH-tamoxifen, DES, and 17β-estradiol were serially diluted in BGG/phosphate buffer on a 96-well plate. A mixture of either ERα or ERβ and ES2 was added to the diluted inhibitors to a final concentration of 13 nM for ERα, 10 nM for ERβ, and 1 nM for ES2, and incubated at room temperature for 2 h. The polarization was measured on a TECAN Polarion using the recommended fluorescein filter set. The polarization (mP) was plotted against the log of the test compound concentration with Prism software. The IC_{50} values were calculated using a nonlinear least squares curve-fitting program.

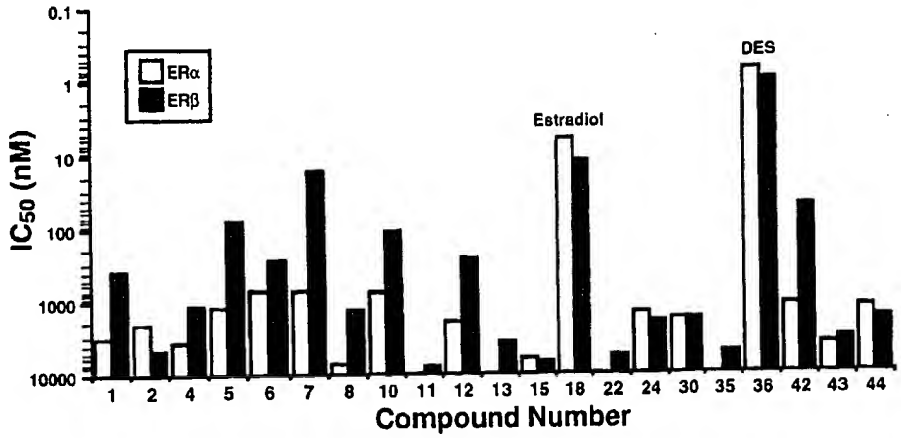

FIG. 5. Binding affinities of 43 lead compounds from an ER-responsive gene reporter assay and 7 controls were determined in a blind study using the FP assay. All compounds were prepared as a 10 mM stock in DMSO. The compounds were then serially diluted in BGG/phosphate buffer on a 96-well plate. A mixture of either ERα or ERβ and ES2 was added to the diluted inhibitors to a final concentration of 13 nM or ERα, 10 nM for ERβ, and 1 nM for ES2, and incubated at room temperature for 2 h; the polarization was then measured on a TECAN Polarion. The polarization (mP) was plotted against the log of the compound concentration with Prism software, and the IC_{50} values were calculated using a nonlinear least squares curve-fitting program. Of the original 50 compounds tested, those with IC_{50} values lower than 10 μM, including estradiol and DES, are plotted here. Higher bars represent higher affinity binding.

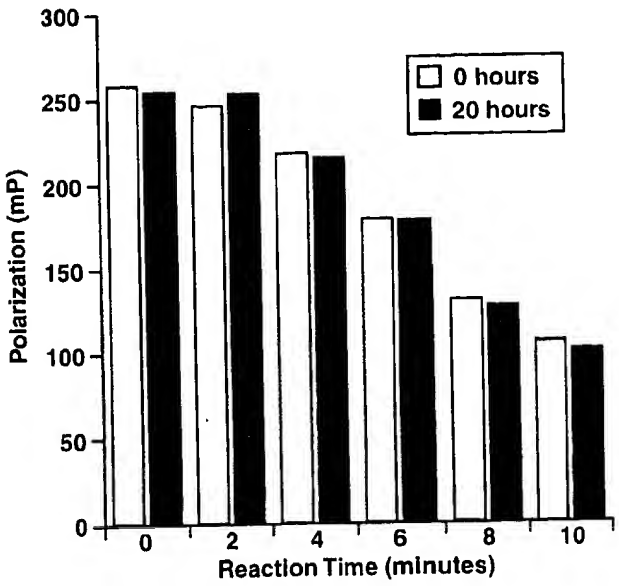

FIG. 6. The PTK activity of the tyrosine kinase c-Src was assayed by measuring the change in FP signal over time in an endpoint experiment. In a 96-well plate, parallel kinase reactions were run at room temperature for a maximum of 10 min in a final volume of 40 μl under the following conditions: 50 mM HEPES (pH 7.4), 6 mM $MgCl_2$, 0.1 ng/μl c-Src, 1.25 mM ATP, and 0.125 mg/μl poly(Glu, Tyr) 4:1 substrate. Just after the addition of ATP to start the reaction and every 2 min after that, 10 μl of 100 mM EDTA was added to quench the reaction. After all of the reactions were quenched, 50 μl of tracer: Ab complex, was added to each well and the reaction was incubated for 5 min. The FP signal was then read at room temperature on a TECAN Polarion. Twenty hours later, the polarization was read again to test the stability of a quenched PTK assay after the addition of the tracer–anti-pY Ab complex.

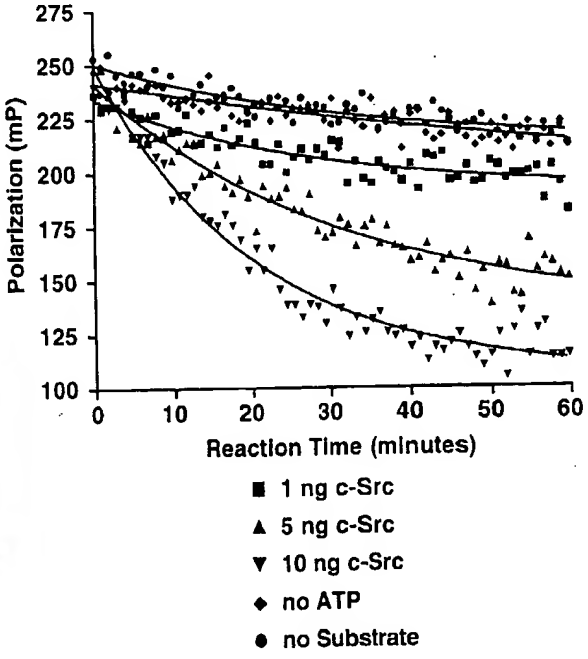

FIG. 7. The PTK activity of c-Src was also assayed in the kinetic mode of the FP instrument by measuring the polarization signal in 1-min intervals over the duration of a 1-h experiment. In a 96-well plate, five separate kinase reactions were run at room temperature in a final volume of 100 μl. All reactions contained 50 μl of the PTK Detection Mix. The first three reactions contained either 1, 5, or 10 ng of c-Src (equal to 0.01, 0.05, and 0.1 ng/μl, respectively), with the following reaction conditions: 50 mM HEPES (pH 7.4), 6 mM $MgCl_2$, 1.25 mM ATP, and 0.125 mg/μl poly(Glu, Tyr) 4:1 substrate. Two control reactions were also run; one did not receive ATP, while the second did not receive the poly(Glu, Tyr) 4:1 substrate. ATP was added last to start each reaction.

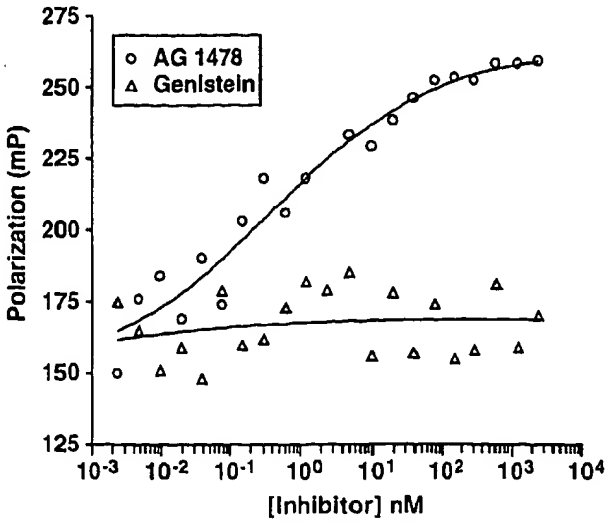

FIG. 8. In a black, round-bottom, 96-well plate, the EGF receptor was preincubated with 2-fold serial dilutions of either AG 1478 or Genistein for 5 min. ATP was then added to start the reactions. Final conditions were 20 mM HEPES (pH 7.4), 5 mM $MgCl_2$, 2 mM $MnCl_2$, 50 μM Na_3VO_4, 1 nM EGF receptor, 1 mM ATP, 1% DMSO, and 1 mg/ml poly(Glu, Tyr) 4:1 substrate. The reaction was run for 2 h at room temperature and quenched with 20 mM EDTA. An equal volume of the PTK Detection Mix was added and the reaction was incubated for 5 min. The polarization of each well was read on a TECAN Polarion, and nonlinear regression analysis was performed on a semi-log plot of the data to determine the IC_{50} of each compound.

ting program (GraphPad), were determined to be 5.6, 189, 26, and 3.5 nM, respectively (Fig. 4).

In Figure 5, only the 21 compounds with IC_{50} values below 10 μM are shown. Note that higher bars represent higher affinity binding. As hoped, several of these lead compounds exhibited receptor isozyme selectivity. For example, compound 7 has an almost 100-fold higher affinity for ERβ over ERα. Two controls, estradiol (compound 18) and DES (compound 36) are also shown. As expected, both of these compounds are high-affinity competitors of both estrogen receptors.

Kinase assays

As shown in Figure 6, in an endpoint c-Src kinase reaction, polarization decreases with time as products from the kinase reaction (phosphopeptides) displace the tracer from the anti-pY Ab. The polarization changed from an initial value of 250 mP to approximately 100 mP over 10 min. The second set of data, obtained 20 h after the addition of EDTA and the PTK Detection Mix, demonstrates the stability of the quenched kinase reactions and the PTK Detection Mix reagents.

In Figure 7, the kinetic c-Src experiment also shows that polarization decreases with time. These data were collected in real time. The "no ATP" control reaction demonstrates that this reaction, and the subsequent decrease in polarization, is phosphate donor dependent, as expected. The "no substrate" control, when compared to the "no ATP" control, indicates that autophosphorylation of c-Src and/or phosphorylation of the anti-pY Ab do not contribute a detectable amount of competitor phosphotyrosine in this assay.

As Figure 8 shows, the experimentally determined IC_{50} of AG 1478, known to inhibit the EGF receptor at nanomolar concentrations, was 400 pM. Genistein, which is a much weaker inhibitor of the EGF receptor, did not inhibit the EGF receptor at the concentrations tested, as expected.

The results obtained in a kinetic tyrosine phosphatase experiment when using TC PTP are shown in Figure 9. Increasing concentrations of TC PTP result in an increased rate of dephosphorylation, which is indicated by a decrease in polarization. This change in polarization was dependent on the presence of TC PTP and could be completely inhibited by 50 μM Na_3VO_4.

The IC_{50} of an unknown phosphatase inhibitor can also be established with this assay, as illustrated in Figure 10. In this experiment, the IC_{50} of the ubiquitous phosphatase inhibitor Na_3VO_4 was determined to be 4 nM for TC PTP.

Figure 11 shows that each PKC isoform has a different turnover rate for this specific peptide substrate. In the control experiment, which contained no ATP and therefore no PKC reaction products, the polarization value was 225 mP (data not shown). This value represented the maximum possible polarization value for the assay. When various amounts of PKC isoforms were tested in the presence of ATP, the decrease in po-

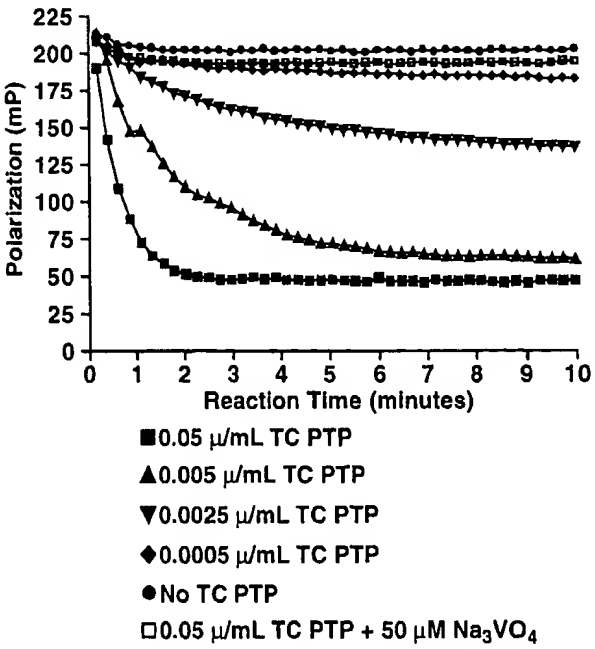

FIG. 9. The enzymatic activity of T-cell protein-tyrosine phosphatase (TC PTP) was measured in a dose-dependent manner by incubating concentration of TC PTP. The TC PTP concentration ranged from 0.05 to 0.0005 U/μl. Each well also contained 50 μl of the PTK Detection Mix in a final volume of 100 μl. Two control assays were performed: one did not receive TC PTP, while the other was supplemented with 50 μM Na_3VO_4, a potent phosphatase inhibitor. In both cases, no dephosphorylation occurred and the polarization remained high throughout the experiment.

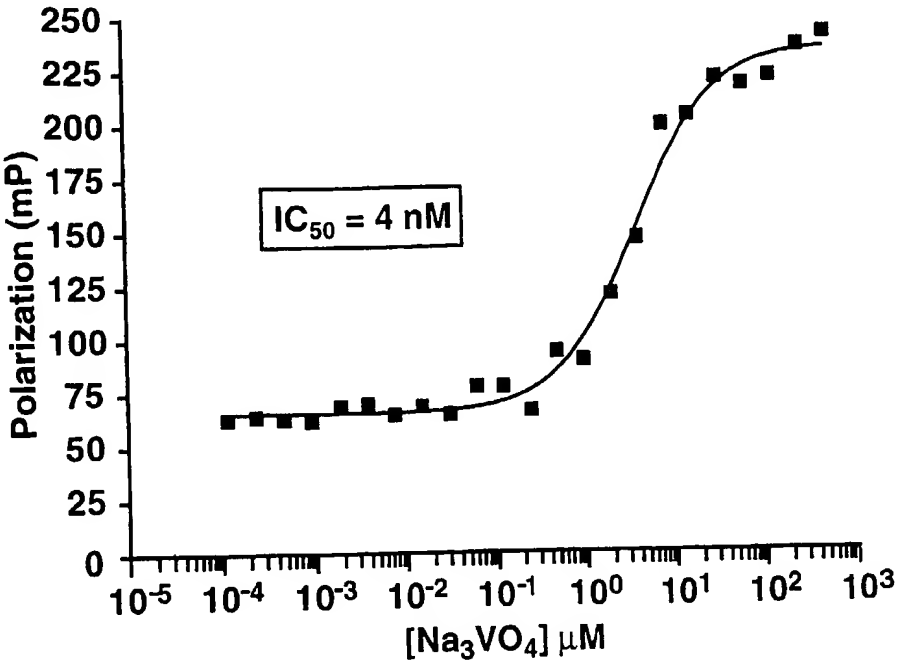

FIG. 10. The IC_{50} value for Na_3VO_4 and TC PTP was determined in the following manner. In a 96-well plate, Na_3VO_4 was serially diluted 2-fold into 24 wells from a starting concentration of 500 nM in a volume of 50 μl. TC PTP was then added to each well so that the final concentration of the enzyme would be 0.005 U/μl per assay. To start the reaction, 50 μl of the PTK Detection Mix was added, and each reaction was incubated for 15 min. At the end of the incubation, 10 μl of 550 μM Na_3VO_4 was added to quench all of the reactions, and the polarization for each sample was measured on a TECAN Polarion. Nonlinear regression analysis of a semi-log plot of the data was used to determine an IC_{50} of approximately 4 nM.

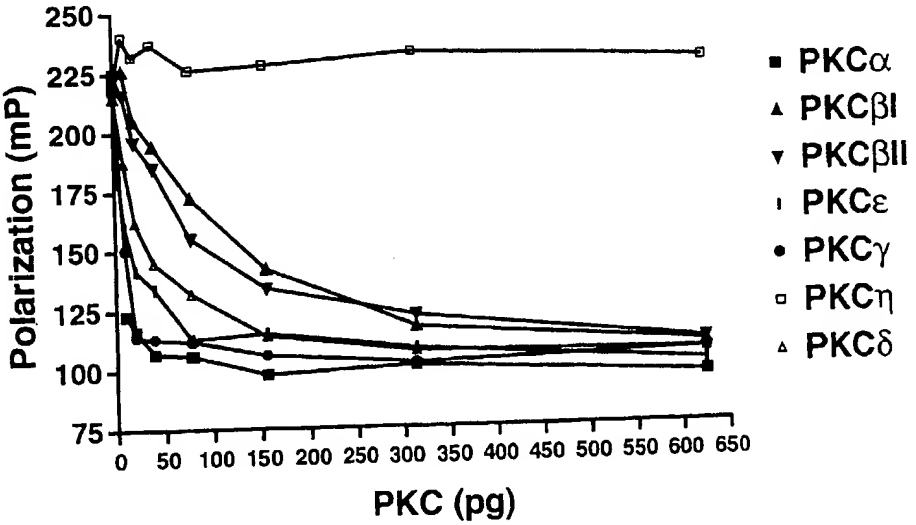

FIG. 11. Seven PKC isoforms were serially diluted in a 96-well plate. The final amount of each PKC ranged from 10 pg to 20 ng per well. After a 5-min incubation with additional PKC reaction components, ATP was added to initiate the reactions. Final reaction conditions (for a 50-μl total reaction volume) were 20 mM HEPES (pH 7.4), 10 mM $MgCl_2$, 100 μM $CaCl_2$, 0.1 mg/ml phosphatidylserine, 0.02 mg/ml diacylglycerol, 2 μM peptide substrate. 2× PKC fluorescent phosphopeptide tracer, 50 μM Na_3VO_4, and 10 μM ATP. After a 90-min incubation at room temperature, 50 μl of quench/detection mixture (containing 130 mM EDTA and anti-phosphoserine antibodies) was added to each well to stop the reaction and initiate the competition for antibody binding. Following an additional 30-min incubation at room temperature, the FP of each well was measured on a TECAN Polarion.

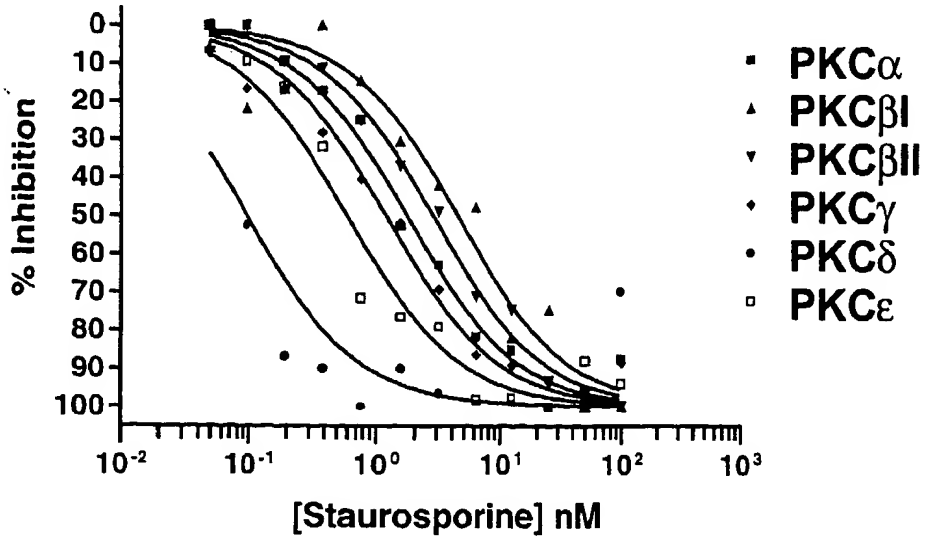

FIG. 12. In a round-bottom, 96-well plate, PKC isoforms (15 ng PKCα, 300 ng PKCβI, 300 ng PKCβII, 17 ng PKCγ, 117 ng PKCδ, and 65 ng PKCϵ) were individually incubated with serial dilutions of staurosporine for 5 min at room temperature. ATP was then added to start the reactions. Final reaction conditions (for 50-μl total reaction volumes) 20 mM HEPES (pH 7.4), 10 mM $MgCl_2$, 100 μM $CaCl_2$, 0.1 mg/ml phosphatidylserine, 0.02 mg/ml diacylglycerol, 2 μM peptide substrate, 2× PKC fluorescent phosphopeptide tracer, 50 μM Na_3VO_4, 0.02% NP40, and 10 μM ATP. After a 90-min incubation at room temperature, 50 μl of a quench/detection mixture (containing 130 mM EDTA and the anti-phosphoserine antibody) was added to stop each reaction and initiate the competition for antibody binding. Results were measured on a TECAN Polarion, and nonlinear regression analysis was performed on a semi-log plot of the data. The IC_{50} values of staurosporine were shown to be less than 10 nM for all PKC isoforms tested.

larization was directly proportional to the amount of PKC present in the reaction. Reactions containing the greatest amount of each PKC isoform produced the most unlabeled phosphopeptide products, which ultimately resulted in the lowest polarization values. The results show that 100 pg of most PKC isoforms can complete 50%–70% of the reaction after a 90-min incubation in the presence of ATP. From these data, it was estimated that 15 ng of PKCα, 300 ng of PKCβI, 300 ng of PKCβII, 17 ng of PKCγ, 117 ng of PKCδ, and 65 ng of PKCϵ would give approximately equal amounts of enzymatic activity over a 90-min period under these reaction conditions.

The results in Figure 12 show that the IC_{50} of staurosporine is less than 10 nM for all PKC isoforms tested, with PKCδ being the most potentially inhibited. This correlates well with published data reporting staurosporine IC_{50} values of 9 nM for PKCα, PKCβ, and PKCγ.[35] A staurosporine concentrations increased, the polarization value of the reaction also increased, indicating that PKC activity was being inhibited to a greater extent. The lowest concentrations of staurosporine yielded low polarization values, indicating that the PKC reaction was able to proceed largely (or totally) uninhibited.

DISCUSSION

Estrogen receptor assays

The data show that an FP-based competitive binding assay can be used to screen diverse compounds with a broad range of binding affinities for ER, and that the assay provides a rank ordering of binding affinity values similar to determinations made with conventional assay methods. It should be noted that these binding analyses were carried out under the conditions recommended for HTS application, that is, a relatively high ES2 concentration to overcome potential background fluorescence from test compounds. These conditions are optimal for qualitative identification of ligands in impure samples, but they do not yield accurate affinity measurements for very-high-affinity ligands; for this reason the binding affinities (IC_{50}) for DES and 4-OH-tamoxifen are underestimated using the FP assay. For analytical purposes, use of a lower ES2 concentration (50–100 pM) in a more sensitive single-tube instrument is recommended.

This assay has proven to be fast, robust, and quantitative for the determination of binding affinity for a wide range of estrogen ligands. The quantitative nature of the data and the ability to run assays for multiple receptors in parallel will significantly aid the efforts to develop new ER-responsive drugs with unique activities.

Kinase assays

These data demonstrate that an assay based on FP can be used to detect PTK activity, PKC activity, and phosphatase activity. These assays are simple, rapid, and inexpensive. The screening of unknown kinases, the optimization of substrates, and the testing of reaction conditions are all possible with this assay. The phosphorylated peptide substrates for several tyrosine kinases—including the EGF receptor; insulin receptor; c-Src, Fyn, Lck, and Lyn; and the general kinase substrate poly(Glu, Tyr) 4:1—have been shown to displace the tracer from the anti-pY Ab, while the PKC assay can detect the ac-

tivity of at least seven different PKC isoforms. The principles described here may also be broadly applied to any other modification of a peptide, small protein, or other molecule that can be fluorescently labeled, that can be recognized by an antibody, and that competes for binding with a nonfluorescent molecule.

CONCLUSION

FP is now a method of choice for screening several types of drug targets. The development of new HTS instrumentation and assay methods utilizing the advantages of FP has made FP a technology easily incorporated into HTS. FP should be considered for ligand displacement assays when the ligand can be fluorescently labeled and the receptor is fairly pure and abundant, or when enzyme reaction products can be quantified by immunoassay. The ligand displacement assay approach is being expanded to other nuclear receptors, such as androgen and progesterone receptors. The same competition immunoassay approach used in the PTK and PKC assays is now being used to develop assays for additional serine/threonine kinases.

NOTE ADDED IN PROOF

Since this article was accepted for publication, we have been able to detect the protein kinase activity of cAMP-dependent protein kinase (PKA), calmodulin-dependent protein kinase (CamKII), and glycogen synthase kinase-3β (GSK-3β) with the reagents, methods, and sensitivity similar to that described herein for the PKC assays.

REFERENCES

1. Drews, J. (1996). Genomic sciences and the medicine of tomorrow. *Nat. Biotechnol.* 14:1516–1517.
2. Gallop, M.A., Barrett, R.W., Dower, W.J., Fodor, S.P., Gordon, E.M. (1994). Applications of combinatorial technologies to drug discovery. 1. Background and peptide combinatorial libraries. *J. Med. Chem.* 37:1233–1251.
3. Pope, A.J., Haupts, U.M., Moore, K.J. (1999). Homogeneous fluorescence readouts for miniaturized high-throughput screening: Theory and practice. *Drug Discov. Today* 4:350–362.
4. Heyduk, T., Ma, Y., Tand, H., Ebright, R.H. (1996). Fluorescence anisotropy: Rapid, quantitative assay for protein-DNA and protein-protein interaction. *Methods Enzymol.* 274:492–503.
5. Jameson, D.M., Sawyer, W.H. (1995). Fluorescence anisotropy applied to biomolecular interactions. *Methods Enzymol.* 246: 283–300.
6. Checovich, W.J., Bolger, R.E., Burke, T. (1995). Fluorescence polarization—a new tool for cell and molecular biology. *Nature* 375:254–256.
7. Bolger, R., Wiese, T.E., Ervin, K., Nestich, S., Checovich, W. (1998). Rapid screening of environmental chemicals for estrogen receptor binding capacity. *Environ. Health Perspect.* 106: 551–557.
8. Lundblad, J.R., Laurance, M., Goodman, R.H. (1996). Fluorescence polarization analysis of protein-DNA and protein-protein interactions. *Mol. Endocrinol.* 10:607–612.
9. Ozers, M.S., Hill, J.J., Ervin, K., Wood, J.R., Nardulli, A.M., Royer, C.A. Gorski, J. (1997). Equilibrium binding of estrogen receptor with DNA using fluorescence anisotropy. *J. Biol. Chem.* 272:30405–30411.
10. Wu, P., Brasseur, M., Schindler, W. (1997). A high-throughput STAT binding assay using fluorescence polarization. *Anal. Biochem.* 249:29–36.
11. Bolger, R., Checovich, W. (1994). A new protease activity assay using fluorescence polarization. *Biotechniques* 17:585–589.
12. Bolger, R., Thompson, D. (1994). A quantitative RNase assay using fluorescence polarization. *Am. Biotechnol. Lab.* 12:113–116.
13. Turner, R.T., Riggs, B.L., Spelsberg, T.C. (1994). Skeletal effects of estrogen. *Endocr. Rev.* 15:275–300.
14. Ciocca, D.R., Roig, L.M. (1995). Estrogen receptors in human nontarget tissues: Biological and clinical implications. *Endocr. Rev.* 16:35–61.
15. Farhat, M.Y., Lavigne, M.C., Ramwell, P.W. (1996). The vascular protective effects of estrogen. *FASEB J.* 10:615–624.
16. Kuiper, G.G.J.M., Enmark, E., Pelto-Huikko, M., Nilsson, S., Gustadsson, J.-A. (1996). Cloning of a novel receptor expressed in rat prostate and ovary. *Proc. Natl. Acad. Sci. U.S.A.* 93:5925–5930.
17. Nilsson, S., Kuiper, G., Gustafsson, J.-A. (1998). ERβ: A novel estrogen receptor offers the potential for new drug development. *Trends Endocrinol. Metab.* 9:387–395.
18. Korach, K.S., McLachlan, J.A. (1995). Techniques for detection of estrogenicity. *Environ. Health Perspect.* 103:5–8.
19. Soto, A.M., Sonnenschein, C., Chung, K.L., Fernandez, M.F., Olea, N., Serrano, F.O. (1995). The E-SCREEN assay as a tool to identify estrogens: An update on estrogenic environmental pollutants. *Environ. Health Perspect.* 7:113–122.
20. Reese, J.C., Katzenellenbogen, B.S. (1991). Mutagenesis of cysteines in the hormone binding domain of the human estrogen receptor: Alterations in binding and transcriptional activation by covalently and reversibly attaching ligands. *J. Biol. Chem.* 266:10880–10887.
21. Haggblad, J., Carlsson, B., Kivela, P., Siitari, H. (1995). Scintillating microtitration plates as a platform for determination of [^{3}H]estradiol binding constants for hER-HBD. *Biotechniques* 18:146–151.
22. Hunter, T. (1995). Protein kinases and phosphatases: The yin and yang of protein phosphorylation and signaling. *Cell* 80:225–236.
23. Hunter, T. (1998). The Croonian Lecture 1997. The phosphorylation of proteins on tyrosine: Its role in cell growth and disease. *Philos. Trans. R. Soc. Lond. B Biol. Sci.* 353:583–605.
24. Pawson, T. (1995). Protein modules and signalling networks. *Nature* 373:573–580.
25. von Deimling, A., Louis, D.N., Wiestler, O.D. (1995). Molecular pathways in the formation of gliomas. *Glia* 15:328–338.
26. Friess, H., Berberat, P., Schilling, M., Kunz, J., Korc, M., Buchler, M.W. (1996). Pancreatic cancer: The potential clinical relevance of alterations in growth factors and their receptors. *J. Mol. Med.* 74:35–42.
27. Wong, A.J., Ruppert, J.M., Bigner, S.H., Grzeschik, C.H., Humphrey, P.A., Bigner, D.S., Vogelstein, B. (1992). Structural alterations of the epidermal growth factor receptor gene in human gliomas. *Proc. Natl. Acad. Sci. U.S.A.* 89:2965–2969.
28. Eppstein, D.A., Marsh, Y.V., Schryver, B.B., Bertics, P.J. (1989). Inhibition of epidermal growth factor/transforming growth factor-alpha-stimulated cell growth by a synthetic peptide. *J. Cell. Physiol.* 141:420–430.
29. Baum, E.Z., Johnston, S.H., Bebernitz, G.A., Gluzman, Y. (1996).

Development of a scintillation proximity assay for human cytomegalovirus protease using ^{33}phosphorus. *Anal. Biochem.* 237:129–134.

30. Kolb, A.J., Kaplita, P.V., Hayes, D.J., Park, Y.-W., Pernell, C., Major, J.S., Mathis, G. (1998). Tyrosine kinase assays adapted to homogeneous time-resolved fluorescence. *Drug Discov. Today* 3:333–342.
31. Nishizuka, Y. (1986). Studies and perspectives of protein kinase C. *Science* 233:305–312.
32. Nishizuka, Y. (1992). Intracellular signaling by hydrolysis of phospholipids and activation of protein kinase C. *Science* 258:607–614.
33. Dekker, L.V., Parker, P.J. (1994). Protein kinase C—a question of specificity. *Trends Biochem. Sci.* 19:73–77.
34. Hu, H. (1996). Recent discovery and development of selective protein kinase C inhibitors. *Drug Discov. Today* 1:438–447.
35. Tamaoki, T., Nomoto, H., Takahaski, I., Kato, Y., Morimoto, M. Tomita, F. (1986). Staurosporine, a potent inhibitor of phospholipid/Ca^{++} dependent protein kinase. *Biochem. Biophys. Res. Commun.* 135:397–402.

Address reprint requests to:
Gregory J. Parker
PanVera Corporation
545 Science Drive
Madison, WI 53711

E-mail: gregp@panvera.com

Niosomes and Polymeric Chitosan Based Vesicles Bearing Transferrin and Glucose Ligands for Drug Targeting

Christine Dufes,[1,4] Andreas G. Schätzlein,[2] Laurence Tetley,[3] Alexander I. Gray,[1] Dave G. Watson,[1] Jean-Christophe Olivier,[4] William Couet,[4] and Ijeoma F. Uchegbu[1,5]

Received March 11, 2000; accepted July 7, 2000

Purpose. To prepare polymeric vesicles and niosomes bearing glucose or transferrin ligands for drug targeting.

Methods. A glucose-palmitoyl glycol chitosan (PGC) conjugate was synthesised and glucose-PGC polymeric vesicles prepared by sonication of glucose-PGC/ cholesterol. N-palmitoylglucosamine (NPG) was synthesised and NPG niosomes also prepared by sonication of NPG/ sorbitan monostearate/ cholesterol/ cholesteryl poly-24-oxyethylene ether. These 2 glucose vesicles were incubated with colloidal concanavalin A gold (Con-A gold), washed and visualised by transmission electron microscopy (TEM). Transferrin was also conjugated to the surface of PGC vesicles and the uptake of these vesicles investigated in the A431 cell line (over expressing the transferrin receptor) by fluorescent activated cell sorter analysis.

Results. TEM imaging confirmed the presence of glucose units on the surface of PGC polymeric vesicles and NPG niosomes. Transferrin was coupled to PGC vesicles at a level of 0.60 ± 0.18 g of transferrin per g polymer. The proportion of FITC-dextran positive A431 cells was 42% (FITC-dextran solution), 74% (plain vesicles) and 90% (transferrin vesicles).

Conclusions. Glucose and transferrin bearing chitosan based vesicles and glucose niosomes have been prepared. Glucose bearing vesicles bind Con-A to their surface. Chitosan based vesicles are taken up by A431 cells and transferrin enhances this uptake.

KEY WORDS: polymeric vesicles; glucose vesicles; transferrin vesicles.

[1] Department of Pharmaceutical Sciences, University of Strathclyde, Strathclyde Institute for Biomedical Sciences, 27 Taylor Street, Glasgow G4 0NR, United Kingdom.

[2] Department of Medical Oncology, University of Glasgow, Garscube Estate, Switchback Road, Glasgow G61 1BD, United Kingdom.

[3] Institute of Biomedical and Life Sciences, University of Glasgow, Joseph Black Building, Glasgow G12 8QQ, United Kingdom.

[4] Laboratoire de Pharmacie Galénique et Biopharmacie, Faculté de Médecine et Pharmacie, 34 rue du Jardin des Plantes, 86000 Poitiers, France.

[5] To whom correspondence should be addressed. (e-mail: i.f.uchegbu@strath.ac.uk)

ABBREVIATIONS: Con-A-gold, concanavalin A gold; DMSI, dimethylsuberimidate; DMSO, dimethylsulphoxide; FACS, Fluorescent activated cell sorter; FITC-dextran, fluorescein isothiocyanate dextran; PGC, palmitoyl glycol chitosan; NPG, N-palmitoyl glucosamine; PBS, phosphate buffered saline; TEM, transmission electron microscopy; TF, transferrin.

INTRODUCTION

Actively targeted therapies have demonstrated their potential in the tumour targeting of polymeric gene delivery systems (1), the central nervous system targeting of peptide analgesics (2) and the targeting of oligonucleotides to the liver hepatocytes and macrophages (3). In our laboratories polymeric vesicles for drug delivery have been developed from a specially designed amphiphilic chitosan derivative-palmitoyl glycol chitosan (PGC) (4). While the passive targeting of anti-cancer phospholipid vesicles (liposomes) (5,6) and non-ionic surfactant vesicles (niosomes) (7) to solid tumours has been well documented, liposomes for gene delivery are predominantly passively targeted to the lung endothelium (8,9). Hence, depending on their potential use it will be necessary to elucidate active targeting strategies for vesicular systems. Additionally the targeting of large hydrophilic molecules across the blood brain barrier (BBB) is invariably problematic. Transferrin bearing proteins however may be targeted across the blood brain barrier when administered via the carotid artery (10) and the exploitation of the BBB glucose transporter, GLUT-1 (11,12), using glucose peptide conjugates results in peptide delivery to the central nervous system (2). The GLUT-1 receptor is also over expressed in some tumour tissue (13,14), hence a glucose targeting ligand may be useful for targeting anti-cancer genes to tumour tissue. It is possible that the active targeting of polymeric vesicles for drug/ gene delivery may be accomplished with targeting ligands. This work reports on the preparation and characterisation of polymeric vesicles and niosomes bearing targeting ligands.

MATERIALS AND METHODS

Materials

Palmitic acid N-hydroxysuccinimide, glucosamine, sorbitan monostearate (Span 60), cholesterol, glycol chitosan (Mw = 164,000), concanavalin A gold (Con A-gold, 20nm), β-D-glucopyranosyl phenylisothiocyanate, N-N-diisopropylethylamine, dimethyl-suberimidate (DMSI), triethanolamine, fluorescein isothiocyanate dextran (FITC-dextran), phosphate buffered saline (PBS, pH = 7.4) tablets, iron-saturated human transferrin (TF), Folin Ciocalteu's reagent, uranylformate, sodium carbonate, sodium potassium tartrate and cupric sulphate, were all purchased from Sigma Aldrich Co, UK. Dialysis tubing was obtained from Medicell International, UK. Chloroform, isopropanol, dimethylsulphoxide (DMSO) and diethylether were all purchased from Merck, UK. Cholesteryl poly-24-oxyethylene ether (Solulan C24) was kindly donated by D.F. Anstead, UK. All tissue culture reagents were obtained from Gibco, UK.

Preparation of Glucose-Bearing Niosomes

Synthesis of N-Palmitoyl Glucosamine (NPG)

This was prepared in a similar manner to that described for the glycoside palmitoyl muramic acid (15) and was derived from the method of Lapidot and others (16). Glucosamine (86.3mg) was dissolved in dimethylsulphoxide (15mL) and triethanolamine (93μL). To this was added palmitic acid N-

0724-8741/00/1000-1250$18.00/0

hydroxysuccinimide (283mg) dissolved in chloroform (4mL). The mixture was stirred at room temperature for 48 h, protected from light. Chloroform was evaporated off at room temperature and the remaining liquid freeze-dried. The resulting powder was purified by washing consecutively with water (200 ml), chloroform (50 ml), and ether (200 ml) and then was freeze-dried again. NPG (Figure 1) was obtained as a white powder.

^{1}H NMR Analysis of NPG

^{1}H NMR (with integration) and ^{1}H correlation spectroscopy experiments (Bruker AMX 400MHz spectrometer, Bruker Instruments, UK) were performed on NPG solutions in deuterated DMSO.

Mass Spectrometry

Analysis of NPG was carried out by mass spectrometry (fast atom bombardment–FAB on a JEOL AX505 mass spectrometer, Jeol Instruments, UK).

Preparation of NPG Niosomes

Niosomes were prepared by shaking a mixture of NPG (16mg), Span 60 (65mg), cholesterol (58mg) and Solulan C24 (54mg) in water (5mL) at 90°C for 1h, followed by probe sonication (Soniprobe Instruments, UK) for 4 minutes with the instrument set at 20% of its maximum capacity.

Synthesis of the PGC- Glucose Conjugate

Palmitoyl glycol chitosan (PGC) (Fig. 2) was synthesised by the reaction of glycol chitosan with palmitic acid N-hydroxysuccinimide in a 4:1 sugar monomer, palmitic acid molar ratio and characterised by ^{1}H NMR analysis as previously described (4). PGC - glucose conjugate was prepared using methods described previously (17). PGC (5mg), β-D-glucopyranosyl phenylisothiocyanate (5mg) and N-N-diisopropylethylamine (4μl) were dissolved in DMSO (5mL). The reaction mixture was stirred at room temperature for 24h, diluted with water (25mL), exhaustively dialysed against 1L of water (over a 24h period with 6 changes), and finally freeze-dried.

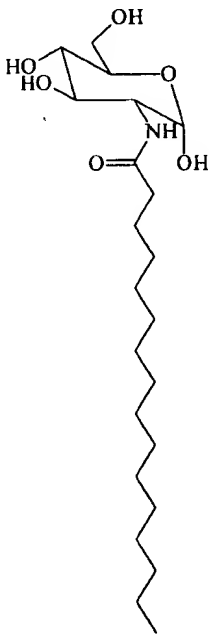

Fig. 1. Chemical structure of N-palmitoyl glucosamine (N-PG).

Preparation of Polymeric Glucose Vesicles

Vesicles were prepared by probe sonicating the PGC-glucose conjugate (4mg) and cholesterol (2mg) in water (4mL) for 4 min with the instrument set at 20% of its maximum output. The temperature of the probe sonicated formulation reached a maximum temperature of ~ 60°C. The vesicle dispersion was then filtered through a 0.45 μm filter.

Preparation Of Control Span 60 Niosomes

Vesicles were prepared by shaking a mixture of Span 60 (73mg), cholesterol (65mg), Solulan C24 (54mg) in water (5mL) at 90°C for 1h followed by probe sonication for 4 minutes with the instrument set at 20% of its maximum capacity.

Transmission Electron Microscopy (TEM)

The presence of glucose on the vesicle surface was evaluated by incubation with a colloidal dispersion of Con A-gold thus exploiting the affinity of the lectin concanavalin A for glucose (18). Glucose bearing vesicles and control plain Span 60 niosome suspensions (0.1mL) were shaken with the Con A-gold dispersion (0.1mL) at 60°C for 1h. To separate unbound Con A-gold from bound Con A-gold, the mixture was then centrifuged (1,000g for 10 min, Beckman L8-55 ultracentrifuge, Beckman Instruments, UK) and the pelleted unbound Con A-gold discarded. Vesicles bearing the bound gold were then imaged by TEM as follows. Droplets of the vesicle preparation were mixed in equal (20 μl) volumes with 1% uranylformate (pH 4.8) on a specimen support grid and immediately dried down using filter paper. The negatively stained grid samples were then imaged on a LEO 902 energy filtering electron microscope at 80 kV.

Preparation of TF-Bearing Polymeric Vesicles Entrapping the Fluorescent Marker FITC-Dextran

Preparation of Plain PGC Vesicles

PGC vesicles were prepared from PGC and cholesterol as previously described (4), by probe sonicating PGC (10mg) and cholesterol (4mg) in PBS (pH = 7.4, 2mL) for 4 min with the instrument set at 20% of its maximum capacity.

Conjugation of TF to PGC Vesicles (TF-PGC)

TF was linked with PGC vesicles by using DMSI as a cross-linking reagent (19) in a similar manner to that reported for TF-coated liposomes (20). To 2mL of the vesicle suspension (2mL), obtained from above (5mg mL^{-1}), was added TF (12mg) and DMSI (24mg) in triethanolamine HCl buffer (pH 7.4, 2mL). The coupling reaction was allowed to take place at room temperature for 2h whilst stirring. Free TF was then removed by ultracentrifugation (2 × 150,000g for 1h). After each ultracentrifugation step the pelleted vesicles were resuspended in PBS (pH = 7.4, 2mL).

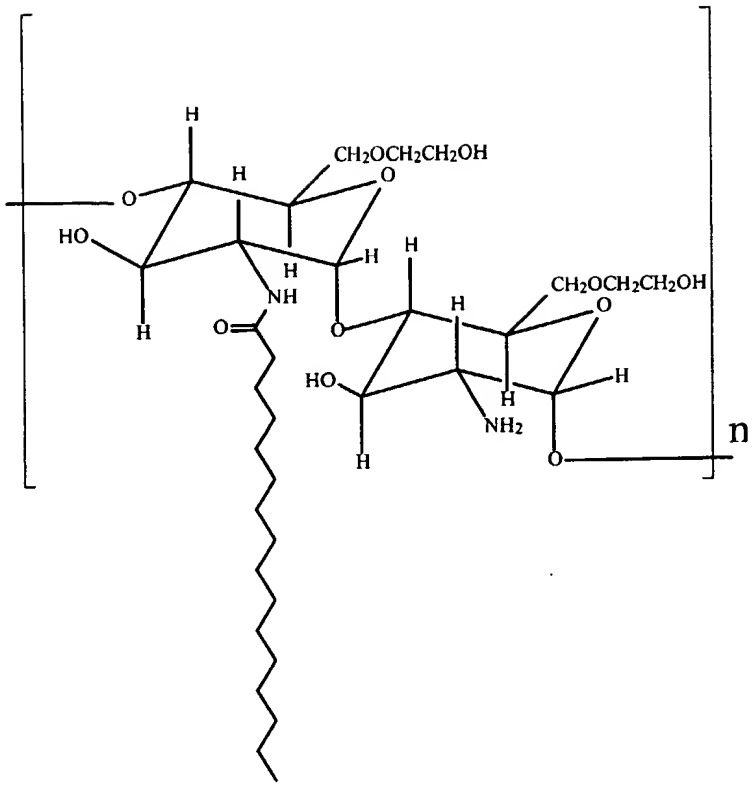

Fig. 2. Chemical structure of palmitoyl glycol chitosan (PGC).

Assay for Conjugated TF

The amount of conjugated TF was determined using the Lowry method (21). TF bearing vesicle suspensions, blank vesicles bearing no TF and vesicle suspensions carried through the TF conjugation reaction but without the cross-linking agent DMSI were used in this assay. The latter vesicles were used to ensure that TF was not merely adsorbed to the vesicle surface. To sodium carbonate solution (25mL, 2%w/v in NaOH 0.1M) was added sodium potassium tartrate (0.5mL, 2%w/v) and cupric sulphate (0.5mL, 1%w/v) with constant stirring to avoid precipitation. To 1mL of this solution (freshly prepared) was added 100μl of each of the vesicle suspensions (5mg mL^{-1} PGC) or the standard TF solutions (0–0.5mg mL^{-1}) and the mixture allowed to stand for 10min. To these samples was then added Folin Ciocalteu's reagent (100μL) with immediate vortexing. All samples were subsequently left to stand for 30min and the colour reaction quantified by measuring the absorbance at 750nm (UV-1, Unicam Ltd., UK). The sample derived from the blank vesicles not containing TF was used in the reference cell, when measuring the absorbance of the vesicle samples. The amount of protein associated with the vesicles was determined with reference to the standard TF solutions.

Loading of FITC-Dextran TF-PGC Vesicles

FITC-dextran loaded TF-PGC vesicles were prepared by probe sonicating on ice TF-coated vesicles, obtained as described above in a solution of FITC-dextran (2mL, 6mg mL^{-1}). Unentrapped FITC-dextran was removed by ultracentrifugation (150,000g × 1h) and the FITC-dextran loaded vesicle pellet resuspended in PBS (2mL).

Assay for the Amount of FITC-Dextran Entrapped by TF- PGC Vesicles

PGC vesicles were disrupted by adding the vesicle suspension (0.1mL) to isopropanol (1mL). This solution was then diluted to 10mL with PBS (pH = 7.4) and the fluorescence measured (Perkin Elmer LS-50 fluorescence spectrometer, Perkin-Elmer Instruments, UK.) at an excitation wavelength of 480nm and an emission wavelength of 560nm. The amount FITC-dextran was computed with reference to standard solutions of FITC-dextran (11μg mL^{-1}–11mg mL^{-1}) in an isopropanol, PBS (pH = 7.4) mixture (10: 90).

Vesicle Sizing

Vesicle sizing was performed by photon correlation spectroscopy on a Malvern Zetasizer 1 (Malvern Instruments, UK.).

Cellular Uptake of FITC-Dextran Loaded TF- PGC Vesicles

The A431-human epidermoid carcinoma cell line (ATCC CRL-1555) (22,23) was grown as a monolayer culture at 37°C in 5% CO_2 and maintained by regular passages in Dulbecco's medium supplemented with 10% foetal bovine serum, L-glutamine (1%w/v). Plated A 431 cells (10^5 cells/well) were incubated (37°C for 4 h) with transferrin-bearing vesicles (0.2 mL, 104μg mL^{-1} PGC) loaded with FITC-dextran (24μg mL^{-1}), blank FITC-dextran vesicles or with FITC-dextran solution. The concentration of FITC-dextran was the same for all the samples.

For the microscopic studies cells were grown and exam-

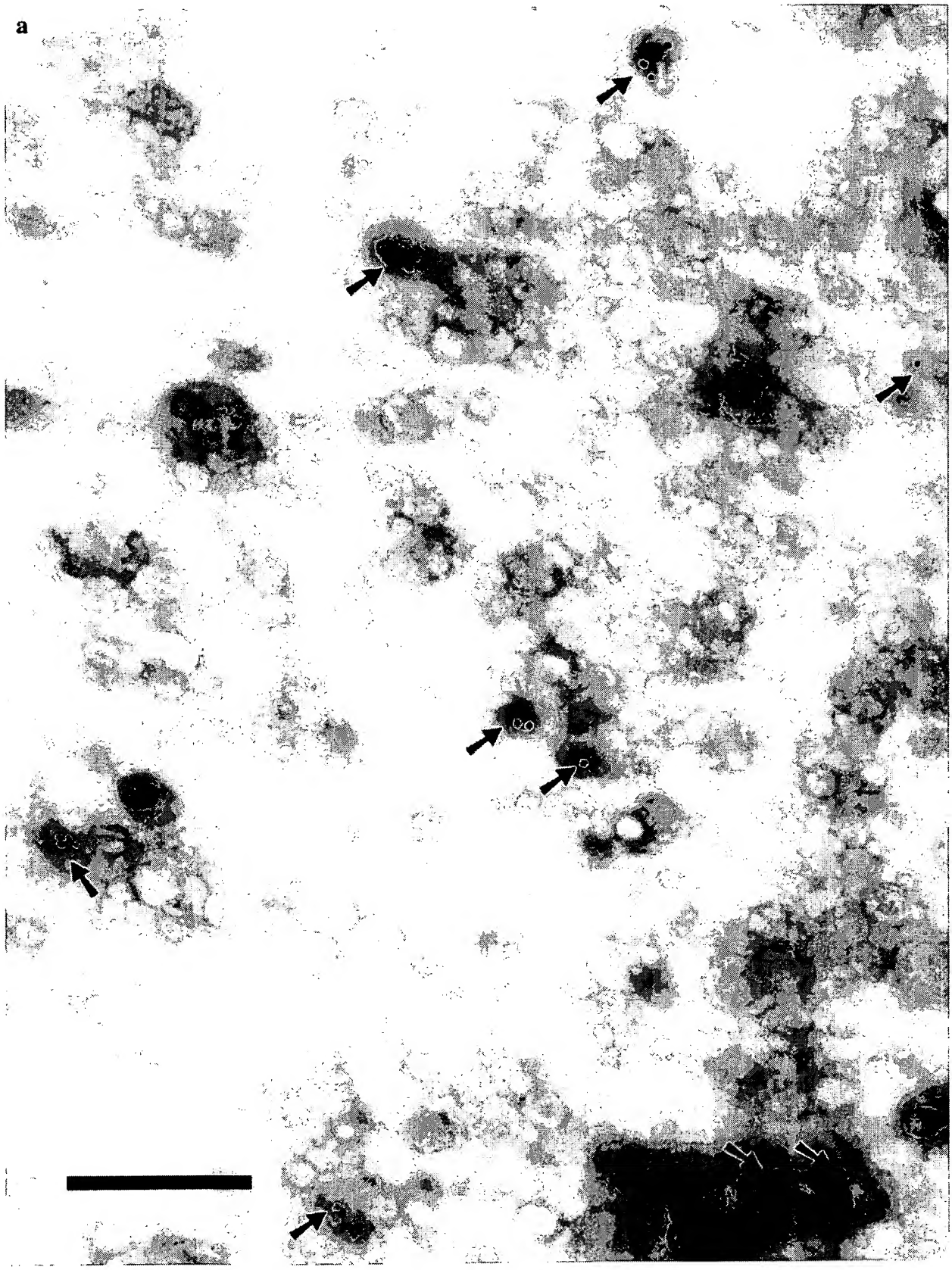

Fig. 3. Continued on facing page.

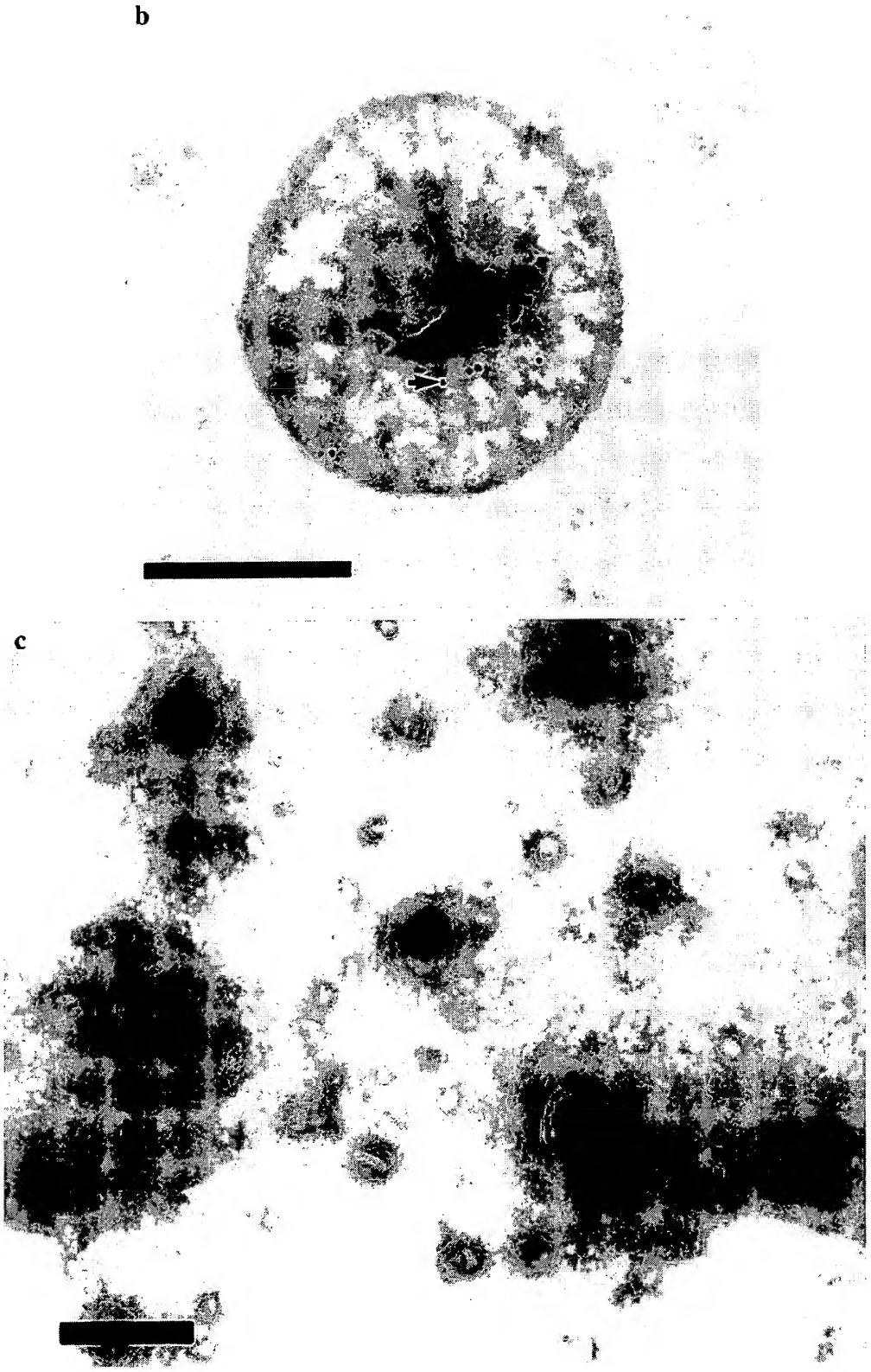

Fig. 3. Transmission electron micrographs with negative staining of Con A-gold (20 nm) associated with a) N-PG vesicles, b) PGC- glucose vesicles, and c) plain Span 60 niosomes. Gold particles are indicated by arrow , bar = 100nm.

ined on coverslips. At the end of the incubation period, cells were washed with PBS (pH = 7.4), transferred to a holder where the cells were immersed in PBS (pH = 7.4) and examined using confocal microscopy (λ_{ex} = 488 nm, Biorad 600 confocal microscope, Biorad, UK). For flow cytometry studies, the cells were trypsinised after the incubation period, washed (PBS , pH = 7.4) and pelleted (1,000g) twice. Cellular FITC-dextran uptake was examined on a FACStar flow cytometer (Becton-Dickinson Instruments, UK). The forward scatter (FSC) and sideward scatter (SSC) of a control cell suspension was used to discriminate cells and debris. 20,000 cells (gated events) were counted for each sample. FITC–dextran fluorescence was detected with logarithmic settings (FL1, λ_{em} = 515–545 nm). Cells were counted as positive when their fluorescence (FL1) was higher than that of 95% of cells from an untreated cell suspension, (i.e. channel 198 to 1024)

RESULTS

Glucose Bearing Vesicles

NPG Niosomes

The characterisation of PGC was as previously described (4). Proton assignments by ^{1}H NMR of NPG were as follows: δ 0.86 ppm = CH3 (palmitoyl), δ 1.25 ppm = CH2 (palmitoyl), δ 1.89 ppm = CH2 (palmitoyl shielded by carbonyl), δ 2.14 ppm = CH2 (adjacent to carbonyl protons), δ 2.71 ppm = CH (C2 sugar proton), δ 3.3–4.0 ppm = non-exchangeable sugar protons. Mass spectrometry data yielded one main peak corresponding to the mass ion 418 (100%, M^+) and further minor peaks 400 (72.75 %, M^+ -OH) and 432 (24.43%, M^+ + OH). These results indicate that NPG was successfully prepared.

Stable vesicles could be formed from NPG, sorbitan monostearate, cholesterol, Solulan C24 (10: 40: 40: 10 mole%). Higher levels of NPG resulted in unstable formulations with the NPG crystallising out of the formulation within hours. Glucose niosomes prepared from NPG had a z-average mean diameter of 164nm.

Glucose-PGC Vesicles

Polymeric (PGC) glucose bearing vesicles had a z-average mean diameter of 155nm.

Con-A Gold Binding

Both types of vesicles effectively bound Con A-gold while the control plain vesicles (devoid of glucose) did not (Figure 3), indicating the presence of accessible glucose units on the surface of these niosomes and polymeric vesicles.

Transferrin Bearing PGC Vesicles

Transferrin was successfully conjugated to PGC in these vesicles, as determined by the Lowry assay at a level of 0.60 ± 0.18g of TF per g polymer (50 ± 15% of the initial transferrin used). FITC-dextran was entrapped in the transferrin bearing vesicles (0.23g per g polymer, corresponding to 10% of the initial FITC-dextran) and in the plain chitosan based vesicles (0.32g per g polymer, corresponding to 13% of the initial FITC-dextran). Plain PGC vesicles had a z-average mean diameter of 420nm, while TF-PGC vesicles had a z-average size of 458nm and TF-PGC vesicles loaded with FITC-dextran had a z-average size of 740nm.

Cellular Uptake of Fluorescently Labelled TF-PGC Vesicles

Fluorescence microscopy images showed a brighter fluorescence (more fluorescently labelled vesicles) associated with cells incubated with the transferrin bearing vesicles when compared to the plain vesicles (Figure 4). Flow cytometry data (Fig. 5) also indicated that there was the greater percentage of positive cells when the transferrin bearing vesicles were incubated with the cells. However it is interesting to note that the polymeric vesicles without TF also associated to a greater degree with the cells than the fluorescent marker (FITC-dextran) in solution. This is indicative of the fact that these latter vesicles are also taken up by the cells or at least enhance the uptake of the fluorescent polymer.

DISCUSSION

This work is the first report of the preparation of polymeric chitosan based vesicles bearing targeting ligands. In addition the synthesis of a new surfactant NPG is described. The synthesis is a simple one-step procedure unlike the synthetic methods previously reported (24). Stable vesicles could not be produced from this surfactant alone or in the presence of cholesterol and the incorporation of more than 10mole% NPG into the bilayer of niosomes resulted in NPG crystallising out within hours. 6-O-alkanoyl-α-D glucose amphiphiles also crystallise out of niosomes prepared with these agents and cholesterol within 3–4 weeks (25). Small niosomes in the colloidal size range may be formed with this new amphiphile, NPG. 1-alkyl glucosides have been reported to form large unilamellar niosomes by Kiwada and others (26). These latter niosomes are 1μm in diameter and were reported to be stable when stored in the dark for up to 25 weeks. The production of colloidal dispersions of the 1-alkyl glucoside niosomes was not however reported by these authors. To our knowledge this is the first report of the production of sub-micron glucose vesicles in which the glucose units are found to be recognisable by the glucose specific lectin-con A. Con A served as a model for the glucose specific receptor.

The PGC-glucose conjugate produced vesicles with a smaller z-average mean diameter than vesicles produced from plain PGC (155nm vs 420nm). The conjugation of glucose to PGC probably resulted in an increase in the size of the hydrophilic portion of the molecule relative to the hydrophobic portion of the molecule. An increase in the hydrophilic head group of an amphiphile or mixture of amphiphiles would result in an increase in vesicle curvature and hence a decrease in vesicle size (27). It appears that with amphiphilic pendant like polymers, a similar increase in the hydrophilic head group area also decreases vesicle size. Vesicles incorporating only 10 mole % of NPG are able to bind Con A, as do vesicles prepared from the PGC-glucose conjugate (Figure 3). This indicates that the glucose units were accessible on the vesicle surface and may be accessible to glucose receptors in vivo. Because human cancer cells have an enhanced need for glucose and hence frequently over express the GLUT receptors

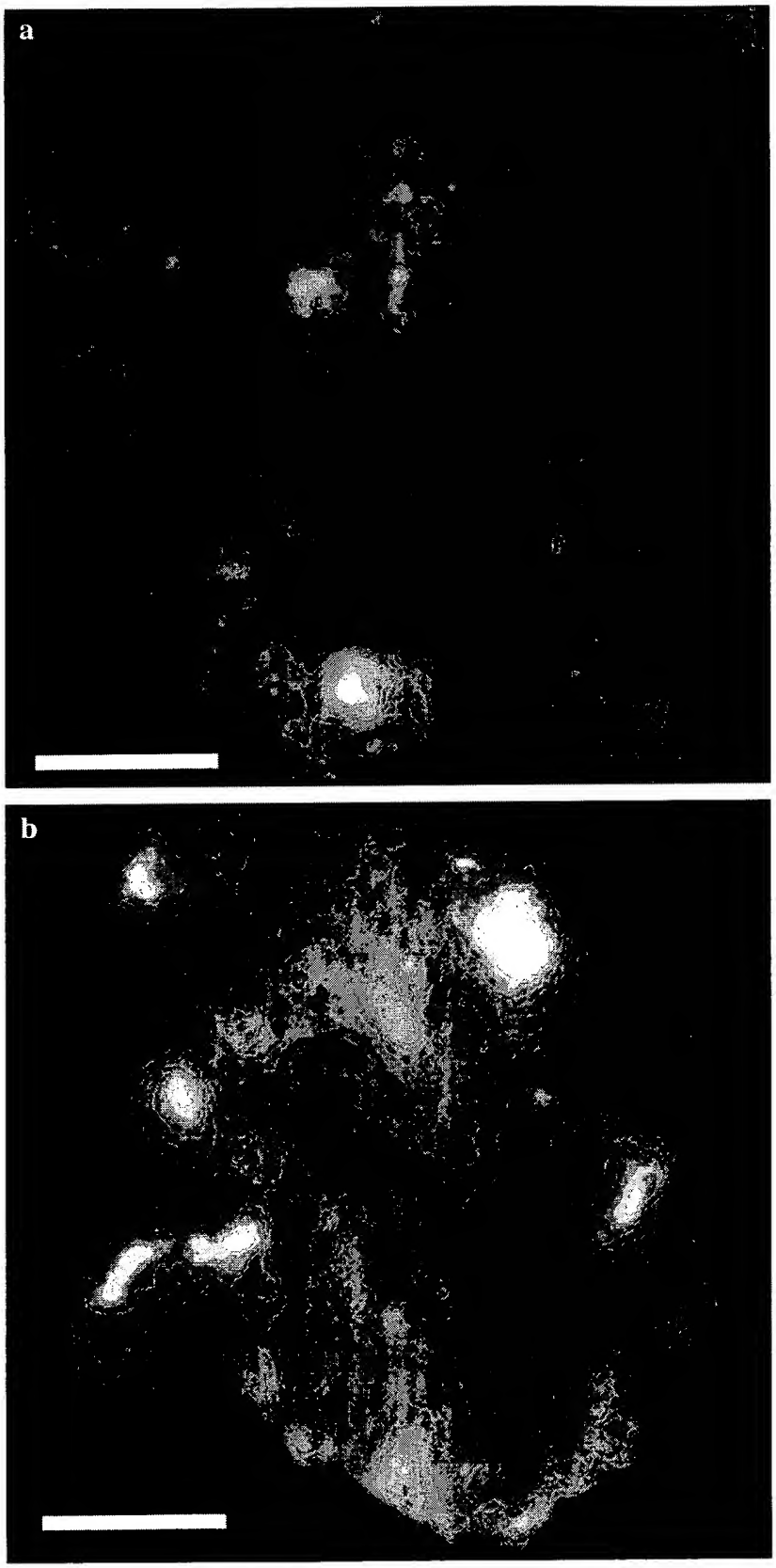

Fig. 4. Fluorescence micrographs of A 431 tumour cells treated with a) plain FITC-dextran loaded vesicles (without transferrin) and b) transferrin bearing FITC-dextran loaded vesicles, bar = 100 nm.

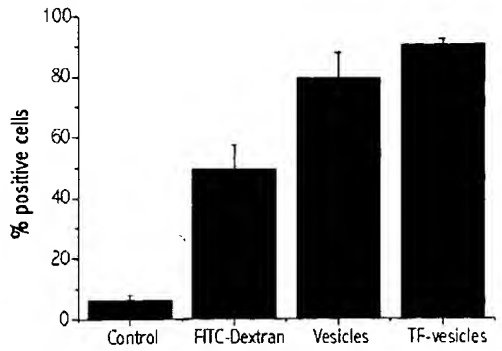

Fig. 5. FACS analysis of the uptake of FITC-D solution ("solution"), FITC-D vesicles without Tf ("vesicles"), and Tf-bearing vesicles loaded with FITC-D ("TF vesicles"), by A 431 cells. "Control": untreated cells. Cells were counted as FITC positive when their fluorescence was higher than that of 95 % of cells from an untreated cell suspension. n = 3.

(14), these glucose bearing vesicles may prove useful as gene targeting agents to tumour cells over-expressing the GLUT receptor isoforms. In addition the presence of GLUT 1 receptors at the BBB (28) may potentially be exploited with these carriers, causing them to increase the transfer of large hydrophilic molecules across the BBB.

Transferrin was coupled to the surface of the polymeric vesicles and appeared to be accessible to the TF receptor in the A431 cell line (Figures 4 and 5). Transferrin receptors are also over expressed on the surface of many proliferating cells (29) and their presence may be exploited for the targeting of gene expression to tumours (1). In addition the administration of transferrin-protein conjugates via the carotid artery resulted in the enhanced transfer of large proteins across the BBB (10). These transferrin bearing vesicles may thus find a use in the targeting to the central nervous system.

CONCLUSION

Glucose niosomes and glucose or transferrin bearing polymeric vesicles have been successfully prepared for drug targeting. The accessibility of these targeting ligands to the glucose specific lectin Con A or to the transferrin receptor have been demonstrated. In addition the encapsulation of FITC-dextran within polymeric vesicles has been shown to promote the uptake of the fluorescent marker. Further studies on the usefulness of these new vesicles in vivo are planned for the very near future.

ACKNOWLEDGMENTS

This work was supported by a University of Strathclyde New Lecturer Starter Grant to IFU.

REFERENCES

1. M. Ogris, S. Brunner, S. Schuller, R. Kircheis, and E. Wagner. PEGylated DNA/transferrin-PEI complexes: Reduced interaction with blood components, extended circulation in blood and potential for systemic gene delivery. *Gene Ther.* **6**:595–605 (1999).
2. R. Polt, F. Porreca, L. Z. Szabo, E. J. Bilsky, P. Davis, T. J. Abbruscato, T. P. Davis, R. Horvath, H. I. Yamamura, and V. J. Hruby. Glycopeptide enkephalin analogs produce analgesia in mice—Evidence for penetration of the blood-brain-barrier. *Proc. Natl. Acad. Sci. USA* **91**:7114–7118 (1994).
3. R. I. Mahato, S. Takemura, K. Akamatsu, M. Nishikawa, Y. Takakura, and M. Hashida. Physicochemical and disposition characteristics of antisense oligonucleotides complexed with glycosylated poly(L-lysine). *Biochem. Pharmacol.* **53**:887–895 (1997).
4. I. F. Uchegbu, A. G. Schatzlein, L. Tetley, A. I. Gray, J. Sludden, S. Siddique, and E. Mosha. Polymeric chitosan-based vesicles for drug delivery. *J. Pharm. Pharmacol.* **50**:453–458 (1998).
5. D. Papahadjopoulos, T. M. Allen, A. Gabizon, E. Mayhew, K. Matthay, S. K. Huang, K. D. Lee, M. C. Woodle, D. D. Lasic, and C. Redemann. Sterically stabilized liposomes: Improvements in pharmacokinetics and antitumor therapeutic efficacy. *Proc. Natl. Acad. Sci. USA* **88**:11460–11464 (1991).
6. F. Yuan, M. Leunig, S. K. Huang, D. A. Berk, D. Papahadjopoulos, and R. K. Jain. Microvascular permeability and interstitial penetration of sterically stabilized (stealth) liposomes in a human tumor xenograft. *Cancer Res.* **54**:3352–3356 (1994).
7. I. F. Uchegbu, J. A. Double, J. A. Turton, and A. T. Florence. Distribution, metabolism and tumoricidal activity of doxorubicin administered in sorbitan monostearate (Span 60) niosomes in the mouse. *Pharm. Res.* **12**:1019–1024 (1995).
8. Y. K. Song and D. X. Liu. Free liposomes enhance the transfection activity of DNA/lipid complexes in vivo by intravenous administration. *Biochim. Biophys. Acta* **1372**:141–150 (1998).
9. L. G. Barron, L. Gagne, and F. C. Szoka, Jr. Lipoplex-mediated gene delivery to the lung occurs within 60 minutes of intravenous administration. *Human Gene Ther.* **10**:1683–1694 (1999).
10. R. D. Broadwell, B. J. Baker-Cairns, P. M. Friden, C. Oliver, and J. C. Villegas. Transcytosis of protein through the mammalian cerebral epithelium and endothelium. III. Receptor-mediated transcytosis through the blood-brain barrier of blood-borne transferrin and antibody against the transferrin receptor. *Experimental Neurol.* **142**:47–65 (1996).
11. C. L. Farrell and W. M. Pardridge. Blood-brain-barrier glucose transporter is asymmetrically distributed on brain capillary endothelial lumenal and ablumenal membranes—An electron-microscopic immunogold study. *Proc. Natl. Acad. Sci. USA* **88**: 5779–5783 (1991).
12. W. M. Pardridge. Molecular regulation of blood-brain barrier GLUT1 glucose transporter. In J.Greenwood, D. J. Begley and M. B. Segal (eds.), *New Concepts of a blood brain barrier,* Plenum Press, New York, 1995, pp. 81–88.
13. T. Higashi, N. Tamaki, T. Honda, T. Torizuka, T. Kimura, T. Inokuma, G. Ohshio, R. Hosotani, M. Imamura, and J. Konishi. Expression of glucose transporters in human pancreatic tumors compared with increased FDG accumulation in PET study. *J. Nucl. Med.* **38**:1337–1344 (1997).
14. T. A. D. Smith. Facilitative glucose transporter expression in human cancer tissue. *Br. J. Biomed. Sci.* **56**:285–292 (1999).
15. I. F. Uchegbu. The biodistribution of novel 200nm palmitoyl muramic acid vesicles. *Int. J. Pharm.* **162**:19–27 (1998).
16. Y. Lapidot, N. D. Groot, and I. Fry-Shafrir. II A general method for the preparation of acylaminoacyl-tRNA. *Biochim. Biophys. Acta* **145**:292–299 (1967).
17. C. R. McBroom, C. H. Samanen, and I. J. Goldstein. Carbohydrate antigens: Coupling of carbohydrates to proteins by diazonium and phenylisothiocyanate reaction. *Meth. Enzymol.* **28**:212–219 (1972).
18. M. Monsigny, A. C. Roche, and P. Midoux. Uptake of neoglycoproteins via membrane lectins of L1210 cells evidenced by quantitative flow cytofluorometry and drug targeting. *Biol. Cell* **51**: 187–196 (1984).
19. N. Benhamou and G. B. Ouellette. Ultrastructural-localization of glycoconjugates in the fungus ascocalyx-abietina, the scleroderris canker agent of conifers, using lectin gold complexes. *J. Histochem. Cytochem.* **34**:855–867 (1986).
20. G. E. Davies and G. R. Stark. Use of dimethyl suberimidate, a cross-linking agent in studying the subunit structure of oligomeric proteins. *Proc. Natl. Acad. Sci. USA* **66**:651–656 (1970).
21. J. C. Stavridis, G. Deliconstantinos, M. C. Psallidopoulos, N. A. Armenakas, D. J. Hadjiminas, and J. Hadjiminas. Construction of transferrin-coated liposomes for in vivo transport of exogenous DNA to bone marrow erythroblasts in rabbits. *Exp. Cell Res.* **164**:568–572 (1986).
22. O. H. Lowry, N. J. Rosenburgh, A. L. Farr, and R. J. Randall.

Protein measurement with the folin phenol reagent. *J. Biol. Chem.* **193**:265–275 (1951).
23. T. Hoshino, M. Misaki, M. Yamamoto, H. Shimizu, Y. Ogawa, and H. Toguchi. In-vitro cytotoxicities and in-vivo distribution of transferrin platinum(Ii) complex. *J. Pharm. Sci.* **84**:216–221 (1995).
24. T. Hoshino, M. Misaki, M. Yamamoto, H. Shimizu, Y. Ogawa, and H. Toguchi. Receptor-binding, in-vitro cytotoxicity, and in-vivo distribution of transferrin-bound cis-platinum(Ii) of differing molar ratios. *J. Control. Rel.* **37**:75–81 (1995).
25. R. Hori and Y. Ikegami. Studies on carbohydrate derivatives V. Synthesis of alkyl galactosides and alkyl glucosides. *Yakugaku Zasshi* **79**:80–83 (1951).
26. G. Vanlerberghe and J. L. Morancais. Niosomes in perspective, STP. *Pharma Sci.* **6**: 5–11 (1996).
27. H. Kiwada, H. Niimura, Y. Fujisaki, S. Yamada, and Y. Kato. Application of synthetic alkyl glycoside vesicles as drug carriers. I Preparation and physical properties. *Chem. Pharm. Bull.* **33**: 753–759 (1985).
28. I. F. Uchegbu and A. T. Florence. Non-ionic surfactant vesicles (niosomes): Physical and pharmaceutical chemistry, some aspects of the niosomal delivery of doxorubicin. *Adv. Coll. Interf. Sci.* **58**:1–55 (1995).
29. W. M. Pardridge, R. J. Boado, and C. R. Farrell. Brain-type glucose transporter (Glut-1) is selectively localized to the blood-brain-barrier—Studies with quantitative western blotting and in situ hybridization. *J. Biol. Chem.* **265**:18035–18040 (1990).
30. A. A. Phylchenkov, I. I. Slukvin, Y. I. Kudryavets, L. P. Didkovskaya, G. A. Kulik, V. P. Chernishov, and A. I. Bykorez. Expression and functional-activity of transferrin receptor in human tumor-cell of different histogenesis. *Eksperimental. Onkol.* **14**:22–27 (1992).

0013-7227/92/1312-0799$03.00/0
Endocrinology

Vol. 131, No. 2
Printed in U.S.A.

Expression of Recombinant Human Follicle-Stimulating Hormone Receptor: Species-Specific Ligand Binding, Signal Transduction, and Identification of Multiple Ovarian Messenger Ribonucleic Acid Transcripts*

JONATHAN L. TILLY†, TOSHIHIKO AIHARA‡, KEIJI NISHIMORI, XIAO-CHI JIA, HAKAN BILLIG, KIM I. KOWALSKI, E. A. PERLAS, AND AARON J. W. HSUEH

Division of Reproductive Biology, Department of Gynecology and Obstetrics, Stanford University School of Medicine, Stanford, California 94305–5317

ABSTRACT

The ligand specificity and biochemical properties of the human (h) FSH receptor are poorly characterized due to the low abundance of these receptors and the limited availability of human tissues. Using a fragment of rat FSH receptor cDNA, we screened a human testicular cDNA library and obtained a FSH receptor cDNA covering the entire amino acid-coding region. After transfection of a human fetal kidney cell line (293) with the hFSH receptor cDNA, radioligand receptor analysis revealed the presence of high affinity (K_d, 1.7×10^{-9} M) FSH-binding sites on the plasma membrane. Both recombinant and wild-type hFSH displaced [^{125}I]hFSH binding, with ED_{50} values of 25 and 70 ng/ml, respectively, whereas hLH, hCG, and hTSH were ineffective. Although human, rat (r), and ovine FSH as well as equine CG competed for rat testicular FSH receptor binding, only hFSH and rFSH interacted effectively with the recombinant hFSH receptor, suggesting that species-specific ligand recognition exists between human and rodent receptors. After incubation of transfected cells with hFSH, but not recombinant hLH or hCG, a dose-dependent increase (ED_{50}, 10 ng/ml) in extracellular cAMP accumulation was observed, indicating a functional coupling of the expressed human receptor with the endogenous adenyl cyclase. In cells cotransfected with the FSH receptor expression plasmid and a luciferase reporter gene driven by the promoter of a cAMP-responsive gene, treatment with hFSH, but not hCG, resulted in a dose-dependent increase in luciferase activity. Northern blot analysis using a cRNA probe derived from the human receptor cDNA indicated the presence of multiple FSH receptor mRNA transcripts (7.0, 4.2, and 2.5 kilobases) in RNA prepared from human follicular phase ovary, but not from human corpus luteum or placenta. Additionally, two FSH-binding sites of 76 and 112 kilodaltons were detected in transfected 293 cells after ligand/receptor cross-linking and sodium dodecyl sulfate-polyacrylamide gel electorphoresis analysis. These results demonstrate the expression of functional hFSH receptor with unique ligand specificity and provide new data on the biochemical properties of the human receptor at the mRNA and protein levels. (*Endocrinology* **131**: 799–806, 1992)

FSH IS a member of the glycoprotein hormone family that also comprises LH, CG, and TSH (1, 2). Hormones of this family are dimers consisting of a common α-subunit and hormone-specific β-subunits joined together by noncovalent binding (3). As with the other glycoprotein hormones, FSH binding to target cells increases adenyl cyclase activity through interaction with membrane-associated G-proteins (4), thus classifying the FSH receptor to the G-protein-coupled receptor family (5–7). The hallmark of G-protein-coupled receptors is the presence of seven transmembrane-spanning segments that possess a homologous cluster of six or seven amino acid residues located on the carboxyl-terminal region of the third cytoplasmic loop. Recent molecular cloning of rat LH and FSH receptors have indicated that this conserved region, which has been implicated in G-protein coupling of the β-adrenergic receptor (8–10) and TSH receptor (11), is also present in the third cytoplasmic loop of gonadotropin receptors (12, 13).

Although the importance of FSH in testicular and ovarian development and reproductive function has been unequivocally established (for review, see Refs. 14–16), the limited availability of human gonadal tissues as well as the paucity of gonadal FSH-binding sites have precluded the study of human (h) FSH receptors. Recent studies from our laboratory have indicated that the ligand specificity of human *vs.* rat (r) LH receptors is dramatically different, suggesting that the properties of human gonadotropin receptors may differ from those of experimental animal models (17). To more clearly elucidate the properties of hFSH receptors, we report here the expression of a functional recombinant hFSH receptor with unique ligand specificity. Furthermore, the distribution of FSH receptor mRNA in human reproductive tissues and the biochemical properties of the expressed receptor are presented.

Materials and Methods

Reagents and hormones

Restriction enzymes were obtained from Bethesda Research Laboratories (BRL; Gaithersburg, MD), Boehringer-Mannheim (Indianapolis, IN), and Stratagene (La Jolla, CA). A λgt11 human testicular cDNA

Received February 7, 1992.
Address all correspondence and requests for reprints to: Dr. Aaron J. W. Hsueh, Division of Reproductive Biology, Department of Obstetrics and Gynecology, Stanford University School of Medicine, 300 Pasteur Drive, Stanford, California 94305–5317.
* This work was supported by NIH Grant HD-23273.
† Postdoctoral fellow supported by the Lalor Foundation.
‡ On leave from the Department of Obstetrics and Gynecology, Hokkaido University, Sapporo, Japan.

library was obtained from Clontech (Palo Alto, CA). The eukaryotic expression vector pCMX was a gift from Dr. K. Umesono of The Salk Institute (San Diego, CA). The recombinant human gonadotropin preparations were derived from serum-free conditioned medium of Chinese hamster ovary (CHO) cell lines transfected with human gonadotropin genes. The recombinant hLH contains a deletion of seven hydrophobic amino acids at the carboxyl-terminus and a substitution of Trp to Arg at position eight of the β-subunit for efficient dimerization and secretion from CHO cells (18). The recombinant hFSH has biological activity and chromatofocusing profiles similar to those of purified pituitary FSH (19). The concentrations of the recombinant gonadotropins were estimated in RIAs using purified pituitary preparations as standards (hLH, hLH I-3, 5,900 IU/mg; hFSH, hFSH I-3, 3,100 IU/mg by the hCG augmentation assay). hFSH (I-3), hCG (CR-127; 14,900 IU/mg), hLH (B1; 4,015 IU/mg), hTSH (B1; 15 IU/mg), rFSH (I-7; 4,714 IU/mg), and ovine (o) FSH (oFSH-17; 25 IU/mg) were obtained from the National Hormone and Pituitary Distribution Program (Bethesda, MD); recombinant hTSH was obtained from Genzyme (Cambridge, MA); equine (e) CG (PMSG; 2,530 IU/mg) was obtained from Calbiochem (La Jolla, CA); and porcine (p) FSH was the gift of Dr. H. Papkoff (University of California-San Francisco). Reagents required for the luciferase assay were purchased from Analytical Luminescence Laboratory (San Diego, CA).

cDNA library screening

A fragment of rFSH receptor cDNA, corresponding to bases 621–1031 of the published sequence (13), was obtained by reverse transcription-polymerase chain reaction of RNA prepared from PMSG-primed rat ovaries (20). This cDNA fragment was radiolabeled by the random priming method (21) and used to screen the human testicular cDNA library (22). Eight positively hybridizing phage clones ranging in size from 1.8–2.2 kilobases (kb) were isolated, subcloned into the pBluescript II SK plasmid (Stratagene), and sequenced using the dideoxy chain termination method (23) with a DNA sequencing kit (U.S. Biochemical Corp., Cleveland, OH) and specific primers. Individual fragments obtained from two separate clones (H37 and G3) were prepared by *Bam*HI restriction enzyme digestion and ligated at nucleotide position 686 to yield the final hFSH receptor cDNA construct containing the entire amino acid-coding region. Clone H37 contains 75-basepairs (bp) of 5′-untranslated region plus 1562 bp of open reading frame, but lacks the 3′-end and polyadenylation signal. Clone G3 starts at 168 bp of the open reading frame and covers the entire amino acid-coding region to the termination codon plus 26 bp of the 3′-untranslated region. These clones contain a 1394-bp overlapping region with identical nucleotide sequence, the identity of which was further confirmed by sequence analysis of the remaining six clones. The DNA sequence of the final clone was determined on both strands and compared to the published sequence of a cloned, but not expressed, human ovarian FSH receptor cDNA (24). Sequence comparison indicated seven individual basepair substitutions between our and the reported clone, resulting in five different amino acids at the following positions: 112 (Thr to Asn), 197 (Ala to Glu), 198 (Val to Leu), 307 (Ala to Thr), and 680 (Ser to Asn).

Expression of full-length cDNA in eukaryotic cells

An *Eco*RI linker (Promega, Madison, WI) was inserted into the *Eco*RV restriction site of the pCMX expression vector (17) to generate a plasmid (designated pCME) containing an *Eco*RI cloning site. The cDNA construct coding for the entire hFSH receptor (−75 to 2085 bp plus 26 bp of the 3′-untranslated region) was then subcloned into the *Eco*RI site of the pCME vector and partially sequenced to determine the orientation of the cDNA insert. Exponentially growing 293 cells derived from human fetal kidney were transiently transfected in 5 ml Dulbecco's Modified Eagle's Medium (DMEM; supplemented with 5% fetal calf serum, 2 mM L-glutamine, 100 U/ml penicillin, and 100 μg/ml streptomycin sulfate; Gibco, Santa Clara, CA) with the expression plasmid (designated pCME-hFSHR) using the calcium phosphate precipitation method (25) used routinely in our laboratory (17). Twenty-four hours after transfection, FSH receptor binding studies were performed by incubating cells (2×10^5/0.4 ml) with [^{125}I]hFSH at 22 C for 20 h or as indicated. Iodination of hFSH (I-3) was performed using the lactoperoxidase method (26). The specific activity and maximal binding of [^{125}I]hFSH, as determined by radioligand receptor assay using rat testicular membranes, were 99,000–110,000 cpm/ng and 7%, respectively. Nonspecific binding was determined by inclusion of a 1,000-fold excess of unlabeled ligand (Pergonal, Serono Laboratories, Randolph, MA). Similar procedures were used to analyze the ligand specificity of FSH-binding sites in testicular homogenates prepared from 15-day-old Sprague-Dawley rats (Johnson Labs, Bridgeview, IL). For cAMP analysis, transfected 293 cells (2×10^5/culture dish) were treated with various gonadotropins in the presence of 0.25 mM 3-isobutyl-1-methylxanthine (MIX; Sigma Chemical Co., St. Louis, MO) for 2 h at 37 C. After incubation, extracellular cAMP levels were determined by specific RIA, using [^{125}I]cAMP (ICN, Costa Mesa, CA) as the labeled ligand and a commercially available cAMP antiserum (ICN) (27). The intra- and interassay coefficients of variation were 6% and 10%, respectively.

Luciferase reporter gene

A 654-bp fragment of the 5′-flanking sequence of the rat tissue plasminogen activator (tPA) gene ligated to the luciferase gene plasmid p19LUC (28) was used (designated ptPA-LUC) (29). This portion of the tPA promoter region contains a cAMP-responsive element capable of mediating gonadotropin-stimulated tPA gene transcription (29). Exponentially growing 293 cells were transiently transfected in 5 ml DMEM with pCME-hFSHR and ptPA-LUC plasmids (at a ratio of 0.8:0.2; 7.5 μg total DNA). After transfection, cells were collected, counted, and dispensed into 12 × 75-mm culture tubes (5×10^4 cells/tube). The total volume was brought to 0.3 ml with DMEM containing 0.25 mM MIX with hFSH or hCG, and cells were incubated for 18 h at 37 C. After incubation, cells were lysed by the addition of 0.3 ml/tube 2 × lysis buffer [50 mM Tris-phosphate (pH 7.8), 4 mM dithiothrietol, 4 mM 1,2-diaminocyclohexane-*N,N,N′,N′*-tetraacetic acid, 20% glycerol, and 2% Triton X-100] at 22 C for 15 min. For estimation of luciferase activity, 10 μl cell lysate mixture were combined with 100 μl assay reagent [20 mM tricine, 1.07 mM $(MgCO_3)_4$ $Mg(OH)_2$–$5H_2O$, 2.67 mM $MgSO_4$, 0.1 mM EDTA, 33.3 mM dithiothrietol, 270 μM coenzyme-A, 470 μM luciferin, and 530 μM ATP], and light production was immediately measured for 10 sec in a luminometer (Monolight 2010, Analytical Luminescence Laboratory).

Preparation of nucleic acid probe for hFSH receptor mRNA

A fragment of the hFSH receptor cDNA, corresponding to bases 744–1026, was isolated after digestion of the hFSH receptor cDNA with the *Hinc*II restriction enzyme. This fragment, which possesses less than 50% nucleotide sequence homology to the hLH receptor cDNA (17), was subcloned into the pGEM4z vector (Promega). The plasmid clone was linearized with the *Sal*I restriction enzyme and served as a template for the production of a cRNA probe using T7 RNA polymerase (BRL) and [α-^{32}P]CTP (3000 Ci/mmol; Amersham, Arlington Heights, IL), as previously described (30).

Northern blot analysis

Human ovarian and placental tissues were provided by Dr. T. Tanaka (Hokkaido University, Sapporo, Japan) and Dr. A. Murphy (University of California-San Diego), respectively. Total RNA was extracted from human tissues using the guanidinium thiocyanate-phenol-chloroform extraction procedure (31). Total RNA samples were enriched for poly(A) mRNA by a single round of oligo(dT) column chromatography (Pharmacia LKB Biotechnology, Piscataway, NJ) and electrophoresed through 1% agarose-2.2 M formaldehyde gels. Samples were blotted onto nitrocellulose membranes (Schleicher and Schuell, Keene, NH) by overnight capillary electrophoresis and covalently cross-linked using a UV cross-linker (Stratagene). Membranes were then prehybridized for 2–4 h at 65 C in the presence of 50% formamide under standard conditions, followed by hybridization with the radiolabeled hFSH receptor cRNA probe at the same temperature for 18–20 h (20, 32, 33). Membranes were washed in 2 × sodium chloride-sodium citrate (SSC)-0.1% sodium dodecyl sulfate (SDS) for 10 min at room temperature, followed by two or three consecutive 15- to 20-min washes in 0.1 × SSC-0.1% SDS at

65 C, and exposed to Kodak X-Omat film (Eastman Kodak, Rochester, NY) for 1–5 days at −70 C.

Ligand receptor cross-linking

Cross-linking of [^{125}I]hFSH to binding sites in transfected 293 cells and rat testicular homogenates was performed using disuccinimidyl suberate (Pierce, Rockford, IL), as previously described (34). Briefly, 6 × 10^6 transfected 293 cells or homogenate from 10 immature rat testes were incubated with 8 × 10^5 cpm [^{125}I]hFSH in the absence or presence of a 1000-fold excess of unlabeled hormone at 22 C for 20 h in a total volume of 0.4 ml. After incubation, cells or homogenates were diluted with 1 ml wash solution (Dulbecco's PBS containing 0.1% BSA, 5 mM EDTA, and 5 mM *N*-ethylmaleimide), pelleted by centrifugation, washed, and recentrifuged. Pellets were then resuspended in 0.5 ml incubation buffer (D-PBS containing 10% dimethylsulfoxide), and disuccinimidyl suberate (freshly prepared in dimethylsulfoxide) was added to a final concentration of 1.5 mM. Cross-linking was carried out at 0 C for 30 min, and the reaction was stopped by the addition of 1 ml termination buffer [50 mM Tris-HCl (pH 7.5) and 100 mM NaCl]. The reaction tubes were centrifuged, and pellets were resuspended in 0.1 ml solubilization buffer [50 mM Tris-HCl (pH 7.5) and 1% Triton X-100]. Solubilization was performed by incubation at 0 C for 60 min, with mixing of samples every 15 min. The samples were centrifuged for 5 min at 13,000 × *g*, and the resultant supernatants were resolved by SDS-polyacrylamide gel electrophoresis (SDS-PAGE), using 8.5% polyacrylamide gels. The gels were then subjected to autoradiography at −70 C for 2–14 days.

Results

Expression and binding kinetics of hFSH receptors in eukaryotic cells

Cells derived from a human fetal kidney cell line (293) were transfected with the plasmid pCME-hFSHR. After a 24-h incubation, cells were analyzed by radioligand receptor binding (Fig. 1). A dose-dependent increase in specifically bound [^{125}I]hFSH was detected in transfected cells incubated with increasing concentrations of labeled FSH, whereas no specific binding was observed in nontransfected cells (data not shown). Analysis of receptor binding indicated a K_d value of 1.7 × 10^{-9} M.

To study the effects of incubation time and temperature on the kinetics of FSH receptor binding, transfected 293 cells were incubated with [^{125}I]hFSH at 4, 22, or 37 C for increasing lengths of time, after which specific binding was determined (Fig. 2). A time-dependent increase in the levels of specific FSH binding was observed in cells incubated at 22 and 37 C, whereas low levels of [^{125}I]hFSH binding were detected at 4 C. Maximal FSH binding was highest in cells incubated at 22 C, although the time required to reach maximal ligand binding was considerably longer in incubations conducted at 22 *vs.* 37 C (Fig. 2).

Interaction of hFSH receptor with recombinant and pituitary/urinary-derived human gonadotropins and TSH

To test the binding specificity of the expressed hFSH receptor for human gonadotropins, transfected 293 cells were incubated with [^{125}I]hFSH in the absence or presence of increasing doses of unlabeled urinary-derived hCG, or hFSH, hLH, or hTSH of both pituitary and recombinant origin. Displacement of labeled FSH from its binding sites was expressed relative to the total amount of specifically bound [^{125}I]hFSH (Fig. 3). Both recombinant and pituitary FSH preparations competed with [^{125}I]hFSH for FSH receptors expressed in 293 cells (ED_{50}: recombinant, 25 ng/ml; pituitary-derived, 70 ng/ml), whereas human pituitary LH and

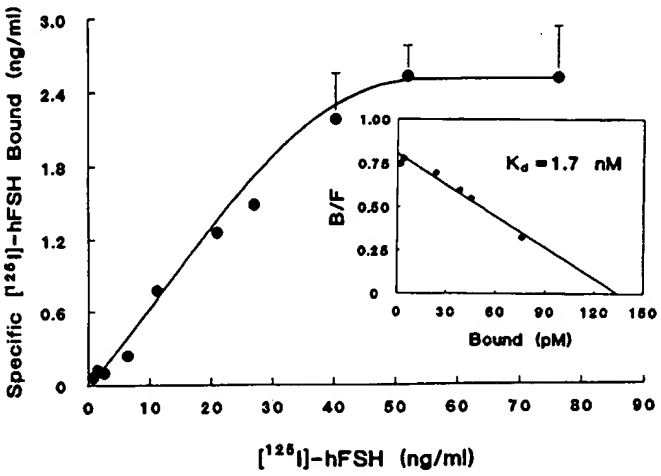

FIG. 1. Binding of [^{125}I]hFSH to hFSH receptors expressed in eukaryotic cells. 293 cells were transfected with the hFSH receptor plasmid pCME-hFSHR, and binding of radiolabeled hFSH was determined 24 h later. Cells (2 × 10^5/tube × 0.4 ml) were incubated with increasing concentrations of [^{125}I]hFSH in the absence or presence of a 1000-fold excess of unlabeled ligand. Levels of specifically bound [^{125}I]hFSH are shown together with the derived Scatchard plot (*inset*; B/F, bound to free ratio). Data are the mean ± SEM of triplicate determinations from a representative experiment.

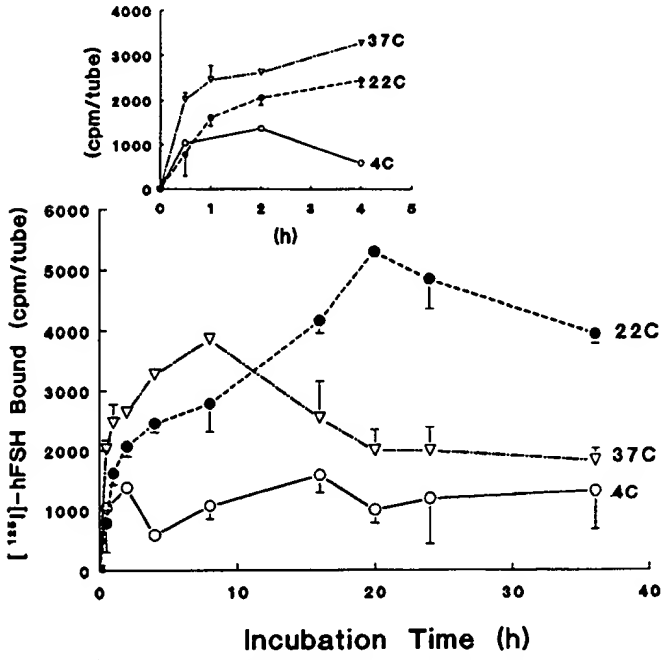

FIG. 2. Effects of incubation time and temperature on rate and extent of [^{125}I]hFSH binding to 293 cells. Transfected 293 cells (2 × 10^5/tube) expressing hFSH receptors were incubated with radiolabeled hFSH in the absence or presence of a 1000-fold excess of ligand at 4, 22, or 37 C for increasing lengths of time, after which levels of specifically bound [^{125}I]hFSH were calculated (mean ± SEM of triplicate determinations from a representative experiment). An enlarged figure for the first 4 h of incubation is presented in the *inset*.

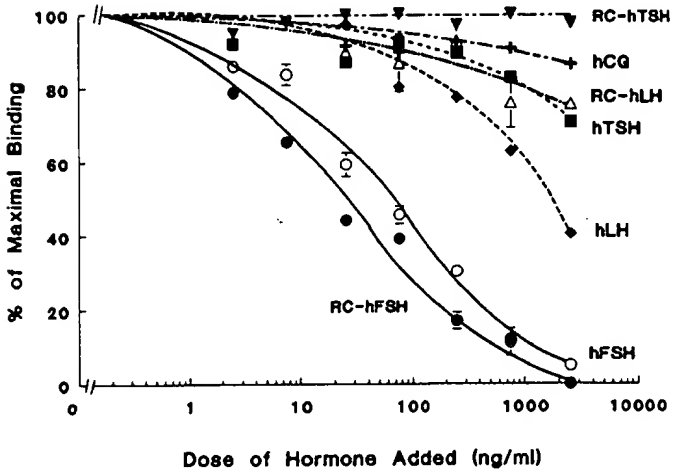

FIG. 3. Interaction of recombinant (RC) and pituitary/urinary-derived human gonadotropins and TSH with hFSH receptors expressed in transfected 293 cells. Displacement of [^{125}I]hFSH binding to hFSH receptors by hFSH, hLH, hCG, or hTSH was determined in radioligand receptor assays (mean ± SEM of three replicate experiments).

TSH were effective only at high doses. In contrast, negligible interaction of hCG or recombinant hLH or hTSH with the expressed FSH receptors was observed (Fig. 3).

Ligand specificity of human vs. rat FSH receptors

To assess the ligand specificity of the hFSH receptor, 293 cells expressing human receptors were incubated with [^{125}I] hFSH in the absence or presence of increasing doses of eCG (PMSG) or FSH from human, rat, ovine, and porcine origin. Displacement of [^{125}I]hFSH by unlabeled hormone in the human receptor was compared to that of testicular homogenates from 15-day-old rats (Fig. 4). hFSH and rFSH preparations were effective in binding to the recombinant hFSH receptor (ED_{50}: hFSH, 70 ng/ml; rFSH, 125 ng/ml), whereas only minimal interaction of oFSH, pFSH, or eCG with hFSH receptors was observed (Fig. 4A). In contrast, FSH from rat, human, and ovine origin as well as eCG effectively competed with radiolabeled FSH for binding sites in rat testicular homogenates (hFSH = rFSH > oFSH > eCG); however, pFSH was effective only at high doses (Fig. 4B).

Gonadotropin stimulation of cAMP production and tPA promoter-luciferase reporter gene by transfected 293 cells expressing hFSH receptors.

The functional capacity of the recombinant hFSH receptor was tested based on gonadotropin stimulation of cAMP production by transfected 293 cells. Treatment of cells with human pituitary FSH caused a dose-dependent increase in cAMP formation (ED_{50}, 10 ng/ml), with a maximal 13-fold increase observed in response to 100 ng/ml FSH (Fig. 5A). Human pituitary LH also increased cAMP production at doses of 100 (4-fold) and 1000 (6.6-fold) ng/ml, whereas neither hCG nor recombinant hLH altered cAMP levels compared to control values (Fig. 5A).

Our earlier data demonstrated the stimulation of rat tPA

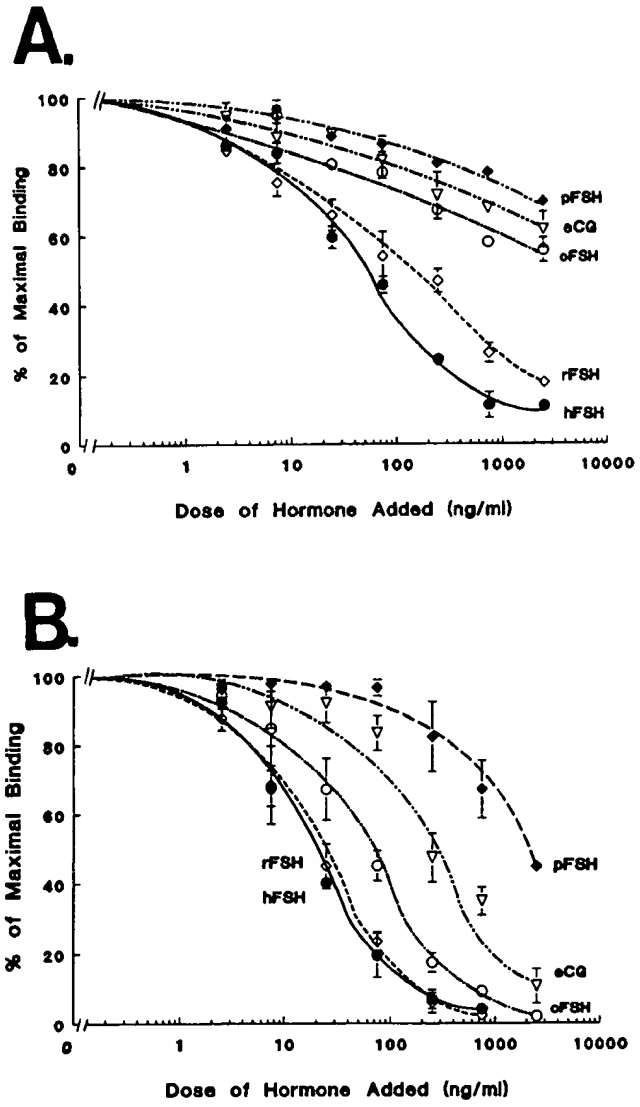

FIG. 4. Displacement of [^{125}I]hFSH binding to human and rat FSH receptors by human, rat, ovine, equine, and porcine gonadotropins. Transfected 293 cells expressing hFSH receptors (A) or rat testicular homogenates (B) were incubated with [^{125}I]hFSH in the absence or presence of hFSH, rFSH, oFSH, or pFSH as well as eCG. Displacement curves are presented as a percentage of maximal binding at each dose of unlabeled hormone (mean ± SEM of three replicate experiments).

gene expression in ovarian granulosa cells (32). In granulosa cells transfected with a luciferase reporter gene driven by a cAMP-responsive region of the rat tPA gene promoter, treatment with FSH increases luciferase expression (29). Using this tPA-luciferase reporter plasmid, we evaluated the ability of human gonadotropins to induce luciferase activity in 293 cells transfected with plasmids for both hFSH receptor and the reporter constructs. Treatment of cells with increasing doses of FSH, but not hCG, caused a dose-dependent increase in luciferase activity, with an estimated ED_{50} of 8 ng/ml and a maximal 2-fold increase at 100 ng/ml (Fig. 5B). These findings demonstrate a functional linkage of recombinant hFSH receptors to the tPA gene.

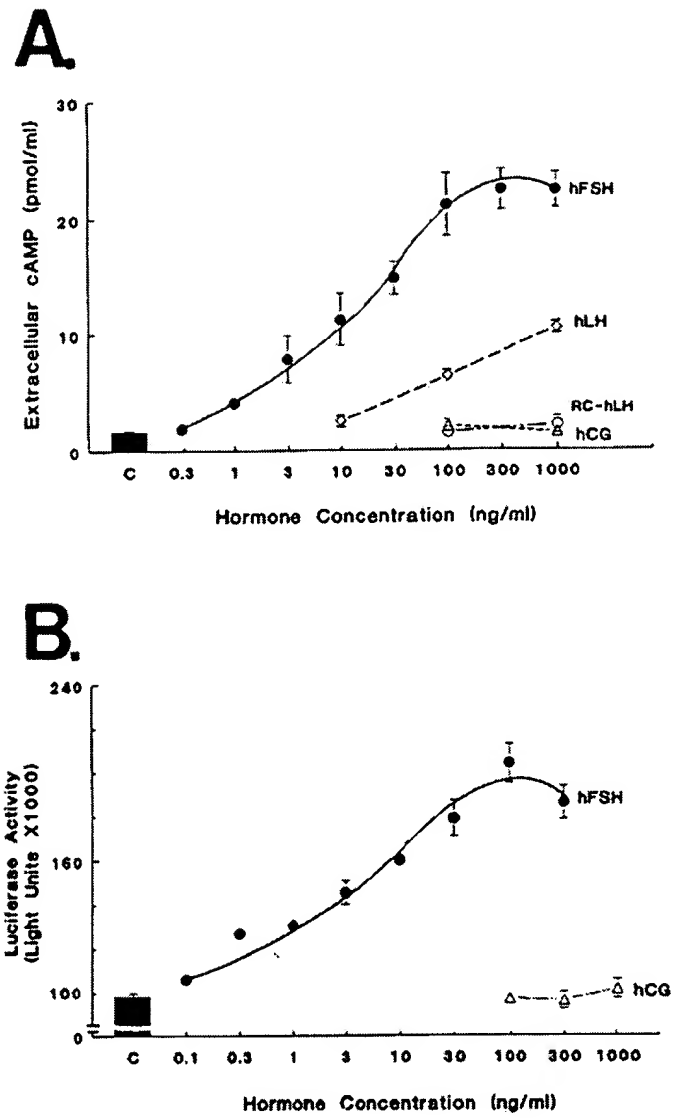

FIG. 5. Gonadotropin stimulation of cAMP production (A) and luciferase activity (B) by 293 cells expressing hFSH receptors. A, Extracellular cAMP accumulation was measured after incubation of transfected 293 cells (2×10^5/culture dish) for 2 h at 37 C with 0.25 mM MIX in the absence or presence of hFSH, hLH, or hCG. Data are the mean ± SEM of six cultures from three replicate experiments (RC, recombinant). B, Dose-dependent stimulation of luciferase activity by hFSH, but not hCG, in 293 cells cotransfected with the hFSH receptor plasmid and a tPA promoter-luciferase reporter gene construct (note the break in the y-axis). Data are the mean ± SEM of triplicate determinations from a representative experiment.

Northern blot analysis of FSH receptor mRNAs in human reproductive tissues

To study the expression of hFSH receptor mRNA, RNA was extracted from human reproductive tissues and analyzed by Northern blot, using a radiolabeled cRNA probe corresponding to the extracellular region of cDNA from our cloned hFSH receptor (Fig. 6). Analysis of poly(A)-enriched mRNA prepared from human follicular phase ovary indicated the

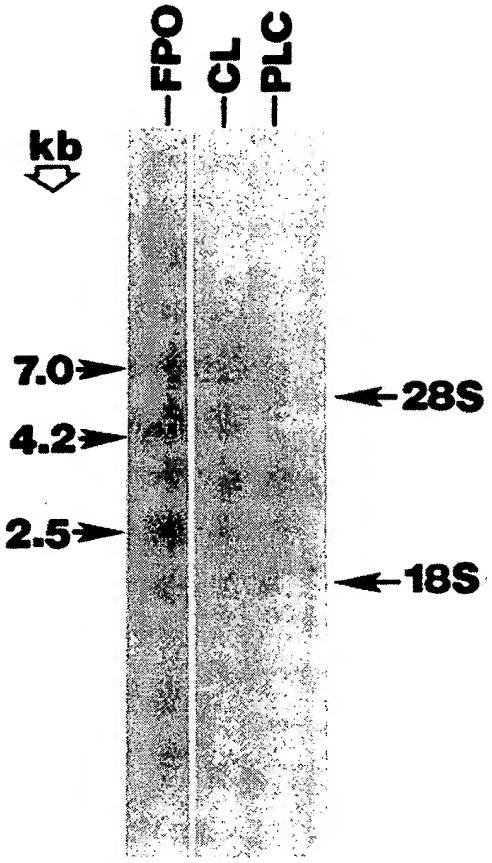

FIG. 6. Northern blot analysis of hFSH receptor mRNAs in human reproductive tissues. Poly(A)-enriched RNA samples prepared from human follicular phase ovary (FPO), 21-day-old corpora lutea (CL), or 19-week-old placenta (PLC) (2 μg/lane) were resolved through denaturing agarose gels, transferred to nitrocellulose filters, and hybridized to a ^{32}P-labeled hFSH receptor cRNA probe. Filters were washed and exposed to photographic films for 5 days at −70 C. Migration distances of the 28S and 18S ribosomal RNAs of a parallel total RNA sample from human ovary are indicated.

existence of three mRNA transcripts (7.0, 4.2, and 2.5 kb) that were not detected in an equivalent amount of mRNA prepared from corpus luteum (day 21 of the menstrual cycle) or placenta (week 19 of pregnancy; Fig. 6).

Cross-linking of [^{125}I]hFSH to FSH-binding sites in transfected cells and immature rat testes

To estimate the molecular size of the recombinant hFSH receptor, [^{125}I]hFSH was cross-linked to FSH-binding sites in transfected 293 cells using disuccinimidyl suberate, followed by SDS-PAGE analysis (Fig. 7). A predominant autoradiographic band of protein, with an estimated molecular mass of 109 kilodaltons (kDa; 76 kDa for the binding protein after correction for mass attributed to the ligand) was detected in transfected cells expressing hFSH receptors, whereas a 1000-fold excess of ligand completely blocked [^{125}I]hFSH binding (Fig. 7). A less abundant protein band of approximately 145 kDa (112 kDa for the binding protein) was also present. These findings were comparable to those observed for FSH

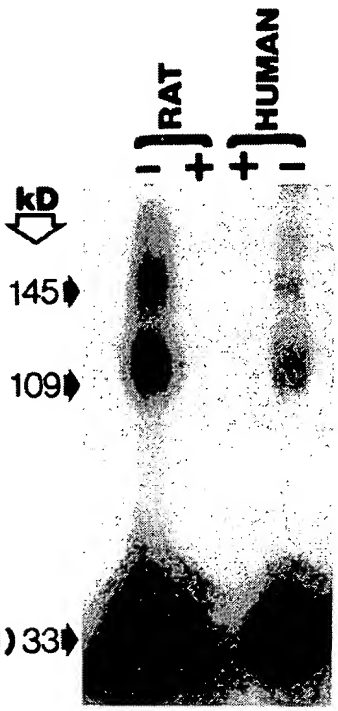

FIG. 7. Cross-linking of hFSH- and rFSH-receptors to [^{125}I]hFSH. Radiolabeled hFSH was cross-linked to FSH receptors in transfected 293 cells expressing hFSH receptors (HUMAN) or rat testicular homogenates (RAT) using disuccinimidyl suberate. Proteins were separated through 8.5% polyacrylamide gels and analyzed by autoradiography (14 days at −70 C). The sizes of the proteins were estimated by comparison to migration distances of known protein mol wt standards. Symbols indicate the absence (−) or presence (+) of a 1000-fold excess of ligand (Pergonal) during the binding incubation period before the cross-linking reaction.

receptors found in testicular homogenates of immature rats under the same experimental conditions (Fig. 7).

Discussion

We report here the ligand specificity and biochemical properties of the recombinant hFSH receptor. Our data indicate that hFSH, but not LH or CG, competes with [^{125}I] hFSH for binding to the recombinant FSH receptor. In addition, hFSH stimulates cAMP production in 293 cells expressing the human receptor, whereas recombinant hLH and hCG are without effect. As a result of stimulation of endogenous cAMP levels by FSH, a tPA promoter-driven luciferase reporter gene was also activated. Similar to the species-specific ligand binding recently reported for the hLH receptor (17), the recombinant hFSH receptor interacts with hFSH and rFSH, but only minimally with eCG or FSH of ovine and porcine origins. We also report here the first identification of FSH receptor mRNA in human ovaries as well as the determination of the molecular size of the recombinant hFSH receptor through ligand cross-linking analysis.

Comparison of the present human testicular FSH receptor cDNA with an ovarian cDNA clone recently reported (24) indicated seven individual basepair substitutions throughout the receptor sequence, resulting in five amino acid changes. Although we are uncertain of the basis for the observed disparity between our and the reported clone, our FSH receptor cDNA could be expressed, whereas no expression data were reported for the ovarian clone. Additionally, four of the five variant amino acids are identical between our hFSH and the reported rFSH receptor sequence (13). The ability of 293 cells transfected with our cDNA to express high affinity FSH receptors coupled to the endogenous adenyl cyclase and a luciferase reporter gene indicates that our clone encodes for a functional protein.

The availability of a cell line that expresses recombinant hFSH receptors has provided an unlimited source of the human receptor and enabled us to perform analysis of the ligand specificity of the human receptor. Radioligand receptor assays demonstrated that the hFSH receptor does not interact with hCG or recombinant hLH or hTSH at physiological or supraphysiological concentrations. However, highly purified human pituitary LH and TSH did cross-react with recombinant FSH receptors, suggesting that the pituitary hormone preparations contain minor FSH contamination. Furthermore, unlike the ability of rat testicular FSH receptors to recognize gonadotropin preparations from diverse species (Ref. 35 and the present study), the human receptor interacted preferentially with human and rat FSH. These findings coupled with a similar species-specific ligand binding of hLH receptors (17) indicate significant evolutionary changes in both human gonadotropin receptors. Alternatively, we cannot rule out subtle differences in posttranslational processing of the receptor in 293 cells *vs.* gonadal cells that may influence its binding characteristics. However, the ligand specificity of hLH-binding sites expressed in 293 cells (17) is identical to that of native LH receptors present in human corpus luteum (36), suggesting that the properties of these recombinant proteins are similar to those of endogenous gonadal receptors.

Saturation binding and Scatchard analysis demonstrated that the recombinant FSH-binding site has an estimated K_d of 1.7 nM, comparable to that reported for FSH receptors in human testes (37). In addition, the effects of incubation time and temperature on the rate and extent of [^{125}I]hFSH binding by recombinant hFSH receptors were similar to those reported for rat testicular FSH (35) and LH (38) receptors. Recombinant hFSH receptors occupied by gonadotropin are also capable of interacting with the endogenous G-proteins of the 293 cells to increase cAMP formation, thus providing a useful model to study FSH-activated signal transduction. Additionally, the use of a luciferase reporter gene driven by the cAMP-responsive promoter of the rat tPA gene (29) has indicated that transfected cells expressing hFSH receptors respond to FSH with increased luciferase activity. These findings provide evidence that FSH-induced signal transduction in cells expressing recombinant hFSH receptors is coupled to the activation of genes that are regulated by gonadotropins under physiological conditions within gonadal cells (32). However, the relatively small magnitude of the FSH response using the luciferase system (compared to cAMP) suggests a potential limitation of this assay in its present form. The reasons for this observation are unclear, but may

be related to the lack of gonadal cell-specific transcription factors in 293 cells that limit the activation of the luciferase reporter gene construct. Nonetheless, future modifications of the present cell model and the cAMP-driven luciferase gene reporter system should provide a useful and sensitive bioassay for hFSH.

The availability of hFSH receptor cDNA enabled us to study FSH receptor mRNA transcripts within human reproductive tissues. Northern blot analysis revealed the existence of several FSH receptor mRNAs within human follicular phase ovary, consistent with those reported for multiple FSH receptor mRNA transcripts in rat gonadal tissues (20, 39, 40). However, RNA prepared from human corpora lutea did not contain detectable levels of this message, suggesting that ovarian FSH receptor mRNA levels undergo up- and down-regulation during the human menstrual cycle in a manner similar to that reported for experimental animal models (20, 41).

Based on the deduced amino acid sequence of the hFSH receptor cDNA, the calculated molecular mass of the mature protein is approximately 75.6 kDa, consistent with the size estimation of recombinant FSH receptor based on ligand cross-linking and SDS-PAGE and comparable to that observed for FSH receptors in immature rat testes. Of interest was the finding of a less abundant 112-kDa FSH-binding site in both transfected 293 cells and rat testes, presumably resulting from posttranslational glycosylations of the protein. Alternatively, the smaller FSH-binding site may arise from proteolytic cleavage of the larger 112-kDa protein, as has been suggested by previous studies on hCG-binding sites in rat gonadal tissues (42).

Previous studies using nonreducing PAGE followed by ligand blotting have estimated the size of the FSH receptor in bovine and rat testicular membranes to be approximately 240 kDa (43, 44), possibly resulting from receptor aggregation and dimer formation. Moreover, photoaffinity labeling of the pFSH receptor revealed the presence of a major cross-linked complex of 104 kDa, which could be reduced with dithiothrietol into two smaller complexes of 75 and 61 kDa (45). Although the reasons for the discrepancy between our and earlier findings are unclear, they may result from varying methodologies (*e.g.* ligand-receptor cross-linking *vs.* ligand blotting) or species differences. Our data, however, suggest that binding of FSH does not require prior dimerization of its receptor on the plasma membrane, although it is possible that receptor aggregation may be important for receptor stability and/or signal transduction (46).

Expression of the hFSH receptor provides unlimited material for future studies of clinical interest. Additionally, the ability to measure cAMP production and luciferase reporter gene activity in a cell line expressing hFSH receptors should allow the establishment of a sensitive bioassay for human gonadotropins and for screening new FSH agonists and antagonists. Because earlier reports have suggested the presence of circulating antibodies against FSH receptor in patients with premature ovarian failure (47–49), the etiology of pathophysiological conditions associated with gonadotropin receptor dysfunction may also be more clearly elucidated.

Note Added in Proof

Amplification of human ovarian and testicular mRNA by reverse transcription polymerase chain reaction with oligonucleotide primers specific for human FSH receptor cDNA sequences, followed by direct sequencing of resultant PCR products after T7 gene 6 exonuclease treatment (50), indicated 100% sequence identity of this human FSH receptor cDNA with our clone obtained by cDNA library screening. Furthermore, independent cloning of human FSH receptor cDNA by R. Dijkema and R. de Leeuw (Organon, Oss, the Netherlands) also indicated 100% sequence identity with our cDNA clone (personal communication). Accession no. M95489.

Acknowledgments

The authors thank Dr. T. Ny (University of Umea, Umea, Sweden) for the rat tPA promoter-luciferase reporter gene; Drs. M. Oikawa and P. S. LaPolt for polymerase chain reaction analysis of the rFSH receptor cDNA; Dr. I. Boime (Washington University, St. Louis, MO) for provision of CHO cells secreting human LH and FSH; Dr. K. Umesono (The Salk Institute, San Diego, CA) for the pCMX expression vector and 293 cell line; Dr. T. Tanaka (Hokkaido University, Sapporo, Japan) for human ovarian tissues; Dr. A. Murphy (University of California-San Diego) for human placental tissue; Dr. H. Papkoff (University of California-San Francisco) for the gift of pFSH; and the National Hormone and Pituitary Distribution Program (Bethesda, MD) for hFSH, hLH, hCG, hTSH, rFSH, and oFSH.

References

1. **Pierce JG, Parsons TF** 1981 Glycoprotein hormones: structure and function. Annu Rev Biochem 50:465–495
2. **Ryan RJ, Charlesworth MC, McCormick DJ, Milius RP, Keutmann HT** 1988 The glycoprotein hormones: recent studies of structure-function relationships. FASEB J 2:2661–2669
3. **Kourides IA, Gurr JA, Wolf O** 1984 The regulation and organization of thyroid stimulating hormone genes. Recent Prog Horm Res 40:79–120
4. **Reichert Jr LE, Dattatreyamurty B** 1989 The follicle-stimulating hormone (FSH) receptor in testis: interaction with FSH, mechanism of signal transduction, and properties of the purified receptor. Biol Reprod 40:13–26
5. **Keinanen KP, Rajaniemi HJ** 1986 Rat ovarian lutropin receptor is a transmembrane protein. Biochem J 239:83–87
6. **Lefkowitz RJ, Caron MG** 1988 Adrenergic receptors. Models for the study of receptors coupled to guanine nucleotide regulatory proteins. J Biol Chem 263:4993–4996
7. **Birnbaumer L, Abramowitz J, Brown AM** 1990 Receptor-effector coupling by G proteins. Biochim Biophys Acta 1031:163–224
8. **Kobilka B** 1992 Adrenergic receptors as models for G protein-coupled receptors. Annu Rev Neurosci 15:87–114
9. **Strader CD, Dixon RAF, Cheung AH, Candelore MR, Blake AD, Sigal IS** 1977 Mutations that uncouple the β-adrenergic receptor from Gs and increase agonist efficiency. J Biol Chem 262:16439–16443
10. **Kobilka BK, Kobilka TS, Daniel K, Regan JW, Caron MC, Lefkowitz RJ** 1988 Chimeric α2 and β2-adrenergic receptors: delineation of domains involved in effector coupling and ligand binding specificity. Science 240:1310–1316
11. **Chazenbalk GD, Nagayama Y, Russo D, Wadsworth HL, Rapoport B** 1990 Functional analysis of the cytoplasmic domains of the human thyrotropin receptor by site-directed mutagenesis. J Biol Chem 265:20970–20975
12. **McFarland KC, Sprengel R, Phillips HS, Kohler M, Rosemblit N, Nikolics K, Segaloff DL, Seeburg PH** 1989 Lutropin-chorionogonadotropin receptor: an unusual member of the G protein-coupled receptor family. Science 245:494–499
13. **Sprengel R, Braun T, Nikolics K, Segaloff DL, Seeburg PH** 1990 The testicular receptor for follicle-stimulating hormone: structure and functional expression of cloned cDNA. Mol Endocrinol 4:525–

530
14. **Means AR, Fakunding JL, Huckins C, Tindall DJ, Vitale R** 1976 Follicle-stimulating hormone, the Sertoli cell, and spermatogenesis. Recent Prog Horm Res 32:477–527
15. **Richards JS** 1980 Maturation of ovarian follicles: actions and interactions of pituitary and ovarian hormones on follicular cell development. Physiol Rev 60:51–89
16. **Hsueh AJW, Bicsak TA, Jia X-C, Dahl KD, Fauser BCJM, Galway AB, Czekala N, Pavlou SN, Papkoff H, Keene J, Boime I** 1989 Granulosa cells as hormone targets: the role of biologically active follicle-stimulating hormone in reproduction. Recent Prog Horm Res 45:209–277
17. **Jia X-C, Oikawa M, Bo M, Tanaka T, Ny T, Boime I, Hsueh AJW** 1991 Expression of human luteinizing hormone (LH) receptor: interaction with LH and chorionic gonadotropin from human but not equine, rat, and ovine species. Mol Endocrinol 5:759–768
18. **Matzuk MM, Spangler MM, Camel M, Suganuma N, Boime I** 1989 Mutagenesis and chimeric genes define determinants in the β subunits of human chorionic gonadotropin and lutropin for secretion and assembly. J Cell Biol 109:1429–1438
19. **Keene JL, Matzuk MM, Otani T, Fauser BCJM, Galway AB, Hsueh AJW, Boime I** 1989 Expression of biologically active human follitropin in Chinese hamster ovary cells. J Biol Chem 264:4769–4775
20. **LaPolt PS, Tilly JL, Aihara T, Nishimori K, Hsueh AJW** 1992 Gonadotropin-induced up- and down-regulation of ovarian FSH receptor gene expression: effects of PMSG, hCG and recombinant FSH. Endocrinology 130:1289–1295
21. **Feinberg AP, Vogelstein B** 1983 A technique for radiolabeling DNA restriction endonuclease fragments to high specific activity. Anal Biochem 132:6–13
22. **Maniatis T, Fritsch EF, Sambrook J** 1982 Molecular Cloning–A Laboratory Manual. Cold Spring Harbor Laboratory, Cold Spring Harbor
23. **Hattori M, Sakai Y** 1986 Dideoxy sequencing method using denatured plasmid templates. Anal Biochem 15:232–238
24. **Minegish T, Nakamura K, Takakura Y, Ibuki Y, Igarashi M** 1991 Cloning and sequencing of human FSH receptor cDNA. Biochem Biophys Res Commun 175:1125–1130
25. **Chen C, Okayama H** 1987 High efficiency transformation of mammalian cells by plasmid DNA. Mol Cell Biol 7:2745–2752
26. **Miyachi Y, Vaitukaitis JL, Nieschlag E, Lipsett MB** 1972 Enzymatic radioiodination of gonadotropins. J Clin Endocrinol Metab 34:23–28
27. **Davoren JB, Hsueh AJW** 1985 Vasoactive intestinal peptide: a novel stimulator of steroidogenesis by cultured rat granulosa cells. Biol Reprod 33:37–52
28. **De Wet JR, Wood KV, DeLuca M, Helinski DR, Subramani S** 1987 Firefly luciferase gene: structure and expression in mammalian cells. Mol Cell Biol 7:725–737
29. **Feng P, Ohlsson M, Ny T** 1990 The structure of the TATA-less rat tissue-type plasminogen activator gene. J Biol Chem 265:2022–2027
30. **Melton DA, Krieg PA, Rebagliati MR, Maniatis T, Zinn K, Green MR** 1984 Efficient *in vitro* synthesis of bioactive RNA and RNA hybridization probes from plasmids containing a bacteriophage SP6 promoter. Nucleic Acids Res 12:7035–7056
31. **Chomczynski P, Sacchi N** 1987 Single-step method of RNA isolation by acid guanidinium thiocyanate-phenol-chloroform extraction. Anal Biochem 162:156–159
32. **Ohlsson M, Hsueh AJW, Ny T** 1988 Hormonal regulation of tissue-type plasminogen activator ribonucleic acid levels in rat granulosa cells: mechanism of induction by follicle-stimulating hormone and gonadotropin-releasing hormone. Mol Endocrinol 2:854–861
33. **LaPolt PS, Oikawa M, Jia X-C, Dargan C, Hsueh AJW** 1990 Gonadotropin-induced up- and down-regulation of rat ovarian LH receptor message levels during follicular growth, ovulation and luteinization. Endocrinology 126:3277–3279
34. **Mathews LS, Vale WW** 1991 Expression cloning of an activin receptor, a predicted transmembrane serine kinase. Cell 65:973–982
35. **Means AR, Vaitukaitis J** 1972 Peptide hormone "receptors:" specific binding of ^{3}H-FSH to testis. Endocrinology 90:39–46
36. **Cole FE, Weed JC, Schneider GT, Holland JB, Geary WL, Levy DL, Huseby RA, Rice BF** 1976 The specificity of gonadotropin binding by the human corpus luteum. Fertil Steril 27:921–928
37. **Wahlstrom T, Huhtaniemi I, Hovatta O, Seppala M** 1983 Localization of luteinizing hormone, follicle-stimulating hormone, prolactin, and their receptors in human and rat testis using immunocytochemistry and radioreceptor assay. J Clin Endocrinol Metab 57:825–830
38. **Catt KJ, Tsuruhara T, Dufau L** 1972 Gonadotropin binding sites of the rat testis. Biochim Biophys Acta 279:194–201
39. **Heckert LL, Griswold MD** 1991 Expression of follicle-stimulating hormone receptor mRNA in rat testis and Sertoli cells. Mol Endocrinol 5:670–677
40. **Tilly JL, LaPolt PS, Hsueh AJW** 1992 Hormonal regulation of follicle-stimulating hormone receptor messenger RNA levels in cultured rat granulosa cells. Endocrinology 130:1296–1302
41. **Camp TA, Rahal JO, Mayo KE** 1991 Cellular localization and hormonal regulation of follicle-stimulating hormone and luteinizing hormone receptor mRNAs in the rat ovary. Mol Endocrinol 5:1405–1417
42. **Roche PC, Ryan RJ** 1989 Purification, characterization, and amino-terminal sequence of the ovarian receptor for luteinizing hormone/human choriogonadotropin. J Biol Chem 264:4636–4641
43. **Dattatreyamurty B, Zhang S-B, Reichert Jr LE** 1990 Purification of follitropin receptor from bovine calf testes. J Biol Chem 265:5494–5503
44. **Reichert Jr LE, Dattatreyamurty B, Grasso P, Santa-Coloma TA** 1991 Structure-function relationships of the glycoprotein hormones and their receptors. Trend Pharmacol Sci 12:199–203
45. **Shin J, Ji TH** 1985 Photoaffinity labeling of the follitropin receptor. J Biol Chem 260:14020–14025
46. **Podesta EJ, Solano AR, Attar R, Sanchez ML, Molina-Veda L** 1983 Receptor aggregation induced by antilutropin receptor antibody and biological response in rat testis Leydig cells. Proc Natl Acad Sci USA 80:3986–3990
47. **Dias JA, Gates SA, Reichert Jr LE** 1982 Evidence for the presence of follicle-stimulating hormone receptor antibody in human serum. Fertil Steril 38:330–338
48. **Chiauzzi V, Cigorra S, Escobar ME, Rivarola MA, Charreau EH** 1982 Inhibition of follicle-stimulating hormone receptor binding by circulating immunoglobulin. J Clin Endocrinol Metab 54:1221–1228
49. **van Weissenbruch MM, Hoek A, van Vliet-Bleeker I, Schoemaker J, Drexhage H** 1991 Evidence for the existence of immunoglobulins that block ovarian granulosa cell growth *in vitro*. A putative role in resistant ovary syndrome. J Clin Endocrinol Metab 73:360–367
50. **Shon M, Gerimo J, Bastia D** 1982 The nucleotide sequence of replication origin β of the plasmid R6K. J Biol Chem 257:13823–13827